

The citation of this M.Sc thesis follows:

Hashim Abdellah Hashim Mohamed, Improved robust adaptive control of high-order nonlinear systems with guaranteed performance. M.Sc, King Fahd University Of Petroleum & Minerals, 2014.

Please contact us and provide details if you believe this document breaches copyrights. We will remove access to the work immediately and investigate your claim.

IMPROVED ROBUST ADAPTIVE CONTROL OF HIGH-ORDER
NONLINEAR SYSTEMS WITH GUARANTEED PERFORMANCE

by

HASHIM ABDELLAH HASHIM MOHAMED

Graduate Program in SYSTEMS Engineering

A thesis submitted in partial fulfillment
of the requirements for the degree of
Masters of Science

SYSTEMS ENGINEERING
KING FAHD UNIVERSITY OF PETROLEUM & MINERALS

© HASHIM ABDELLAH HASHIM MOHAMED

December 2014

Abstract

This thesis presents fuzzy- \mathcal{L}_1 adaptive controller and Model Reference Adaptive Control (MRAC) with Prescribed Performance Function (PPF) as two adaptive approaches for high nonlinear systems as two original contribution to the literature. Firstly, \mathcal{L}_1 adaptive controller has a structure that allows decoupling between robustness and adaption owing to the use of a low pass filter with adjustable gain in the feedback loop. The trade-off between performance and robustness is a key factor in the tuning of the filter's parameters. In fuzzy- \mathcal{L}_1 adaptive controller, we consider the class of strictly proper low pass filters with fixed structure but with the feedback gain as the only tunable parameter. A practical new fuzzy based approach for the tuning of the feedback filter of \mathcal{L}_1 adaptive controller is proposed. The fuzzy controller is optimally tuned using Particle Swarm Optimization (PSO) to minimize the tracking error and the control signal range. The main function of the fuzzy logic controller is the on-line tuning of the feedback gain of the filter. Secondly, an adaptive control of multi-input multi-output uncertain high-order nonlinear system capable of guaranteeing a predetermined prescribed performance is presented as MRAC with PPF. In this work, prescribed performance is defined in terms of the tracking error converging to a smaller residual set at a rate no less than a predefined value and exhibiting a maximum overshoot/undershoot less than a sufficiently small fixed constant. The key step in such approach is to transform the constrained system into an equivalent unconstrained one through an adequate transformation of the output error. This will show that the robust stabilization of the transformed error, guaranties the stability and convergence of the constrained tracking error within the set of time varying constraints representing the performance limits. Finally, simulations are presented to illustrate the simplicity, the performance and the robustness of each new technique.

Acknowledgments

This thesis is the result of my Master degree from January 2013 to December 2014. It has taken place at the Department of System Engineering at King Fahd University of Petroleum and Minerals under the counseling of my supervisor Dr. Sami El Ferik. First I would like to thank Dr. Sami El Ferik. His exceptional motivational skills and ability to continuously guide me in the right directions have been much needed assets in my struggle towards finishing the Master Degree. I would like to thank also Dr. Mustafa El-Shafei, and Dr. Mohamed Abido for being my thesis committee members.

Contents

Certificate of Examination	ii
Abstract	ii
Abstract	iii
List of Figures	vii
List of Tables	x
1 INTRODUCTION	1
1.1 Introduction And Motivation	1
1.2 Possible Applications of The Outcomes	1
1.3 Contribution to The Literature	3
1.3.1 Thesis Objectives and Contribution	4
1.4 Methodologies	4
1.5 Thesis Organization	5
2 LITERATURE REVIEW	6
2.1 Introduction	6
2.2 Feedback Control of UVS	6
2.3 \mathcal{L}_1 Adaptive Controller	7
2.4 Adaptive Control with Prescribed Performance Function	10
2.5 Adaptive Observers	11
2.6 Conclusions	11
3 \mathcal{L}_1 ADAPTIVE CONTROLLER	13
3.1 Introduction	13
3.2 \mathcal{L}_1 Adaptive Controller for Uncertain SISO Systems	13
3.2.1 Problem Formulation	13
3.2.2 \mathcal{L}_1 Adaptive Control Architecture	14

3.2.3	\mathcal{L}_1 Adaptive Control Stability Analysis	16
3.2.4	Problem Formulation and Simulation	18
3.3	\mathcal{L}_1 Adaptive Controller for Uncertain MIMO Systems	20
3.3.1	Problem Formulation	20
3.3.2	\mathcal{L}_1 Adaptive Control Architecture	20
3.3.3	\mathcal{L}_1 Adaptive Control Stability Analysis	22
3.3.4	Problem Formulation and Simulation	24
3.4	\mathcal{L}_1 Adaptive Controller for MIMO Systems in the Presence of Unmatched Non-linear Uncertainties and Strong Coupling Effect	34
3.4.1	Problem Formulation	34
3.4.2	Definitions and \mathcal{L}_1 -Norm Sufficient Condition for Stability	36
3.4.3	\mathcal{L}_1 Adaptive Control Architecture	37
3.4.4	\mathcal{L}_1 Adaptive Control Stability Analysis	38
3.4.5	Problem Formulation and Simulation	40
3.5	Conclusion	43
4	A Fuzzy Logic Feedback Filter Design Tuned with PSO for \mathcal{L}_1 Adaptive Controller	44
4.1	Introduction	44
4.2	Review of \mathcal{L}_1 adaptive controller	47
4.3	Optimal Fuzzy-tuning of the feedback filter	49
4.3.1	Structure of Fuzzy Logic Controller	49
4.4	Particle Swarm Optimization	50
4.5	Results and Discussions	51
4.5.1	Fuzzy \mathcal{L}_1 adaptive controller implementation:	51
4.5.2	Membership Function Optimization	52
4.5.3	PSO Simulation results	54
4.5.4	PSO Results	54
4.6	Conclusion	57
5	NEURO-ADAPTIVE FOR STRICT FEEDBACK MIMO SYSTEMS WITH PPF	61
5.1	Introduction	61
5.2	Introduction of Prescribed Performance	61
5.3	Problem Formulation and Preliminaries	62
5.3.1	Performance Functions	64
	Error Transformation	65
5.4	Neural Approximations	66
5.5	Robust Adaptive Control Design	67

5.6	Problem Simulation and Results	68
5.7	Conclusion	69
6	ROBUST MRAC WITH PPF FOR NONLINEAR MIMO SYSTEMS	71
6.1	Introduction	71
6.2	Problem Formulation	71
6.3	Controller Structure	72
6.4	Stability Analysis	75
6.5	Simulation Examples	77
6.6	Conclusion	78
7	ROBUST ADAPTIVE OBSERVER FOR \mathcal{L}_1 ADAPTIVE CONTROLLER	83
7.1	Introduction	83
7.2	Problem formulationn	83
7.3	Robust adaptive observer	84
7.3.1	Lyapunov function	86
7.4	Results and Discussions	87
7.5	Conclusion	90
8	CONCLUSIONS AND FUTURE WORK	94
8.1	Summary of Conclusions and Contributions	94
8.2	Future Work	95
	Bibliography	95

List of Figures

3.1	Closed loop \mathcal{L}_1 adaptive control system.	16
3.2	The output performance of \mathcal{L}_1 adaptive controller for unknown nonlinear SISO system.	18
3.3	Control signal of \mathcal{L}_1 Adaptive controller for unknown nonlinear SISO system. .	19
3.4	The output performance of \mathcal{L}_1 adaptive controller for unknown nonlinear SISO system.	19
3.5	Control signal of \mathcal{L}_1 Adaptive controller for unknown nonlinear SISO system. .	19
3.6	\mathcal{L}_1 adaptive control of two link planar robot with reference and actual tracking	26
3.7	Control signal of \mathcal{L}_1 adaptive control for two link planar robot	26
3.8	\mathcal{L}_1 adaptive control of two link planar robot with reference and actual tracking	27
3.9	Control signal of \mathcal{L}_1 adaptive control for two link planar robot	27
3.10	\mathcal{L}_1 adaptive controller with reference and actual tracking positions for quadrotor.	28
3.11	\mathcal{L}_1 adaptive controller with reference, desired and actual tracking angles of a quadrotor system.	29
3.12	Control input of \mathcal{L}_1 adaptive controller of a quadrotor system.	29
3.13	The 3D space tracking trajectory for both reference and actual output of a quadrotor system.	29
3.14	\mathcal{L}_1 adaptive controller with reference and actual tracking positions for quadrotor.	30
3.15	\mathcal{L}_1 adaptive controller with reference, desired and actual tracking angles of a quadrotor system	30
3.16	Control input of \mathcal{L}_1 adaptive controller of a quadrotor system	31
3.17	The 3D space tracking trajectory for both reference and actual output of a quadrotor system.	31
3.18	\mathcal{L}_1 adaptive controller with reference and actual tracking positions of MARES. .	32
3.19	\mathcal{L}_1 adaptive controller with reference, desired and actual tracking angles of MARES	32
3.20	Control input of \mathcal{L}_1 adaptive controller of MARES.	33
3.21	The 3D space tracking trajectory for both reference and actual output of MARES.	33

3.22	Tracking output of \mathcal{L}_1 adaptive control with reference and desired outputs for unmatched MIMO uncertain system.	41
3.23	Control signal of \mathcal{L}_1 adaptive control for unmatched MIMO uncertain system.	42
3.24	Laboratory set-up of TRMS.	42
3.25	Tracking output of \mathcal{L}_1 adaptive control with reference and desired outputs for TRMS.	43
3.26	Control signal of \mathcal{L}_1 adaptive control for TRMS.	43
4.1	The general structure of L1 adaptive controller.	44
4.2	Proposed fuzzy- adaptive control structure.	46
4.3	Flowchart of particle swarm Optimization [1].	51
4.4	Fuzzy- \mathcal{L}_1 adaptive controller for nonlinear SISO system.	52
4.5	Error and rate of error membership functions.	53
4.6	Graphical illustration of output membership functions.	54
4.7	Objective function minimization with PSO search process.	55
4.8	Performance of fuzzy- \mathcal{L}_1 adaptive controller after 100 iterations search process.	56
4.9	Performance of fuzzy- \mathcal{L}_1 adaptive controller and \mathcal{L}_1 adaptive controller for nonlinear system of case 1.	57
4.10	Feedback gain and output error of fuzzy- \mathcal{L}_1 adaptive controller and \mathcal{L}_1 adaptive controller of case 1.	58
4.11	Performance of fuzzy- \mathcal{L}_1 adaptive controller and \mathcal{L}_1 adaptive controller for nonlinear system of case 2.	59
4.12	Feedback gain and output error of fuzzy- \mathcal{L}_1 adaptive controller and \mathcal{L}_1 adaptive controller of case 2.	59
4.13	Performance of fuzzy- \mathcal{L}_1 adaptive controller for nonlinear system of case 3.	60
5.1	Graphical illustration of PPF for the tracking error behavior (a) graphical illustration of (5.4); (b) graphical illustration of (5.5).	64
5.2	Output response of the robust adaptive control with PPF for q_1 and q_2 versus desired trajectory q_{d1} and q_{d2}	69
5.3	Control input provided by robust adaptive control with PPF where u_1 is τ_1 and u_2 is τ_2	70
5.4	Prescribed error bounds between ρ_0 and ρ_∞ and ϵ for both joints (a) q_1 and (b) q_2	70
6.1	Output Performance of robust MRAC-PPF and \mathcal{L}_1 adaptive controller for case 1.	79
6.2	Control Signal of robust MRAC-PPF and \mathcal{L}_1 adaptive controller for case 1.	79
6.3	e_2 and ϵ_2 of robust MRAC-PPF and \mathcal{L}_1 adaptive controller for case 1.	80

6.4	e_2 and ϵ_2 of robust MRAC-PPF and \mathcal{L}_1 adaptive controller for case 1.	80
6.5	Output Performance of robust MRAC-PPF, \mathcal{L}_1 adaptive controller and <i>Neuro – Adaptive</i> with PPF for case 2.	81
6.6	Control Signal of robust MRAC-PPF, \mathcal{L}_1 adaptive controller and <i>Neuro – Adaptive</i> controller with PPF for case 2.	81
6.7	e_2 and ϵ_2 of robust MRAC-PPF, \mathcal{L}_1 adaptive controller and <i>Neuro – Adaptive</i> controller with PPF for case 2.	82
6.8	e_2 and ϵ_2 of robust MRAC-PPF, \mathcal{L}_1 adaptive controller and <i>Neuro – Adaptive</i> controller with PPF for case 2.	82
7.1	Robust adaptive observer design with \mathcal{L}_1 adaptive controller.	85
7.2	Output performance of \mathcal{L}_1 adaptive controller with robust adaptive observer. . .	88
7.3	x and \check{x} of robust observer with \mathcal{L}_1 adaptive controller.	88
7.4	$\check{\beta}$ of robust observer with \mathcal{L}_1 adaptive controller.	89
7.5	Output performance of \mathcal{L}_1 adaptive controller with robust observer for 2 DOF planner robot.	89
7.6	x and \check{x} of robust observer with \mathcal{L}_1 adaptive controller for 2-DOF planer robot. .	90
7.7	$\check{\beta}$ in the estimate robust observer with \mathcal{L}_1 adaptive controller.	90
7.8	Position performance of \mathcal{L}_1 adaptive controller with robust observer for quadrotor. .	91
7.9	Angles performance of \mathcal{L}_1 adaptive controller with robust observer for quadrotor. .	91
7.10	Control signal of \mathcal{L}_1 adaptive controller with robust observer for quadrotor. . . .	92
7.11	Angles performance of \mathcal{L}_1 adaptive controller with robust observer for quadrotor. .	92
7.12	Actual and estimated angles of robust observer with \mathcal{L}_1 adaptive controller for quadrotor.	93

List of Tables

3.1	Description of symbols and their units	25
3.2	System parameters	25
4.1	Rule base of FLC.	53
4.2	Parameters setting for PSO.	54
5.1	Prescribed performance function parameters	69
5.2	Adaptive PPF Controller parameters	69
6.1	Robust Neuro Adaptive Control with PPF parameters	78

Chapter 1

INTRODUCTION

1.1 Introduction And Motivation

The presence of uncertainties, nonlinearities, disturbances and lack in the precise modeling of nonlinear systems are common problems in dynamical applications. Over the last few decades, adaptive control has been developed to tackle the foregoing problems by providing fast adaptation and ensure robustness. In this work, \mathcal{L}_1 adaptive controller will be discussed briefly from different perspectives for different systems structures. \mathcal{L}_1 adaptive controller has been inspired originally from MRAC. Improving the feedback filter of \mathcal{L}_1 adaptive control will enhance the performance of the controller and the robustness margin. Fuzzy filter will be proposed for \mathcal{L}_1 adaptive controller in order to ensure fast closed loop dynamics with increasing the robustness margin. Neuro adaptive control with prescribed performance function will be investigated. Robust Model Reference Adaptive Control (MRAC) with Prescribed Performance Function (PPF) will be proposed to tackle problems of neuro-adaptive control and comparing the controller performance versus \mathcal{L}_1 adaptive controller. Robust adaptive observer will be implemented with \mathcal{L}_1 adaptive controller in order to check the performance of the controller in case of inaccessible states. These controllers will be applied on high nonlinear systems including Unmanned Vehicle Systems (UVS).

1.2 Possible Applications of The Outcomes

Unmanned Vehicle Systems (UVS) are important for different areas nowadays because they can be controlled and operated remotely without human interference. UVS is a research key because of the increase in demand of remote sensing and control in wide range of applications such as scientific surveys, traffic surveillance, transportation aids, and inspection in addition

to operation in harsh environments. UVS have various configurations, characteristics, shapes and sizes which will be reflected on system dynamics. The development in miniaturization of UVS offers high potential effort for small size and low cost of UVS compared to manned applications especially in certain applications. Rapid growing of UVS comes with promising future because of its size, cost, construction simplicity and maneuverability.

UVS can be classified into two categories either remotely control vehicles, or autonomous vehicles. Each of these categories includes different types of UVS such as: Unmanned Aerial Vehicles, Underwater Vehicles, Unmanned Surface Vehicle, Unmanned Spacecraft and Unmanned Grounded Vehicle. Importance of UVS relies on performance and mission targets. Generally, each type is considered as a mechanical rigid body with different equations of motion. The majority of UVS can be represented by nonlinear dynamics. The dynamic of UVS have their own features as affine nonlinear systems with normal coupling or with strong coupling. Usually, the controller is required to drive the system to the desired trajectory with smooth transition and fast response. Smooth transition in both control signal and output response will contribute in protecting the life cycle of system rotors and other parts in the UVS.

Developing UVS in the absence of the operator is costly in the controller complexity for tracking and vision. The controller is demanded to overcome many drawbacks, starting with stabilizing the system, driving the system to the desired trajectory in the shortest possible time, adapt against any variations of system dynamics and finally be robust against any disturbances. All these requirements ended up making the control design as an important issue and an interested subject to be investigated.

In order to design a controller for UVS, accurate models are needed to reflect system dynamics either by precise modeling or real time identification. UVS have a framework of rigid body dynamics and can be described by a set of differential equations using Euler-Lagrange. The definition of exact model is a struggling problem because nominal model is usually defined under certain operating conditions with neglecting any uncertainties and disturbances that may exist during the control process. Classical controller will not be sufficient due to nonexact model represented by presence of uncertainties and/or disturbances. Other types of controllers have to be considered in order to overcome classical controller drawbacks.

In the literature, several control design approaches have been adopted for Euler-Lagrange systems like adaptive control, nonlinear control, robust control and so forth. The weakness of many control approaches resides in defining the appropriate model for nonlinearity cancellation. In nonlinear control, it is often difficult to use the approximated nonlinear Euler-Lagrange equations of the system without adding a robustifying term to ensure system operation in the stability region. Including a robustifying term in the control law introduces discontinuity and chattering on the control signal. On the other hand, estimation of system nonlinearities nor-

mally experienced with discontinuity or singularity in the estimation process which may take the system out of the stability region.

1.3 Contribution to The Literature

In our work, two robust adaptive control approaches will be proposed for high nonlinear systems with guaranteed performance. Firstly, A fuzzy logic feedback filter will be designed for \mathcal{L}_1 adaptive controller mainly to improve the tracking capability and reduce the control signal range. The trade off between robustness range and fast closed loop dynamics will be averted and the proposed controller will contribute in solving this major problem. Next, robust MRAC-PPF will be proposed to tackle limitations of robust neuro-adaptive control with PPF. Also, it will be compared versus \mathcal{L}_1 adaptive control to highlight merits of the new controller. The controller will be studied on affine and not-affine systems. Finally, the performance of \mathcal{L}_1 adaptive controller with adaptive observers will be examined on Single-Input Single-Output (SISO) and Multi-Input Multi-Output (MIMO) systems.

The main features of the \mathcal{L}_1 adaptive controller are:

- Estimating the system to be controlled.
- For linear and nonlinear case without strong coupling, procedures consist of estimating uncertainties of the states, unmodelled input parameters and disturbances. For nonlinear case with strong coupling and/or unmatched uncertainties, it has same previous estimation process in addition to the estimate of unmatched part.
- The control law is based on Lyapunov function with compact set for previous item will be computed numerically.

The main features of robust neuro adaptive control with PPF are:

- Assign the prescribed function.
- Derive the transformed error.
- Estimating nonlinearities by neural network.
- Computing the control signal based on Lyapunov function.

1.3.1 Thesis Objectives and Contribution

This thesis contributes to literature on several routes all aiming at improving \mathcal{L}_1 adaptive controller in terms of adaptation and robustness. Therefore, there are several problems to be considered in this thesis:

1. We design a stabilizing controller based on fuzzy- \mathcal{L}_1 adaptive controller and examine the controller performance for nonlinear systems.
2. We design a stabilizing controller based on MRAC with PPF and examine the controller performance for nonlinear systems.
3. We compare fuzzy- \mathcal{L}_1 adaptive controller to \mathcal{L}_1 adaptive controller.
4. We compare MRAC to PPF versus neuro adaptive control with PPF and \mathcal{L}_1 adaptive controller.
5. Furthermore, we develop and implement adaptive observer with \mathcal{L}_1 adaptive control for nonlinear systems.

1.4 Methodologies

Developing thesis objective as mentioned in the previous section will go through several steps as following

1. Different UVS and nonlinear models have to be addressed as equation of motions.
2. Reproduce recent results upon literature of \mathcal{L}_1 adaptive control for nonlinear systems including UVS.
3. Reproduce recent results upon the literature on robust neuro adaptive control with prescribed performance function for nonlinear systems.
4. Formulate fuzzy- \mathcal{L}_1 adaptive controller and validate the new controller assuming complete unknown of nonlinear dynamics.
5. Formulate MRAC with PPF and validate the new controller assuming complete unknown of nonlinear dynamics.
6. Evaluating the performance of the controller by benchmarking the results to results in the literatures.

7. Develop and implement adaptive observer with \mathcal{L}_1 adaptive controller and benchmarking the results to results of \mathcal{L}_1 adaptive controller with accessible states.

Out of this work I have succeeded to publish [2–4]

1.5 Thesis Organization

The thesis is organized as the following

Chapter 1 includes introduction of the main work, motivation, thesis objective, methodology and finally thesis organization.

Chapter 2 includes literature review of different control methods especially adaptive control for nonlinear systems. Literature review presents last research activities on \mathcal{L}_1 adaptive control. Literature review of adaptive control with prescribed performance presents the main research activities over the last few years. Literature review of observer design shows the main research activities on this field.

Chapter 3 includes \mathcal{L}_1 adaptive controller for uncertain SISO systems, for uncertain MIMO systems and for MIMO systems in the presence of unmatched nonlinear uncertainties with strong coupling. Stability analysis, problem formulation and simulations will be validated for all foregoing cases.

Chapter 4 includes a brief review of \mathcal{L}_1 adaptive controller. It proposes a design of fuzzy logic control to tune the feedback filter of \mathcal{L}_1 adaptive controller. PSO is presented to design the output membership function of FLC. The controller will be examined on highly nonlinear system.

Chapter 5 includes robust neuro adaptive controller for strict feedback MIMO system with PPF mainly functioned to capture the idea of PPF in addition to evaluate its performance by reproducing recent papers.

Chapter 6 proposes a design of MRAC with PPF for high uncertain nonlinear systems. \mathcal{L}_1 adaptive controller and neuro-adaptive control with PPF are compared to the proposed controller.

Chapter 7 presents robust adaptive observer with \mathcal{L}_1 adaptive controller for highly nonlinear systems with complete unknown dynamics.

Chapter 8 concludes the work and suggests possible future works.

Chapter 2

LITERATURE REVIEW

2.1 Introduction

This chapter summarizes the research activities of \mathcal{L}_1 adaptive controller and adaptive control with PPF on different nonlinear systems with complete unknown dynamics. The first section include an introduction. The second section presents literature review of various control methods of UVS and a literature review of adaptive control techniques. The main contribution of this work is developed. Section three presents a brief review on \mathcal{L}_1 adaptive control including the main recent research activities. The fourth section is a review on adaptive control with PPF including including main research activities and recent works. Section five presents a study review on observer design. The last section is a conclusion.

2.2 Feedback Control of UVS

Adaptive control emerged in order to tackle time variant uncertainties, unmodeled dynamics and disturbances. Over the last few decades, various types of adaptive control has been proposed and modified to manipulate with aforementioned problems such as self-tuning regulators [5–8], gain scheduling [9–11], model reference adaptive control system [12–15] and adaptive neuro fuzzy control system [16–18]. In the recent few years, new adaptive control techniques were proposed rely on previous methods in terms of stability criteria and control law formulation. Immersion and Invariance adaptive control which is based on system immersion and manifold invariance was developed in order to reduce the control law and to ensure the asymptotic stability of the system [19–22]. Robust adaptive control with prescribed performance function mainly developed to force the error to start within large set and end within

pre-assigned small set [23–25]. \mathcal{L}_1 adaptive control was developed to guarantee boundedness of transient and steady state performance in the absence knowledge of system nonlinearities, uncertainties and any disturbance [26–28].

UVS control had been studied by many researchers trying to find a solution for improving the transient response and tracking trajectory. Sliding mode control for twin rotor MIMO system has been proposed in [29, 30] where fuzzy control in [29] and adaptive rule technique in [30] were used to cancel nonlinearities. Both techniques applied integral sliding mode for the vertical part with robust behavior against parameters variations and they showed great results. However, it has some intrinsic limitations due to design complexity, chattering on the sliding surface and manipulation of the controller only with strict feedback systems. Feedback linearization with sliding mode control for quadrotor has been implemented in [31] and for micro unmanned automated vehicle was studied in [32]. Limitations of feedback linearization is that the model should be in the strict feedback form and full knowledge of nonlinear model should be valid. In addition, uncertainties in model parameters should be within specific range. Backstepping control for quadrotor developed with neural nets mainly to estimate system dynamics in [33]. Chattering in the control signal and complexity of developing control law are limitations of backstepping controller. Model Predictive Control (MPC) with friction compensation for mobile robot with inverse kinematics has been proposed in [34] and the work has been validated experimentally. The main drawback of MPC is the complexity of the optimization algorithm for linear and nonlinear case which takes more time for computations.

In our work, \mathcal{L}_1 adaptive controller will be studied on different classes of systems. Fuzzy- \mathcal{L}_1 adaptive controller will be proposed to tackle problems of \mathcal{L}_1 adaptive controller in terms of robustness margin and control signal range. Recent study of neuro-adaptive control with PPF will be studied to evaluate the main role of PPF. MRAC with PPF will be proposed to tackle problems of neuro-adaptive control with PPF and \mathcal{L}_1 adaptive controller in a proper way. Robust adaptive observer will be implemented with \mathcal{L}_1 adaptive controller to examine the performance under inaccessible states. All foregoing tools will be applied on different classes of high nonlinear systems including UVS. Moreover, the nonlinearities will be assumed to be unknown with uncertainties in parameters.

2.3 \mathcal{L}_1 Adaptive Controller

\mathcal{L}_1 adaptive control was first inspired from MRAC. MRAC has been developed initially to control linear systems with uncertainty in parameters [12]. MRAC stability performance relies on Lyapunov function.

\mathcal{L}_1 adaptive controller has been built to enable fast adaption and ensuring robustness. \mathcal{L}_1 adaptive

controller ensures uniformly bounded in the transient response and steady state tracking for both regulated output and control signal owing to the low pass filter in the feedback loop. Through the use of low pass filter in the feedback loop will increase the adaptation gain, \mathcal{L}_1 adaptive control has been proposed to solve several issues that may exist in the control design. Output of the actual system will be compared to the output of the predicted system and the difference will be addressed into the projection function to help in estimating the uncertainties and disturbances. The output of the projection function will be used in building the required control signal. \mathcal{L}_1 adaptive controller design could be adopted to control linear and nonlinear systems with uncertainties in both dynamics and input parameters in the presence of disturbances.

Nonlinearities, uncertainties, disturbances and unmodelled input will be represented by compact regions and all these regions will give a complete view of system nonlinearities. The major advantage of \mathcal{L}_1 adaptive controller is that the worst scenario of all previous unexact modeling can be represented by compact regions with upper and lower bounds without accurate knowledge of nonlinearities structure. \mathcal{L}_1 adaptive controller can be defined as a robust controller for improving the transient and tracking response with appropriate assumptions of foregoing compact regions. All previous approximations have to be concerned to build approximated model allows us to build \mathcal{L}_1 adaptive controller with satisfactory performance.

\mathcal{L}_1 adaptive controller has been proposed successfully for a simple SISO system in [35]. In this work, the controller and stability analysis was mainly designed for an unstable linear system with constant uncertain parameters in the level of the states which assumed to be unknown. The output response shows a satisfactory transient and tracking performance with different values of a step input. In the following year, The work has been modified including control law and stability analysis in order to be able to deal with nonlinear time varying unknown uncertainties and disturbances for nonlinear SISO systems [36]. The output performance of shows good results for both tracking, transient response and smooth control signal. Therefore, the controller has been tested on the same nonlinear system and with higher level of time varying uncertainties. Although, the output performance showed good results similar to previous case, the control signal included chattering in contrast to the first case. Finally, the work has been formulated in the following year as a journal paper [26] considering the foregoing two cases SISO systems in [35, 36] in addition to the investigation of different feedback filter structures.

\mathcal{L}_1 adaptive control for nonlinear systems with unmatched uncertainties has been formulated in [37] for NASA AIRSTAR flight. It was designed for single flight condition and data recorded during flight test and compared to simulated output data. The comparison study showed satisfactory results and good flight control although results were not very close due to insufficient representations of nonlinearities, disturbances and unmodeled input in the control

law.

\mathcal{L}_1 adaptive controller was successfully designed for high nonlinear SISO systems [27]. The control law formulation considered nonlinear time variant for each of uncertainties, system nonlinearities and disturbances in addition to unmodeled input parameters. The controller performance has been validated on high nonlinear SISO system including nonlinearities in the input signal. The transient and tracking performance showed great results with cosine reference input. The same procedure can be applied on MIMO nonlinear systems.

\mathcal{L}_1 adaptive controller for MIMO nonlinear systems in the presence of strong coupling and unmatched uncertainties has been proposed successfully in [28]. The work in [28] approximated the system into two parts where the first was matched and the second was unmatched part. The control law was developed successfully and stability analysis ensured the robustness of the proposed controller. The output performance showed impressive results for tracking capabilities.

\mathcal{L}_1 adaptive control has been tested for different applications and specifically for flight tests in [37–42] where it shows promising results with flight applications. It has been formulated for different aspects of control problems in [43]. The structure of \mathcal{L}_1 adaptive control theory depends on three features and one of them is the implementation of a low pass filter in order to limit the frequency range of the control signal and reduce the effect of uncertainties. The low pass filter should be selected such that the system output tracks properly the reference input and the undesirable uncertainties and frequencies are filtered [35,43]. Using the low pass filter, \mathcal{L}_1 ensures decoupling between robustness, fast adaptation, infinity norm boundedness of the transient and steady state responses.

The optimal structure of filter has been studied extensively in [43] by investigating different type of structures and identifying the optimal filter coefficients. Indeed, the determination of the appropriate parameters of the best filter within a certain class of predefined structure has attracted a particular attention and several attempts on identifying these optimal coefficients have been made. This includes convex optimization based on linear matrix inequality [43,44] and multi-objective optimization using MATLAB optimization solver [45]. Limitations of \mathcal{L}_1 adaptive controller and the interconnection between adaptive estimates and the feedback filter were studied in [46], where Several filter designs were considered based on disturbance observer. More recent, Systematic approach was presented in [47] to determine the optimal feedback filter coefficients in order to increase the zone of robustness margin. The authors proposed the use of greedy randomized algorithms during the analysis of the system performance and robustness in the presence of uncertainties.

The trade-off between fast desired closed loop dynamics and filter parameters relies on error values. However, all previous studies assume constant coefficients of the feedback filter and

the effort of tuning the filter's parameters is performed off-line. Increasing the bandwidth of the low pass filter will reduce robustness margin, which will require slowing the desired closed loop performance in order to regain the robustness. However, slower selection of desired closed loop performance will deteriorate the output performance especially during the transient period [43]. We argue that increasing the robustness with fast closed loop dynamics requires dynamic on-line tuning of the feedback filter gain. The method should be practical and implementable. Therefore, in this thesis, we propose a fuzzy tuning of the filter coefficients function based on the rate and value of the tracking error between the model output and the system output.

2.4 Adaptive Control with Prescribed Performance Function

Prescribed performance is considered as convergence the tracking error into an arbitrarily small residual set and the convergence error should be within range. Prescribed performance with robust adaptive control will provide a smooth control signal for soft tracking. It comes to solve the problem of accurate computation of the upper bounds for systematic convergence owing to nonexistence adaptive control nonlinear systems for error convergence into a predefined small set.

The main function of the prescribed performance is the ability of tracking the error into a defined small set. Prescribed performance should guarantee many factors

- The convergence has to be less than a prescribed value.
- Maximum overshoot is sufficiently less than small prescribed value.
- Uniform ultimate boundedness property for the transformed output error.
- Adaptive and smooth tracking.

Several studies included in their design the use of PPF with linearly parameterized neural network as approximation model to handle unknown nonlinearities and disturbances with or without fuzzy techniques [23–25, 48–50]. PPF has been applied in different applications and showed promising results. It was first introduced with neuro-adaptive control feedback for strict MIMO systems with unknown nonlinearities; linearly parameterized neural network has been used to approximate the model [23]. Although the control law prove robust performance and track the output performance into the desired trajectory, defining radial basis neural network weights offline by try and error is considered the main drawback in [23]. In addition, values of other constant parameters are sensitive. Overall, the output performance showed great results for 2-DOF planar robot.

Robust adaptive controller with prescribed performance has been modified to deal with uncertain MIMO nonlinear systems [49]. Linearly parameterized neural network has been used to compute the control signal and avoid the need of observer from the measured output. Although output performance proves robustness and control law refers to system stability, but limitations of [23] still exist in [49]. Also, [49] mentioned another flaw that even structure of each neuron in the neural network will be defined by try and error.

SISO system with unknown nonlinearities for strict feedback systems studied in [51]. The work in [51] is mostly similar to that in [23] and the only difference was the way of developing control law. The output showed good performance and it had same limitations of [23]. Adaptive compensation control for uncertain nonlinear strict feedback systems with constrained input proposed in [52]. The control law mainly based on two adaptive backstepping controller with prescribed performance bound. Adaptive control with PPF has been proposed for nonlinear systems with unknown dead zone and in order to compensate nonlinearities and uncertainties in the system [25]. In [53], A fuzzy adaptive prescribed performance control for MIMO uncertain chaotic systems is presented. The system is in a non-strict feedback form. A proportional integral adaptation law is proposed for updating the parameters of the fuzzy logic controller.

2.5 Adaptive Observers

Adaptive observer design is an active area of research and it was studied extensively for linear time invariant SISO systems in [54, 55]. Robust observer for uncertain linear systems with solution provided by algebraic Riccati equation presented in [56]. Generally, sliding mode observers such as [57, 58] are suitable with certain model structures. Neural network has been studied widely for observer design and showed efficacy in observing system states. Radial Basis Function (RBF) in [59, 60] and Chebyshev neural network observer in [61] are designed as adaptive observers for nonlinear systems. Try and error are significant problem in adaptive Neural Network (NN) observer design in addition to the need of multi layers in certain cases. Adaptive observer design for nonlinear uncertain systems has been proposed in [62, 63]. The advantage of [63] is being effective for unmodeled dynamics in addition to the possibility of building the adaptation law of observer in the absence of control signal knowledge.

2.6 Conclusions

This chapter included overview of adaptive control research also included several research works on nonlinear systems especially UVS. The main work of research focused on \mathcal{L}_1 adaptive

controller and neuro-adaptive control with PPF. The main contribution in this work has been presented.

Chapter 3

\mathcal{L}_1 ADAPTIVE CONTROLLER

3.1 Introduction

This chapter investigates the transient and tracking performance of \mathcal{L}_1 adaptive controller on nonlinear systems with different structures. The control signal will be evaluated with respect to the foregoing features. The controller structure, stability analysis as well as simulations will be presented. The trade-off between fast closed loop dynamics and filter coefficients will be examined. The chapter consists of five sections with first section includes an introduction. The second section discusses \mathcal{L}_1 adaptive controller for uncertain SISO systems. The third section handles \mathcal{L}_1 adaptive controller for uncertain MIMO systems. The fourth section presents \mathcal{L}_1 adaptive controller for uncertain MIMO systems in the presence of strong coupling and unmatched uncertainties. Finally, we conclude in the last section.

3.2 \mathcal{L}_1 Adaptive Controller for Uncertain SISO Systems

3.2.1 Problem Formulation

Consider the following class of systems:

$$\begin{aligned}\dot{x}(t) &= A_m x(t) + B(\omega u(t) + \theta^\top x(t) + \sigma(t)) \\ y(t) &= Cx(t)\end{aligned}\tag{3.1}$$

where $x(t) \in \mathbb{R}^n$ is the system state vector (measured); $u(t) \in \mathbb{R}$ the control input; $y(t) \in \mathbb{R}$ is the system output; B and C are constant matrices (known); $A_m \in \mathbb{R}^{n \times n}$ is Hurwitz matrix (known) and refers to the desired closed-loop dynamics; $\omega \in \mathbb{R}$ is an unknown matrix with known sign; $\theta(t) \in \mathbb{R}^n$ is a vector of time-varying unknown parameters; and $\sigma(t) \in \mathbb{R}$ models

input disturbances.

Assumption 1 *(The control input is partially known with known sign) Let the upper and lower input gain bounds be defined by ω_l and ω_u respectively, where*

$$\omega \in \Omega \triangleq [\omega_l, \omega_u], \quad |\dot{\omega}| < d_\omega$$

where Ω is assumed to be known convex compact set and $0 < \omega_l < \omega_u$ are uniformly known conservative bounds.

Assumption 2 *(Unknown parameters are uniformly bounded) Let Θ, Δ_0 be known convex compact where $\Theta, \Delta_0 \in \mathbb{R}^+$ are known (conservative) bound of θ and σ where*

$$\theta(t) \in \Theta, \quad |\sigma(t)| \in \Delta_0, \quad \forall t \geq 0$$

Assumption 3 *(Partial derivatives are semiglobal uniformly bounded) Let $\theta(t)$ and $\sigma(t)$ be continuously differentiable with $\dot{\theta}$ and $\dot{\sigma}$ they are bounded by d_θ and d_σ where*

$$\|\dot{\theta}\| \leq d_\theta < \infty, \quad \|\dot{\sigma}\| \leq d_\sigma < \infty, \quad \forall t \geq 0$$

The work in this section aims at designing a full-state feedback adaptive controller to ensure that $y(t)$ tracks a given bounded piecewise-continuous reference signal $r(t)$ with quantifiable performance bounds. We will apply the controller on many case studies to evaluate the output performance in terms of transient and tracking response and the control signal in terms of smoothness and boundedness.

3.2.2 \mathcal{L}_1 Adaptive Control Architecture

State predictor: We consider the following state predictor:

$$\begin{aligned} \dot{\hat{x}}(t) &= A_m \hat{x}(t) + B(\hat{\omega}u(t) + \hat{\theta}^\top x(t) + \hat{\sigma}) \\ \hat{y}(t) &= C\hat{x}(t) \end{aligned} \tag{3.2}$$

The state predictor has the same structure as defined in (3.1) except that the unknown

parameters ω , $\theta(t)$, and $\sigma(t)$ are being replaced by their adaptive estimates $\hat{\omega}$, $\hat{\theta}(t)$ and $\hat{\sigma}(t)$.

$$\begin{aligned}\dot{\hat{\omega}} &= \Gamma \text{Proj}(\hat{\omega}, -\tilde{x}^\top P b u(t)), \quad \hat{\omega}(0) = \hat{\omega}_0 \\ \dot{\hat{\theta}} &= \Gamma \text{Proj}(\hat{\theta}, -\tilde{x}^\top P b x(t)) \quad \hat{\theta}(0) = \hat{\theta}_0 \\ \dot{\hat{\sigma}} &= \Gamma \text{Proj}(\hat{\sigma}, -\tilde{x}^\top P b) \quad \hat{\sigma}(0) = \hat{\sigma}_0\end{aligned}\tag{3.3}$$

where $\tilde{x} \triangleq \hat{x} - x(t)$, $\Gamma \in \mathbb{R}^+$ is the adaptation gain, and $P = P^\top > 0$ is defined by solving the algebraic Lyapunov equation $A_m^\top P + P A_m = -Q$ for arbitrary symmetric $Q = Q^\top > 0$. The projection operator ensures that $\hat{\omega} \in \Omega_0 \triangleq [\omega_l, \omega_u]$, $\hat{\theta} \in \Theta \triangleq [-\theta_b, \theta_b]$, $|\hat{\sigma}| \leq \Delta_0$, while Ω_0 and Δ_0 are being replaced by Ω and Δ to satisfy

$$\Omega_0 < \Omega, \quad \Delta_0 < \Delta,$$

Control Law: Control signal can be calculated as follows

$$u(s) = -kD(s)(\hat{\eta}(s) - k_g r(s))\tag{3.4}$$

where $r(s)$ and $\hat{\eta}(s)$ are the Laplace transforms of $r(t)$ and $\hat{\eta}(t) = \hat{\omega}u(t) + \hat{\theta}x(t) + \hat{\sigma}$ respectively; and the necessary feedforward gain in order to get unity steady state may be calculated by $k_g \triangleq -1/(CA_m^{-1}B)$; Both of the feedback gain $k > 0$ and a strictly proper transfer function $D(s)$ will lead to a strictly proper stable closed loop system.

$$C(s) \triangleq \frac{\omega k D(s)}{1 + \omega k D(s)}, \quad \forall \omega \in \Omega_0\tag{3.5}$$

with DC gain $C(0) = 1$. One simple choice is $D(s) = 1/s$, which yields a first-order strictly proper $C(s)$ of the form

$$C(s) \triangleq \frac{\omega k}{s + \omega k}$$

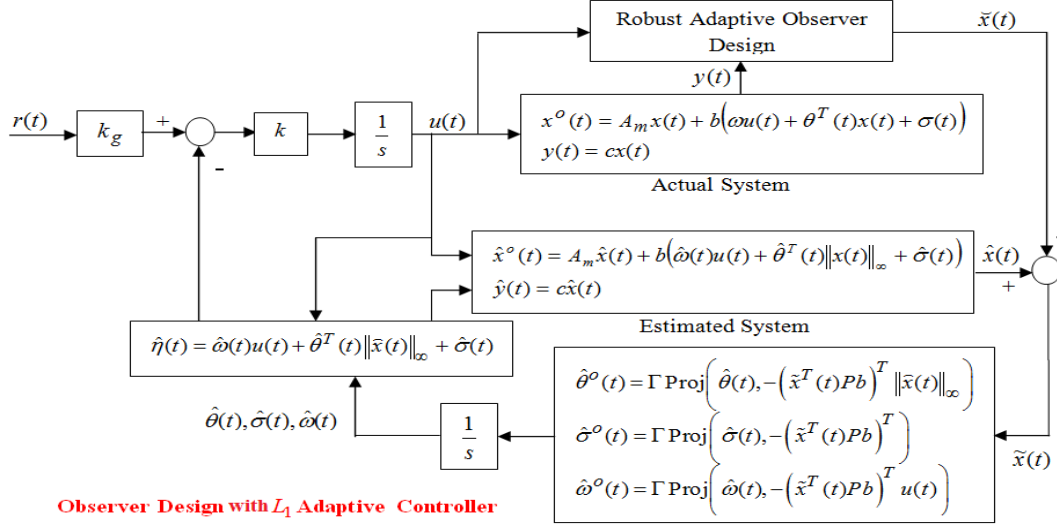
Let

$$L \triangleq \max_{\theta \in \Theta} \|\theta(t)\|_{\mathcal{L}_1}, \quad H(s) = (sI - A_m)^{-1}b, \quad G(s) \triangleq H(s)(1 - C(s))\tag{3.6}$$

Then the \mathcal{L}_1 norm of \mathcal{L}_1 adaptive controller will be

$$\|G(s)\|_{\mathcal{L}_1} L \leq 1$$

Figure 3.1 shows the structure of closed loop \mathcal{L}_1 adaptive controller for uncertain SISO systems.

Figure 3.1: Closed loop \mathcal{L}_1 adaptive control system.

3.2.3 \mathcal{L}_1 Adaptive Control Stability Analysis

Transient and Steady-State Performance: The error dynamics between system dynamics in (3.1) and state predictor in (3.2) can be written as

$$\dot{\tilde{x}}(t) = A_m \tilde{x}(t) + b(\tilde{\omega}u(t) + \tilde{\theta}^T x(t) + \tilde{\sigma}(t)) = A_m \tilde{x}(t) + b\tilde{\eta}(t) \quad (3.7)$$

Where $\tilde{x} = \hat{x} - x$, $\tilde{\theta} = \hat{\theta} - \theta$, $\tilde{\omega} = \hat{\omega} - \omega$ and $\tilde{\sigma} = \hat{\sigma} - \sigma$. The nonlinear part is $\tilde{\eta}(t)$ and its Laplace transform $\tilde{\eta}(s)$ where $\tilde{\eta}(t) \triangleq \tilde{\omega}u(t) + \tilde{\theta}^T x(t) + \tilde{\sigma}(t)$. The Laplace transform of the error dynamics in (3.7) can be rewritten as

$$\tilde{x}(t) = (sI - A_m)^{-1} B \tilde{\eta}(s) = H(s) \tilde{\eta}(s) \quad (3.8)$$

Lemma 1 *The prediction error $\tilde{x}(t)$ is uniformly bounded,*

$$\|\tilde{x}\|_\infty \leq \sqrt{\frac{\theta_m}{\lambda_{\min}(P)\Gamma}} \quad (3.9)$$

where

$$\theta_m \triangleq \max_{\theta \in \Theta} \|\theta\|^2 + 4\Delta^2 + (\omega_l - \omega_u)^2 + 4 \frac{\lambda_{\max}(P)}{\lambda_{\min}(Q)} (d_\theta \max_{\theta \in \Theta} \|\theta\| + d_\sigma \Delta) \quad (3.10)$$

which will be verified as follows.

Stability proof: Consider the Lyapunov function candidate

$$V(\tilde{x}, \tilde{\theta}, \tilde{\omega}, \tilde{\sigma}) = \tilde{x}^T P \tilde{x} + \frac{1}{\Gamma} (\tilde{\theta}^T \tilde{\theta} + \tilde{\omega}^T \tilde{\omega} + \tilde{\sigma}^T \tilde{\sigma}) \quad (3.11)$$

Since $\hat{x}(0) = x(0)$ then we can verify that

$$\begin{aligned}
 V(0) &\leq \max_{\theta \in \Theta} \|\theta\|^2 + 4\Delta^2 + (\omega_l - \omega_u)^2 \leq \frac{\theta_m}{\Gamma} \\
 \dot{V} &\leq \tilde{x}^\top P \dot{\tilde{x}} + \dot{\tilde{x}}^\top P \tilde{x} + \frac{1}{\Gamma} (\tilde{\theta}^\top \dot{\tilde{\theta}} + \dot{\tilde{\theta}}^\top \tilde{\theta} + \tilde{\sigma}^\top \dot{\tilde{\sigma}} + \dot{\tilde{\sigma}}^\top \tilde{\sigma} + \tilde{\omega}^\top \dot{\tilde{\omega}} + \\
 &\quad \dot{\tilde{\omega}}^\top \tilde{\omega} - \tilde{\theta}^\top \dot{\tilde{\theta}} - \dot{\tilde{\theta}}^\top \tilde{\theta} - \tilde{\sigma}^\top \dot{\tilde{\sigma}} - \dot{\tilde{\sigma}}^\top \tilde{\sigma}) \\
 \dot{V} &\leq \tilde{x}^\top Q \tilde{x} + \frac{2}{\Gamma} (\dot{\tilde{\theta}} + \tilde{x}^\top P B x) + \frac{2}{\Gamma} (\dot{\tilde{\sigma}} + \tilde{x}^\top P B) + \frac{2}{\Gamma} (\dot{\tilde{\omega}} + \tilde{x}^\top P B u) \\
 &\quad - \frac{2}{\Gamma} (\tilde{\theta}^\top \dot{\tilde{\theta}} + \tilde{\sigma}^\top \dot{\tilde{\sigma}}) \\
 \dot{V} &\leq -\tilde{x}^\top Q \tilde{x} + \frac{2}{\Gamma} (|\dot{\tilde{\theta}}| + |\dot{\tilde{\sigma}}|)
 \end{aligned} \tag{3.12}$$

As mentioned in Assumption 1, 2 and 3, the projection operator ensures that $\theta(t) \in \Theta$, $|\sigma(t)| \in \Delta$ for all $t \geq 0$, and therefore, the upper bounds in assumption 2 lead to the following upper bound:

$$\tilde{\theta}^\top \dot{\tilde{\theta}} + \tilde{\sigma}^\top \dot{\tilde{\sigma}} \leq 2(d_\theta \max_{\theta \in \Theta} \|\theta\| + d_\sigma \Delta) \tag{3.13}$$

Moreover, the projection operator also ensures that

$$\max_{t \geq 0} \left(\frac{1}{\Gamma} (\tilde{\theta}^\top \tilde{\theta} + \tilde{\omega}^\top \tilde{\omega} + \tilde{\sigma}^\top \tilde{\sigma}) \right) \leq \frac{1}{\Gamma} (\max_{\theta \in \Theta} \|\theta\|^2 + 4\Delta^2 + (\omega_l - \omega_u)^2) \tag{3.14}$$

which holds for all $t \geq 0$. If at any time $t_1 > 0$, one has $V(t_1) \geq \theta_m/\Gamma$, then it follows from (3.10) and (3.11) that

$$\tilde{x}^\top(t_1) P \tilde{x}(t_1) > 4 \frac{\lambda_{\max}(P)}{\lambda_{\min}(Q)} (d_\theta \max_{\theta \in \Theta} \|\theta\| + d_\sigma \Delta) \tag{3.15}$$

and thus

$$\tilde{x}(t_1)^\top Q \tilde{x}(t_1) \geq \tilde{x}^\top(t_1) P \tilde{x}(t_1) > \frac{4}{\Gamma} (d_\theta \max_{\theta \in \Theta} \|\theta\| + d_\sigma \Delta) \tag{3.16}$$

Hence, if $V(t_1) \geq \theta_m/\Gamma$, then from (3.12) and (3.16) we have

$$\dot{V} \leq 0 \tag{3.17}$$

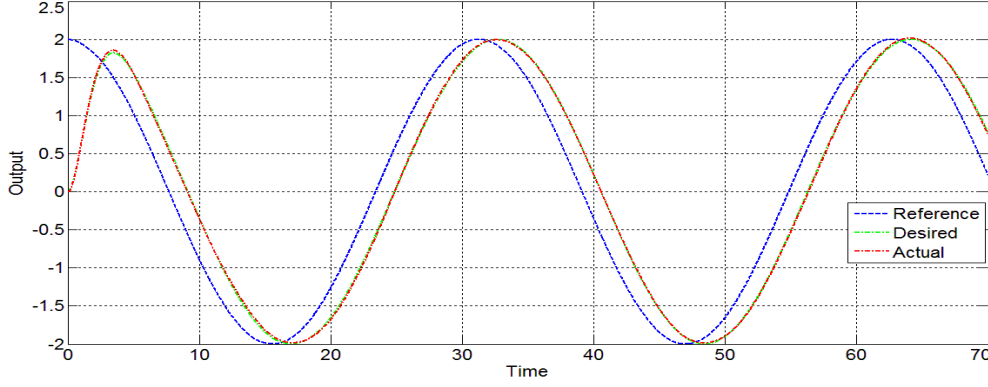


Figure 3.2: The output performance of \mathcal{L}_1 adaptive controller for unknown nonlinear SISO system.

3.2.4 Problem Formulation and Simulation

Example 3.2.1 Consider the following unknown nonlinear system [27]

$$\begin{aligned}\dot{x}(t) &= A_m x(t) + b(\omega u(t) + f(x(t), u(t), t)) \\ y(t) &= cx(t)\end{aligned}$$

where $x(t) = [x_1(t), x_2(t)]^\top$ are the system states, $u(t)$ is the system control input, $f(x(t), u(t), t)$ is assumed to be unknown nonlinear function, $y(t)$ is the output of the system and the system parameters are presented as following

$$A_m = \begin{bmatrix} 0 & 1 \\ -1 & -1.4 \end{bmatrix}, \quad b = \begin{bmatrix} 0 \\ 1 \end{bmatrix}, \quad c = \begin{bmatrix} 1 & 0 \end{bmatrix}$$

$$\begin{aligned}f(x(t), u(t), t) &= x_1(t) + 1.4x_2(t) + (2 + 0.2\sin(t))u(t) + \sin(u(t))\sin(x_1(t)) \\ &\quad + x_1^2(t) + x_2^2(t) + \sin(0.5t)\end{aligned}$$

Parameters of \mathcal{L}_1 can be computed numerically and they are chosen to be $\omega_l = 0.5$, $\omega_u = 3$, $\theta_b = 10$, $\sigma_b = 10$ and the adaptation gain $\Gamma = 100000$. \mathcal{L}_1 adaptive control parameters are defined as $Q = \begin{pmatrix} 1 & 0 \\ 0 & 1 \end{pmatrix}$, $k = 20$, hence $P = \begin{pmatrix} 1.4144 & 0.5001 \\ 0.5001 & 0.7144 \end{pmatrix}$. Figure (3.2) and (3.3) are the output response and control signal respectively with reference input $r(t) = 2\cos(0.2t)$ while figure (3.4) and (3.5) are the output response and control signal respectively with 0.23Hz square wave reference input for the same problem

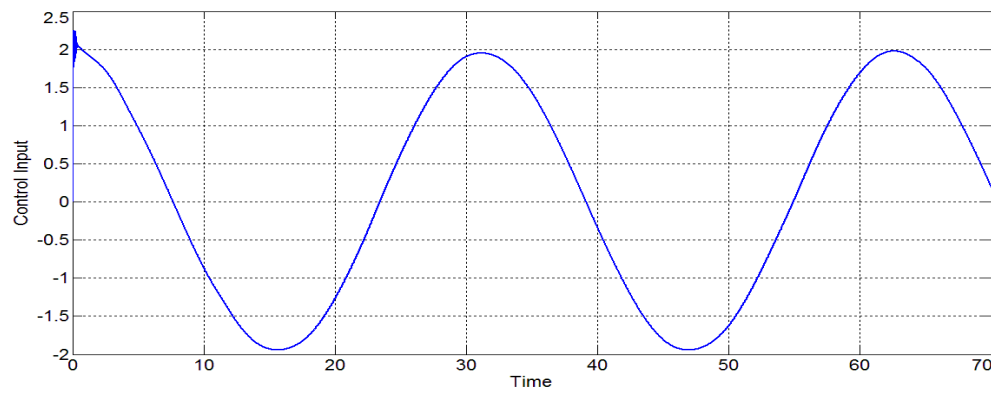


Figure 3.3: Control signal of \mathcal{L}_1 Adaptive controller for unknown nonlinear SISO system.

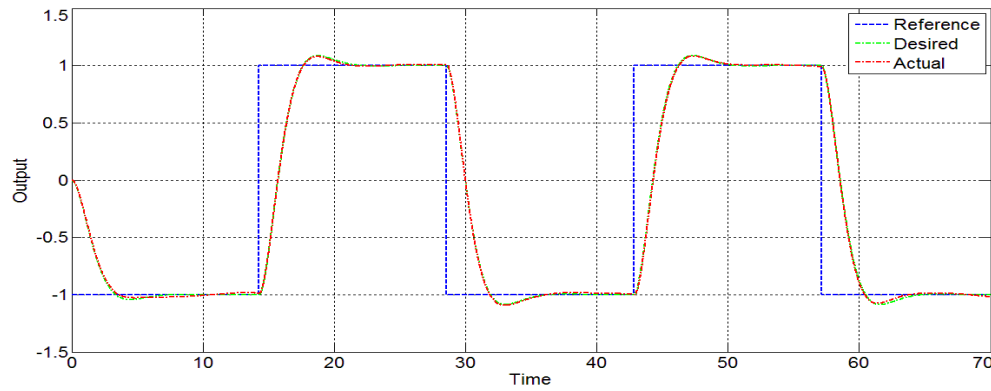


Figure 3.4: The output performance of \mathcal{L}_1 adaptive controller for unknown nonlinear SISO system.

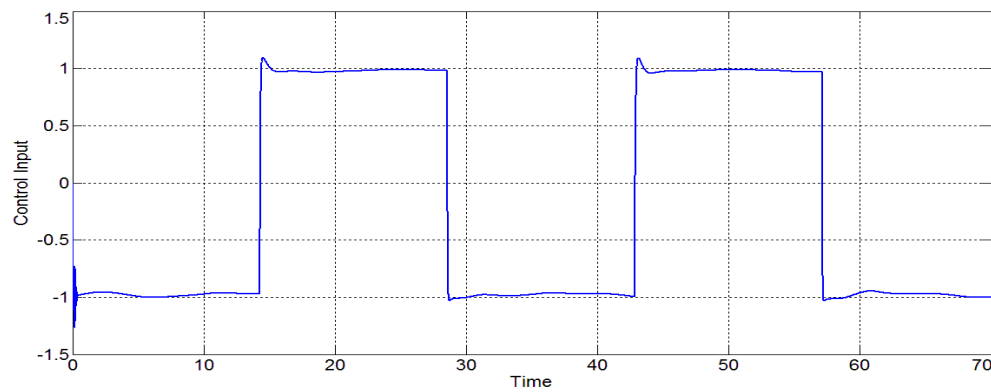


Figure 3.5: Control signal of \mathcal{L}_1 Adaptive controller for unknown nonlinear SISO system.

3.3 \mathcal{L}_1 Adaptive Controller for Uncertain MIMO Systems

3.3.1 Problem Formulation

Consider in the following class of systems:

$$\begin{aligned}\dot{x}(t) &= A_m x(t) + B(\omega u(t) + f(x(t), t)) \\ y(t) &= Cx(t)\end{aligned}\tag{3.18}$$

where $x(t) \in \mathbb{R}^n$ is the system state vector (measured); $u(t) \in \mathbb{R}^m$ the control input; $y(t) \in \mathbb{R}^m$ is the system output; $b \in \mathbb{R}^{n \times m}$ and $C \in \mathbb{R}^{m \times n}$ are constant matrices (known); $A_m \in \mathbb{R}^{n \times n}$ is Hurwitz matrix (known) and refers to the desired closed-loop dynamics; $\omega \in \mathbb{R}^{m \times m}$ is an unknown constant matrix with known sign; $f(x(t), t)$ is an unknown nonlinearity.

Assumption 4 (*Uniform boundedness of $f(0, t)$*) Let $B > 0$ such that $f(0, t) \leq B_l$ for all $t \geq 0$

Assumption 5 (*Partial derivatives are semiglobal uniformly bounded*) For any $\delta > 0$, there exist $d_{f_x}(\delta) > 0$ and $d_{f_t}(\delta) > 0$ such that for arbitrary $\|x\|_\infty \leq \delta$ and any u , the partial derivatives of $f(x(t), t)$ is piecewise-continuous and bounded,

$$\left\| \frac{\partial f(x(t), t)}{\partial x} \right\| \leq d_{f_x}(\delta), \quad \left\| \frac{\partial f(x(t), t)}{\partial t} \right\| \leq d_{f_t}(\delta)$$

Assumption 6 (*Asymptotically stable of initial conditions*) The system is assumed to start initially with x_0 inside an arbitrarily known set ρ_0 i.e., $\|x_0\|_\infty \leq \rho_0 < \infty$.

Assumption 7 (*The control inputs are partially known with known sign*) Let upper and lower input gain bounds are defined by ω_l and ω_u respectively, where

$$\omega \in \Omega \triangleq [\omega_l, \omega_u], \quad |\dot{\omega}| < \omega$$

3.3.2 \mathcal{L}_1 Adaptive Control Architecture

State Predictor: We consider the following state predictor:

$$\begin{aligned}\dot{\hat{x}}(t) &= A_m \hat{x}(t) + b(\hat{\omega} u(t) + \hat{\theta} \|x(t)\|_\infty + \hat{\sigma}) \\ \hat{y}(t) &= c \hat{x}(t)\end{aligned}\tag{3.19}$$

The system in (3.18) can be defined as

$$\begin{aligned}\dot{\hat{x}}(t) &= A_m x(t) + b(\omega u(t) + \theta \|x(t)\|_\infty + \sigma) \\ \hat{y}(t) &= c\hat{x}(t)\end{aligned}\tag{3.20}$$

which is similar to (3.19) except that the unknown parameters ω , $\theta(t)$, and $\sigma(t)$ are being replaced by their adaptive estimates $\hat{\omega}(t)$, $\hat{\theta}(t)$ and $\hat{\sigma}(t)$.

$$\begin{aligned}\dot{\hat{\omega}} &= \Gamma \text{Proj}(\hat{\omega}, -\tilde{x}^\top P b u(t)), \quad \hat{\omega}(0) = \hat{\omega}_0 \\ \dot{\hat{\theta}} &= \Gamma \text{Proj}(\hat{\theta}, -\tilde{x}^\top P b x(t)) \quad \hat{\theta}(0) = \hat{\theta}_0 \\ \dot{\hat{\sigma}} &= \Gamma \text{Proj}(\hat{\sigma}, -\tilde{x}^\top P b) \quad \hat{\sigma}(0) = \hat{\sigma}_0\end{aligned}\tag{3.21}$$

where $\tilde{x} \triangleq \hat{x} - x(t)$, $\Gamma \in \mathbb{R}^+$ is the adaptation gain, and $P = P^\top > 0$ is defined by solving the algebraic Lyapunov equation $A_m^\top P + P A_m = -Q$ for arbitrary symmetric $Q = Q^\top > 0$. The projection operator ensures that $\hat{\omega} \in \Omega_0 \triangleq [\omega_l, \omega_u]$, $\hat{\theta} \in \Theta \triangleq [-\theta_b, \theta_b]$, $|\hat{\sigma}| \leq \Delta_0$, while Ω_0 and Δ_0 are being replaced by Ω and Δ to satisfy

$$\Omega_0 \subset \Omega, \quad \Delta_0 \subset \Delta,$$

Control Law: Control signal can be calculated as following

$$u(s) = -kD(s)(\hat{\eta}(s) - k_g r(s))\tag{3.22}$$

where $r(s)$ and $\hat{\eta}(s)$ are the Laplace transforms of $r(t)$ and $\hat{\eta}(t) = \hat{\omega}u(t) + \hat{\theta}x(t) + \hat{\sigma}$ respectively; and the necessary feedforward gain in order to get unity steady state is calculated by $k_g \triangleq -1/(CA_m^{-1}B)$; $k > 0$ is a feedback gain and $D(s)$ is a strictly proper transfer function such that both of them lead to a strictly proper stable closed loop system.

$$C(s) \triangleq \frac{\omega k D(s)}{1 + \omega k D(s)}, \quad \forall \omega \in \Omega_0\tag{3.23}$$

with DC gain $C(0) = 1$. One simple choice is $D(s) = 1/s$, which yields a first-order strictly proper $C(s)$ of the form

$$C(s) \triangleq \frac{\omega k}{s + \omega k}$$

Let

$$L \triangleq \max_{\theta \in \Theta} \|\theta(t)\|_{\mathcal{L}_1}, \quad H(s) = (sI - A_m)^{-1}b, \quad G(s) \triangleq H(s)(1 - C(s))\tag{3.24}$$

Then the \mathcal{L}_1 norm of \mathcal{L}_1 adaptive controller will be

$$\|G(s)\|_{\mathcal{L}_1} L \leq 1$$

Now, for a given ρ_0 as in assumption 6, k and $D(s)$ should be chosen such that there exist $\rho_r > \rho_{in}$ such that the following \mathcal{L}_1 norm condition verified

$$\|G(s)\|_{\mathcal{L}_1} < \frac{\rho_r - \|H(s)C(s)k_g\|_{\mathcal{L}_1}\|r\|_{\mathcal{L}_\infty} - \rho_{in}}{L_{\rho_r}\rho_r + B} \quad (3.25)$$

let

$$\gamma_1 \triangleq \frac{\|C(s)\|_{\mathcal{L}_1}}{1 - \|C(s)\|_{\mathcal{L}_1} L_{\rho_r}} \gamma_0 + \beta \quad (3.26)$$

where γ_0 and β are arbitrarily small positive constants.

let

$$\rho_u \triangleq \rho_{ur} + \gamma_2 \quad (3.27)$$

where ρ_{ur} and γ_2 are defined as following

$$\rho_{ur} \triangleq \|\omega^{-1}C(s)\|_{\mathcal{L}_1} (\|k_g\|_{\mathcal{L}_1}\|r\|_{\mathcal{L}_\infty} + L_{\rho_r}\rho_r + B) \quad (3.28)$$

$$\gamma_2 \triangleq \|\omega^{-1}C(s)\|_{\mathcal{L}_1} L_{\rho_r} \gamma_1 + \|\omega^{-1}C(s)(c_0^\top H(s))^{-1}c_0^\top\|_{\mathcal{L}_1} \gamma_0 \quad (3.29)$$

and finally let

$$\theta_b \triangleq d_{f_x}(\delta), \quad \Delta \triangleq B + \epsilon \quad (3.30)$$

where ϵ is an arbitrary positive constant.

3.3.3 \mathcal{L}_1 Adaptive Control Stability Analysis

Transient and Steady-State Performance: The error dynamics between system dynamics in (3.20) and state predictor in (3.19) can be written as

$$\dot{\tilde{x}}(t) = A_m \tilde{x}(t) + b(\tilde{\omega}u(t) + \tilde{\theta}\|x(t)\|_\infty + \tilde{\sigma}(t)) = A_m \tilde{x}(t) + b\tilde{\eta}(t) \quad (3.31)$$

Where $\tilde{x} = \hat{x} - x$, $\tilde{\theta} = \hat{\theta} - \theta$, $\tilde{\omega} = \hat{\omega} - \omega$ and $\tilde{\sigma} = \hat{\sigma} - \sigma$. The nonlinear part is $\tilde{\eta}(t)$ and its Laplace transform $\tilde{\eta}(s)$ where $\tilde{\eta}(t) \triangleq \tilde{\omega}u(t) + \tilde{\theta}^\top x(t) + \tilde{\sigma}(t)$. The Laplace transform of the error dynamics in (3.7) can be rewritten as

$$\tilde{x}(t) = (sI - A_m)^{-1} B \tilde{\eta}(s) = H(s) \tilde{\eta}(s) \quad (3.32)$$

Assume

$$\|x(t)\|_\infty \leq \rho \quad (3.33)$$

$$\|u(t)\|_\infty \leq \rho_u \quad (3.34)$$

Lemma 2 *The prediction error $\tilde{x}(t)$ is uniformly bounded,*

from Lemma 2 and equations 3.33 and 3.34, the derivatives of ω , θ and σ are bounded:

$$|\dot{\omega}| \leq d_\omega < \infty \quad (3.35)$$

$$|\dot{\theta}| \leq d_\theta < \infty \quad (3.36)$$

$$|\dot{\sigma}| \leq d_\sigma < \infty \quad (3.37)$$

Then we have

$$\|\tilde{x}\|_\infty \leq \sqrt{\frac{\theta_m}{\lambda_{\min}(P)\Gamma}} \quad (3.38)$$

where

$$\theta_m \triangleq 4\left(\theta_b^2 m + \Delta^2 m + \max_{\omega \in \Omega} \text{tr}(\omega^\top \omega) + m \frac{\lambda_{\max}(P)}{\lambda_{\min}(Q)} (d_\theta \max_{\theta \in \Theta} \|\theta\| + d_\sigma \Delta)\right) \quad (3.39)$$

which will be verified as follows **Stability proof:** Consider the Lyapunov function candidate

$$V(\tilde{x}, \tilde{\theta}, \tilde{\omega}, \tilde{\sigma}) = \tilde{x}^\top P \tilde{x} + \frac{1}{\Gamma} (\tilde{\theta}^\top \tilde{\theta} + \text{tr}(\tilde{\omega}^\top \tilde{\omega}) + \tilde{\sigma}^\top \tilde{\sigma}) \quad (3.40)$$

Since $\hat{x}(0) = x(0)$ then we can verify that

$$V(0) \leq \frac{4}{\Gamma} (\theta_b^2 m + \Delta^2 m + \max_{\omega \in \Omega} \text{tr}(\omega^\top \omega)) \leq \frac{\theta_m}{\Gamma}$$

$$\begin{aligned} \dot{V} &\leq \tilde{x}^\top Q \tilde{x} + \frac{2}{\Gamma} (\dot{\hat{\theta}} + \tilde{x}^\top P B \|x\|_\infty) + \frac{2}{\Gamma} (\dot{\hat{\sigma}} + \tilde{x}^\top P B) + \frac{2}{\Gamma} (\dot{\hat{\omega}} + \tilde{x}^\top P B u) \\ &\quad - \frac{2}{\Gamma} (\tilde{\theta}^\top \dot{\hat{\theta}} + \tilde{\sigma}^\top \dot{\hat{\sigma}}) \end{aligned}$$

$$\dot{V} = -\tilde{x}^\top Q \tilde{x} + \frac{2}{\Gamma} (|\dot{\hat{\theta}} \tilde{\theta}| + |\dot{\hat{\sigma}} \tilde{\sigma}|) \quad (3.41)$$

$$\dot{V} \leq -\tilde{x}^\top Q \tilde{x} + \frac{4}{\Gamma} (d_\theta \theta_b + d_\sigma \Delta) \quad (3.42)$$

As mentioned in Assumption 4, 5, 6 and 7, the projection operator ensures that $\theta(t) \in \Theta$, $|\sigma(t)| \in \Delta$ for all $t \geq 0$, and therefore, the upper bound in assumption 7 lead to the following

upper bound:

$$\tilde{\theta}^\top \dot{\theta} + \tilde{\sigma}^\top \dot{\sigma} \leq d_\theta \theta_b + d_\sigma \Delta \quad (3.43)$$

Moreover, the projection operator ensures that

$$\max_{t \geq 0} \left(\frac{1}{\Gamma} (\tilde{\theta}^\top \tilde{\theta} + \text{tr}(\tilde{\omega}^\top \tilde{\omega}) + \tilde{\sigma}^\top \tilde{\sigma}) \right) \leq \frac{1}{\Gamma} (\theta_b^2 m + \Delta^2 m + \max_{\omega \in \Omega} \text{tr}(\omega^\top \omega)) \quad (3.44)$$

which holds for all $t \geq 0$. If at any time $t_1 > 0$, one has $V(t_1) \geq \theta_m/\Gamma$, then from (3.39) and (3.40), one has

$$\tilde{x}^\top(t_1) P \tilde{x}(t_1) > 4 \frac{\lambda_{\max}(P)}{\lambda_{\min}(Q)} (d_\theta \theta_b + d_\sigma \Delta) \quad (3.45)$$

and thus

$$\tilde{x}(t_1)^\top Q \tilde{x}(t_1) \geq \frac{\lambda_{\min}(Q)}{\lambda_{\max}(P)} \tilde{x}^\top(t_1) P \tilde{x}(t_1) > \frac{4}{\Gamma} \frac{\lambda_{\max}(P)}{\lambda_{\min}(Q)} (d_\theta \theta_b + d_\sigma \Delta) \quad (3.46)$$

Hence, if $V(t_1) \geq \theta_m/\Gamma$, then from (3.42) and (3.46),

$$\dot{V} \leq 0 \quad (3.47)$$

3.3.4 Problem Formulation and Simulation

Example 3.3.1 Simulation Problem of Two Link Planar Robot [23]

$$M(q)\ddot{q} + C(\dot{q}, q)\dot{q} + G_0(q) = \tau$$

where $q = [q_1 \ q_2]^\top$ are the angular position and $\tau = [\tau_1 \ \tau_2]^\top$ are representing the applied torques.

The inertia matrix is represented by

$$M(q) = \begin{bmatrix} M_{11} & M_{12} \\ M_{21} & M_{22} \end{bmatrix}$$

with

$$M_{11} = I_{z_1} + I_{z_2} + \frac{m_1 l_1^2}{2} + m_2 (l_1^2 + \frac{l_2^2}{4} + l_1 l_2 c_2)$$

$$M_{12} = M_{21} = I_{z_2} + m_2 (\frac{l_2^2}{4} + \frac{1}{2} l_1 l_2 c_2)$$

$$M_{22} = I_{z_2} + m_2 \frac{l_2^2}{4}$$

$C(\dot{q}, q)$ is the Coriolis and centrifugal torques matrix, \dot{q} is angular speed and $C(\dot{q}, q)\dot{q}$ is actuator

joint friction forces where

$$C(\dot{q}, q)\dot{q} = \begin{bmatrix} cq_2 + k_1 & -c(q_1 + q_2) \\ cq_1 & k_2 \end{bmatrix} \begin{bmatrix} \dot{q}_1 \\ \dot{q}_2 \end{bmatrix}$$

with $c = \frac{1}{2}m_2l_1l_2s_2$. and $G_0(q)$ is the vector of gravitational torques

$$G_0(q) = \begin{bmatrix} \frac{1}{2}m_1gl_1c_1 + m_2g(l_1c_1 + \frac{1}{2}l_2c_{12}) \\ \frac{1}{2}m_2gl_2c_{12} \end{bmatrix}$$

with $c1 = \cos(q_1)$, $c12 = \cos(q_1 + q_2)$, $s1 = \sin(q_1)$ and $c2 = \cos(q_2)$. Table (3.1) and (3.2) defines the necessary symbols, description and their associated values.

Table 3.1: Description of symbols and their units

Symbol	Description	Unit
q_i	Angular position of joint- i	rad
\dot{q}_i	Angular velocity of joint- i	rad/sec
τ_i	Applied torque at joint- i	N/m
m_i	Mass of link- i	kg
l_i	Length of link- i	m
I_{Z_i}	Moment Inertia of link- i	$kg.m^2$
k_i	Friction coefficient of joint- i	$kg.m^2/s$
g	Gravity acceleration	m/s^2

Table 3.2: System parameters

m_1	l_1	I_{Z_1}	k_1	m_2	l_2	I_{Z_2}	k_2	g
3.2	0.5	0.96	1	2.0	0.4	0.841	1	9.81

The equation of motion of the nonlinear plant can be represented as following

$$\ddot{q} = -M^{-1}(q)(C(\dot{q}, q)\dot{q} + G_0(q)) + M^{-1}(q)\tau$$

Case 1: Parameters of \mathcal{L}_1 can be computed numerically where their bounds were chosen to be $\omega_l = 0.5$, $\omega_u = 10$, $\theta_b = 100$, $\sigma_b = 10$ and the adaptation gain $\Gamma = 100000$. Assuming the desired poles are $-300 \pm j5$ and $-400 \pm j5$. The feedback controller was set to be $30diag(4)$. The

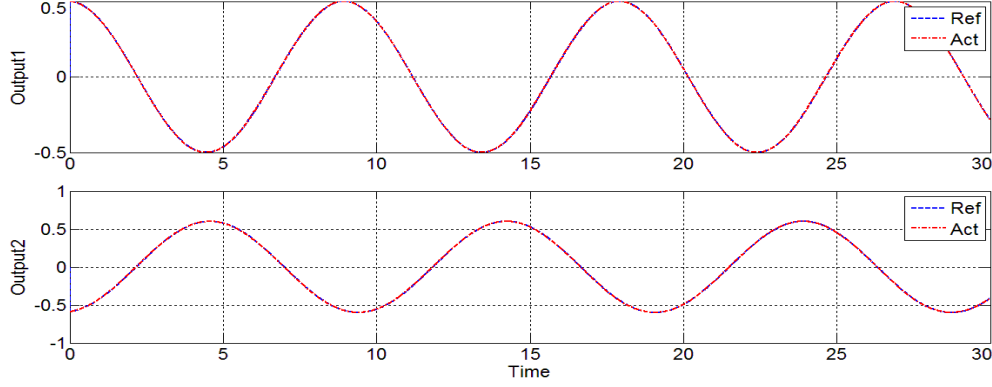


Figure 3.6: \mathcal{L}_1 adaptive control of two link planar robot with reference and actual tracking

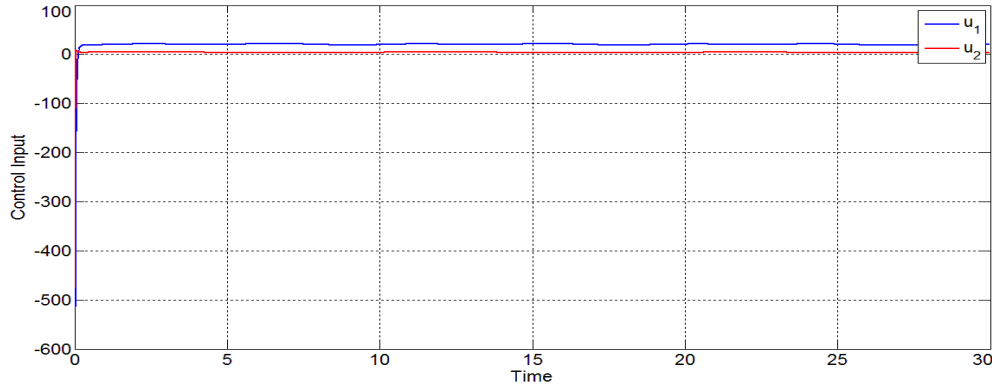


Figure 3.7: Control signal of \mathcal{L}_1 adaptive control for two link planar robot

simulated response will be demonstrated in figure (3.6) and (3.7) for \mathcal{L}_1 output performance and control signal respectively.

Case 2: Figure 3.8 and 3.9 present the outputs of \mathcal{L}_1 adaptive control and control signals respectively considering same assumptions as in case 1 except setting desired poles $-30 \pm j0.5$ and $-40 \pm j0.5$ in order to investigate the relation between fast and slow desired dynamics with respect to the control signal and tracking performance.

Figures (3.6), (3.7), (3.8) and (3.9) describe the relation between robustness and fast tracking response from one hand and control signal range from the other hand. Increasing the speed of transient and tracking performance has a direct relation with how far the desired poles can be located in the left hand side from the origin of $(\sigma - j\omega)$ axis. However, it reduces the robustness of the zone wish demand reducing the feedback gain value. On the other hand, the narrow range of control signal has adverse relation with transient speed.

Example 3.3.2 Simulation Problem of Quadrotor

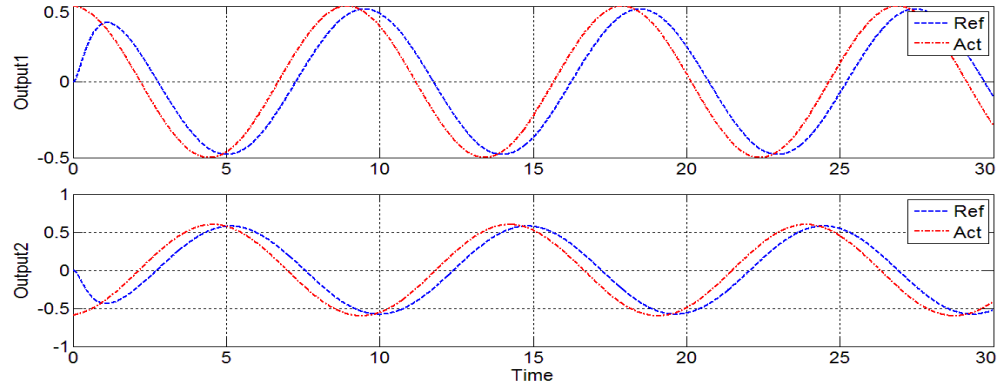


Figure 3.8: \mathcal{L}_1 adaptive control of two link planar robot with reference and actual tracking

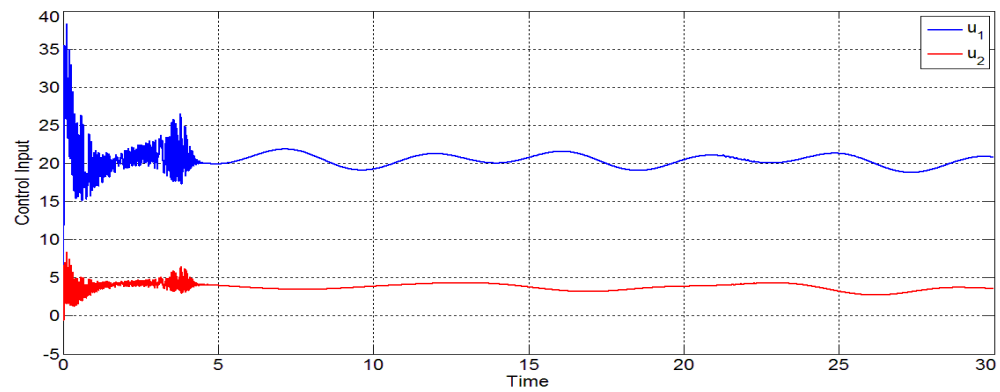


Figure 3.9: Control signal of \mathcal{L}_1 adaptive control for two link planar robot

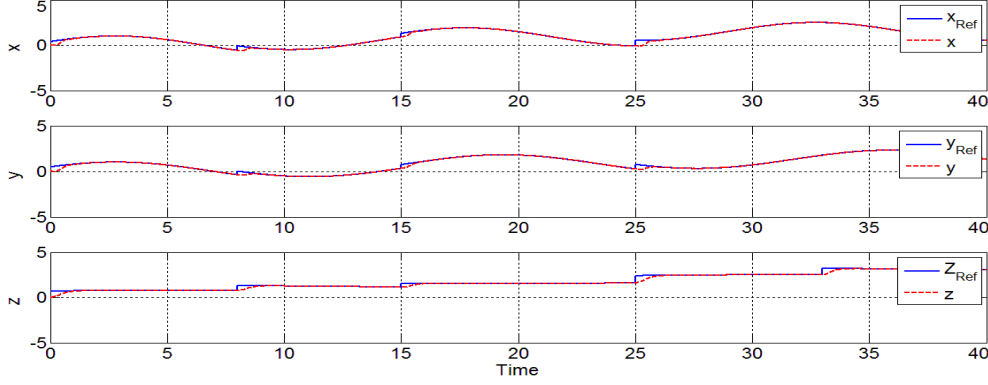


Figure 3.10: \mathcal{L}_1 adaptive controller with reference and actual tracking positions for quadrotor.

Consider the quadrotor model in [33] with model parameters presented in [64]

$$\begin{aligned}\ddot{\eta}_1 &= \frac{1}{m}R(\eta_2)\begin{bmatrix} 0 & 0 & \tau_z \end{bmatrix}^\top - g\begin{bmatrix} 0 & 0 & 1 \end{bmatrix}^\top \\ \ddot{\eta}_2 &= f(\eta_2) + G(\eta_2)\begin{bmatrix} \tau_p & \tau_q & \tau_r \end{bmatrix}^\top\end{aligned}$$

Where R is the Euler transformation angle matrix, η_2 is the Euler angles, $f(\eta_2) \in \mathbb{R}^{3 \times 1}$ is the nonlinear function and $G(\eta_2) \in \mathbb{R}^{3 \times 3}$ is the inverse of the inertia matrix.

Case 1: We assume exact modeling and system with free disturbances where projection bounds of adaptation laws were defined numerically. Parameters of \mathcal{L}_1 can be computed numerically where their bounds were chosen such as $\omega_l = 0.5$, $\omega_u = 10$, $\theta_b = 100$, $\sigma_b = 100$ and the adaptation gain $\Gamma = 100000$. The control input is constrained to $\tau_z = 15$ while other control signals are set free. The desired poles were set to $-30 \pm j0.5$, $-35 \pm j0.5$ and $-40 \pm j0.5$ and the feedback gain were set to $\text{diag}(30, 30, 30)$. Figures (3.10), (3.11), (3.12) and (3.13) represent the output positions, angles, control signals and 3D trajectory of quadrotor system by \mathcal{L}_1 adaptive control respectively.

Case 2: Same assumptions and given data as mentioned in part 1 are considered here except the model is no longer exact. Uncertainties in the level of the states, disturbances and unmodeled input represented will be addressed into the system.

$$\begin{aligned}\ddot{\eta}_1 &= \frac{1}{m}R(\eta_2)\begin{bmatrix} 0 & 0 & \tau_z \end{bmatrix}^\top - g\begin{bmatrix} 0 & 0 & 1 \end{bmatrix}^\top \\ \ddot{\eta}_2 &= f(\eta_2) + f_\Delta(\eta_2) + G_\Delta(\eta_2)G(\eta_2)\begin{bmatrix} \tau_p & \tau_q & \tau_r \end{bmatrix}^\top + D(s)\end{aligned}$$

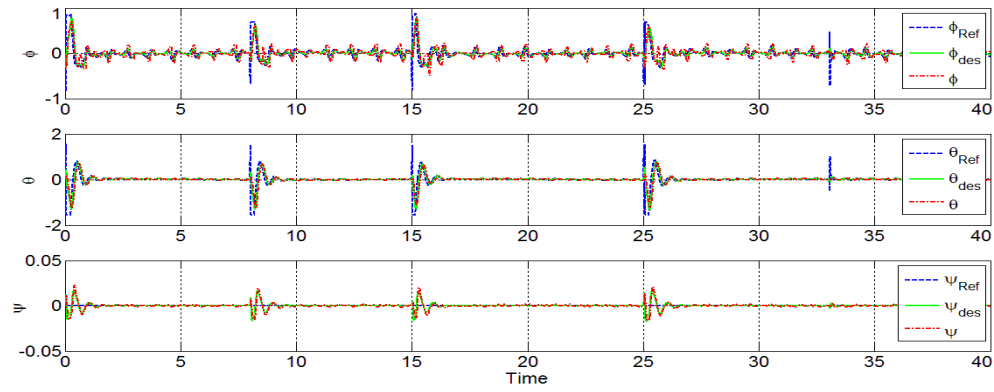


Figure 3.11: \mathcal{L}_1 adaptive controller with reference, desired and actual tracking angles of a quadrotor system.

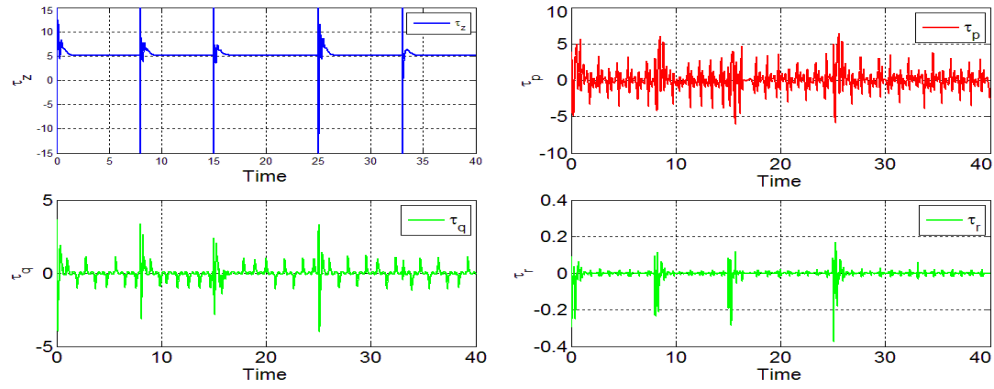


Figure 3.12: Control input of \mathcal{L}_1 adaptive controller of a quadrotor system.

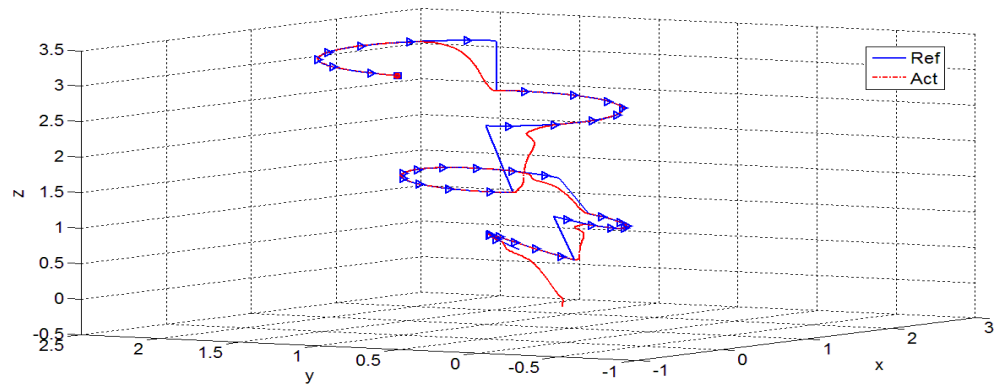


Figure 3.13: The 3D space tracking trajectory for both reference and actual output of a quadrotor system.

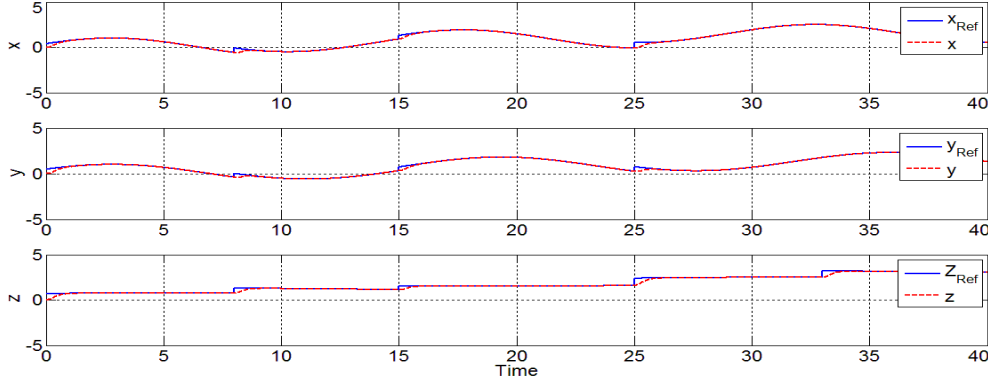


Figure 3.14: \mathcal{L}_1 adaptive controller with reference and actual tracking positions for quadrotor.

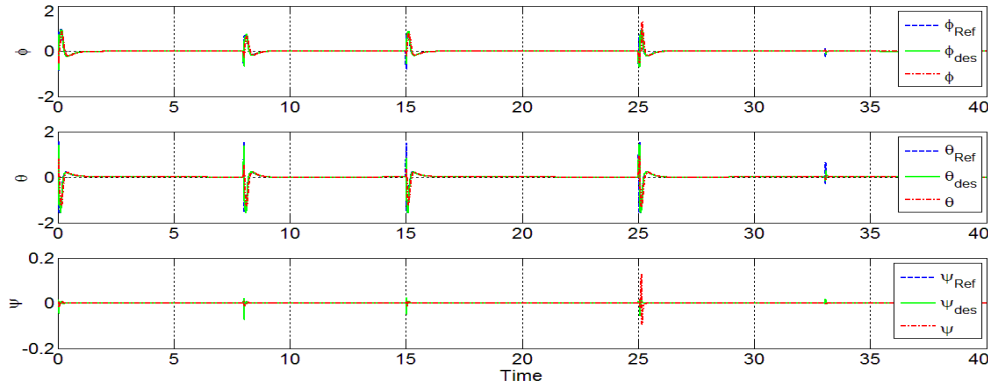


Figure 3.15: \mathcal{L}_1 adaptive controller with reference, desired and actual tracking angles of a quadrotor system.

$$f_{\Delta}(\eta_2) = \begin{bmatrix} 0.2\cos(\phi)\sin(\theta) + 0.2\phi\psi \\ 0.2\cos(\phi)\sin(\psi) + 0.2\phi\psi^2 \\ 0.2\cos(\theta)\sin(\phi) + 0.2\phi\theta\psi \end{bmatrix}, \quad D(s) = \begin{bmatrix} \frac{0.2}{s+1}u_{d1}(s) \\ \frac{0.24}{s^2+2s+3}u_{d2}(s) \\ \frac{0.15}{s^2+3s+2}u_{d3}(s) \end{bmatrix}$$

$$G_{\Delta}(\eta_2) = \begin{bmatrix} 1.6 & 0 & 0 \\ 0 & 0.7 & 0 \\ 0 & 0 & 1.23 \end{bmatrix}$$

$$u_{d1}(t) = \sin(0.4t), \quad u_{d2}(t) = \sin(0.6t), \quad u_{d3}(t) = \sin(0.5t),$$

Figures (3.14), (3.15), (3.16) and (3.17) are describing the output positions, angles, control signals and 3D trajectory of quadrotor system by \mathcal{L}_1 adaptive control after admitting uncertainties, unmodeled input and disturbances.

Example 3.3.3 Simulation Problem of Fully Actuated MARES Autonomous Underwater Vehicle

MARES underwater vehicle model and parameters were defined in [65–68]. The submarine

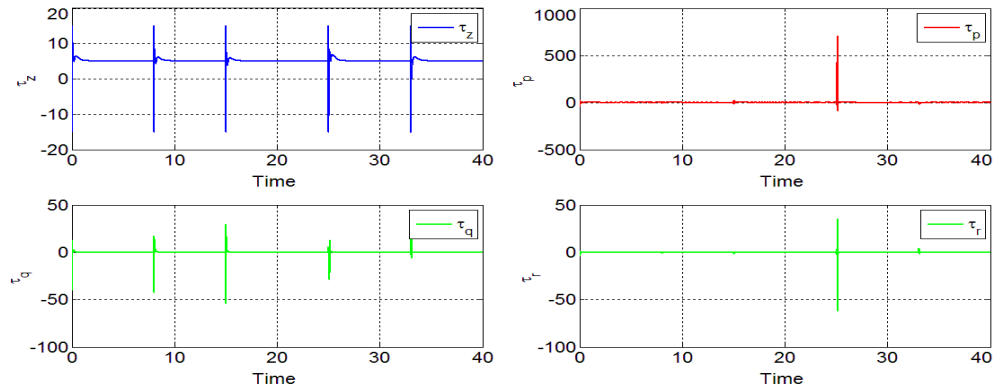


Figure 3.16: Control input of \mathcal{L}_1 adaptive controller of a quadrotor system

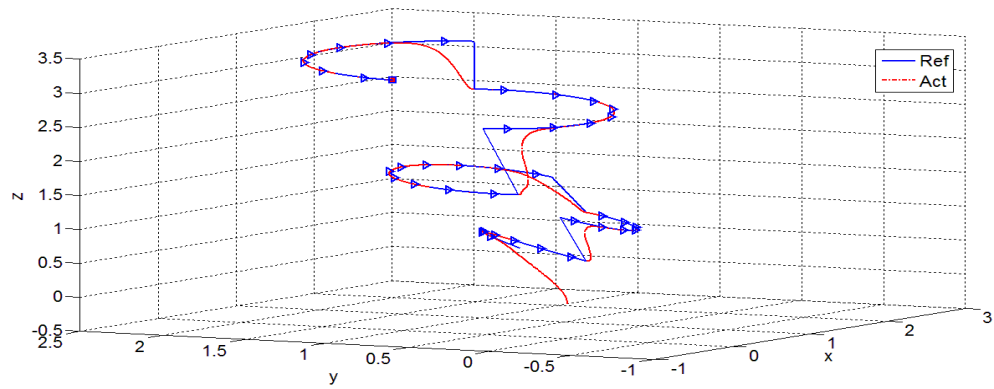


Figure 3.17: The 3D space tracking trajectory for both reference and actual output of a quadrotor system.

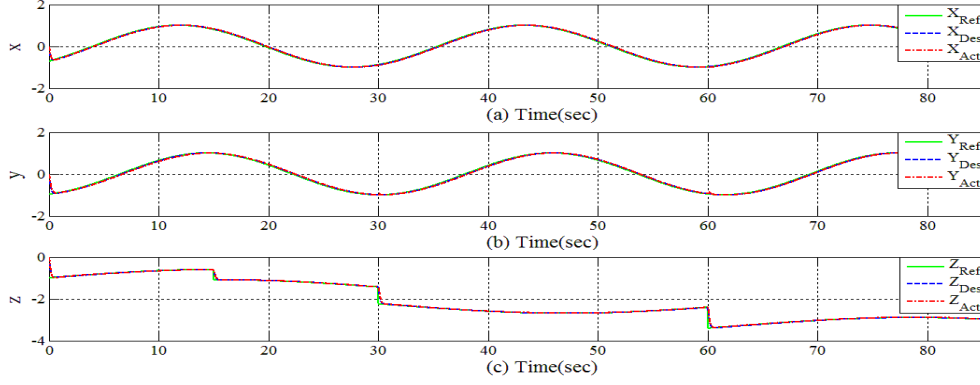


Figure 3.18: \mathcal{L}_1 adaptive controller with reference and actual tracking positions of MARES.

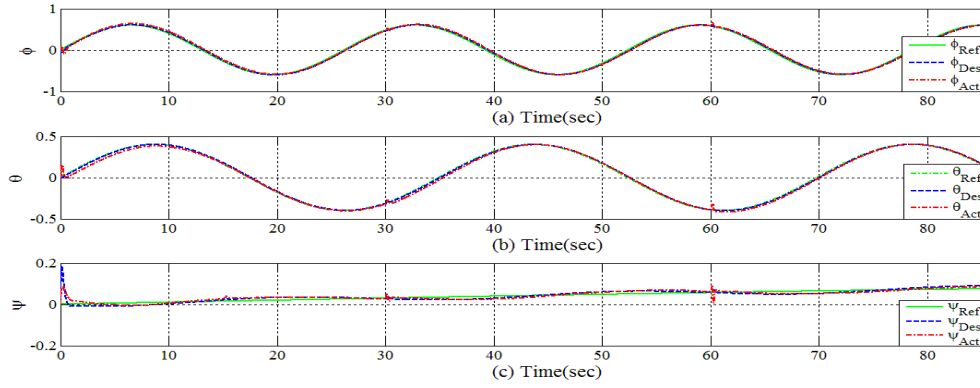


Figure 3.19: \mathcal{L}_1 adaptive controller with reference, desired and actual tracking angles of MARES

model can be represented as following

$$\tau_\eta(\eta) = M_\eta(\eta)\ddot{\eta} + C_\eta(\eta, \nu)\dot{\eta} + D_\eta(\eta, \nu)\dot{\eta} + G_\eta(\eta)$$

Where η is the earth coordinate frame, $G_\eta(\eta)$ is vector of gravitational/buoyancy forces and moments, $D_\eta(\eta, \nu)$ is damping matrix, $C_\eta(\eta, \nu)$ is coriolis-centripetal matrix (including added mass), $M_\eta(\eta)$ is system inertia matrix (including added mass) and $\tau_\eta(\eta)$ is the control input vector.

Parameters of \mathcal{L}_1 can be computed numerically where their bounds were chosen to $\omega_l = 0.5$, $\omega_u = 20$, $\theta_b = 100$, $\sigma_b = 100$ and the adaptation gain $\Gamma = 100000$. The desired poles are $-9 \pm j0.1$, $-10.5 \pm j0.1$, $-12 \pm j0.1$, $-13.5 \pm j0.1$, $-15 \pm j0.1$ and $-16.5 \pm j0.1$. Finally, the feedback gain is $\text{diag}(30, 30, 30, 30, 30, 30)$. Figures (3.18), (3.19), (3.20) and (3.21) are describing the output positions, angles, control signals and 3D trajectory respectively of MARES submarine using \mathcal{L}_1 adaptive control.

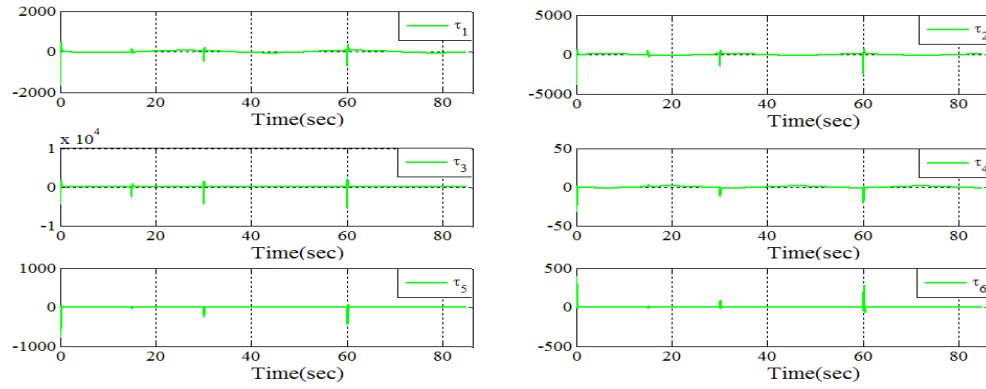


Figure 3.20: Control input of \mathcal{L}_1 adaptive controller of MARES.

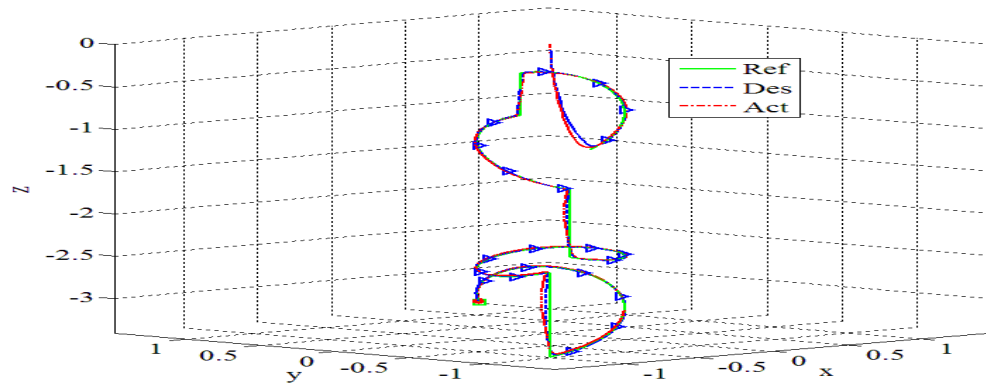


Figure 3.21: The 3D space tracking trajectory for both reference and actual output of MARES.

3.4 \mathcal{L}_1 Adaptive Controller for MIMO Systems in the Presence of Unmatched Nonlinear Uncertainties and Strong Coupling Effect

This section presents \mathcal{L}_1 adaptive control for MIMO uncertain system in the presence of high nonlinearities with strong coupling effect. All uncertainties and nonlinearities are assumed unknown.

3.4.1 Problem Formulation

Consider in the following class of systems:

$$\begin{aligned}\dot{x}(t) &= A_m x(t) + B_m \omega u(t) + f(x(t), z(t), t), \quad x(0) = x_0 \\ \dot{x}_z &= g(x(t), x_z(t), t), \quad x_z(0) = x_{z_0} \\ z(t) &= g_0(x_z(t), t) \\ y(t) &= Cx(t)\end{aligned}\tag{3.48}$$

where $x(t) \in \mathbb{R}^n$ is the system state vector (measured); $u(t) \in \mathbb{R}^m$ is the control input; $y(t) \in \mathbb{R}^m$ is the system output; $B_m \in \mathbb{R}^{n \times m}$ is a known full column-rank constant matrix where (A_m, B_m) is controllable and $C \in \mathbb{R}^{m \times n}$ is a known full-row rank constant matrix (known) where (A_m, C_m) is observable; $A_m \in \mathbb{R}^{n \times n}$ is a known Hurwitz matrix that defines the desired dynamics for the closed-loop system; $\omega \in \mathbb{R}^{m \times m}$ is a gain matrix defines uncertain system input, $x_z(t)$ are the output and the state vector of internal unmodeled dynamics; also $f : \mathbb{R} \times \mathbb{R}^n \times \mathbb{R}^p \rightarrow \mathbb{R}^n$, $g_0 : \mathbb{R}^l \times \mathbb{R} \rightarrow \mathbb{R}^p$ and $g : \mathbb{R} \times \mathbb{R}^l \times \mathbb{R}^n \rightarrow \mathbb{R}^l$ are unknown nonlinear continuous functions.

The system in (3.48) can also be written in the form

$$\begin{aligned}\dot{x}(t) &= A_m x(t) + B_m (\omega u(t) + f_1(x(t), z(t), t)) \\ &\quad + B_{um} (\omega u(t) + f_2(x(t), z(t), t)), \quad x(0) = x_0 \\ \dot{x}_z &= g(x(t), x_z(t), t), \quad x_z(0) = x_{z_0} \\ z(t) &= g_0(x_z(t), t) \\ y(t) &= Cx(t)\end{aligned}\tag{3.49}$$

Where $B_{um} \in \mathbb{R}^{n \times (n-m)}$ is a constant matrix has the property of $B_m \times B_{um} = 0$ with $\text{rank}([B_m, B_{um}]) = n$, while $f : \mathbb{R} \times \mathbb{R}^n \times \mathbb{R}^p \rightarrow \mathbb{R}^m$ and $f : \mathbb{R} \times \mathbb{R}^n \times \mathbb{R}^p \rightarrow \mathbb{R}^{n-m}$ are unknown nonlinear functions

that verify

$$\begin{bmatrix} f_1(x(t), z(t), t) \\ f_2(x(t), z(t), t) \end{bmatrix} = \begin{bmatrix} B_m & B_{um} \end{bmatrix}^{-1} f(x(t), z(t), t) \quad (3.50)$$

where $f_1(\cdot)$ represents the matched component of the unknown nonlinearities and $f_2(\cdot)$ represents the unmatched uncertainties. Let $X \triangleq [x^\top, z^\top]^\top$ and let $F(X(t), t) \triangleq f_i(x(t), z(t), t), i = 1, 2$. The system in (3.49) verifies the following assumptions:

Assumption 8 *(The control input are partially known with known sign) The system input gain matrix ω assumed to be nonsingular and unknown with known diagonal sign with strictly row-diagonally dominant matrix.*

$$\omega \in \Omega \subset \mathbb{R}^{m \times m}$$

where Ω is assumed to be known convex compact set.

Assumption 9 *(Uniform boundedness of $f(0, t)$) Let $B > 0$ such that $f_i(0, t) \leq B$ for all $t \geq 0$.*

Assumption 10 *(Partial derivatives are semiglobal uniform bounded) For any $\delta > 0$, there exist $d_{f_x}(\delta) > 0$ and $d_{f_t}(\delta) > 0$ such that for arbitrary $\|x\|_\infty \leq \delta$ and any u , the partial derivatives of $f(x(t), t)$ is piecewise-continuous and bounded,*

$$\left\| \frac{\partial f_i(x(t), t)}{\partial x} \right\| \leq d_{f_{xi}}(\delta), \quad \left\| \frac{\partial f_i(x(t), t)}{\partial t} \right\| \leq d_{f_{ti}}(\delta) \quad \text{where } i = 1, 2$$

Assumption 11 *(Asymptotically stability of initial conditions) The system assumed to start initially with x_0 inside an arbitrarily known set ρ_0 i.e., $\|x_0\|_\infty \leq \rho_0 < \infty$.*

Assumption 12 *(BIBO stability of internal dynamics) The states x_z of internal dynamics are BIBO stable with respect to x_{z0} and $x(t)$ and there exist $L_z, B_z > 0$ such that for all $t \geq 0$*

$$\|z_t\|_{\mathcal{L}_\infty} \leq L_z \|x(t)\|_{\mathcal{L}_\infty} + B_z$$

Assumption 13 *(Stability of Transmission zeros) The transmission zeros of the transfer matrix $H_m(s) = C(sI - A_m)^{-1} B_m$ lie in the open left half complex plane.*

The objective in this section aims at designing a full-state feedback adaptive controller to ensure that $y(t)$ tracks a given bounded piecewise-continuous reference signal $r(t)$ with quantifiable performance bounds given $M(s)$.

$$M(s) = C(sI - A_m)^{-1} B_m K_g(s)$$

where $K_g(s)$ is a feedforward pre-filter,

3.4.2 Definitions and \mathcal{L}_1 -Norm Sufficient Condition for Stability

Let

$$H_{xm}(s) \triangleq (sI - A_m)^{-1} B_m,$$

$$H_{xum}(s) \triangleq (sI - A_m)^{-1} B_{um},$$

$$H_m(s) \triangleq C(sI - A_m)^{-1} B_m,$$

$$H_{um}(s) \triangleq C(sI - A_m)^{-1} B_{um},$$

and let $x_{in}(t)$ be the signal with Laplace transform $x_{in}(s) \triangleq (sI - A_m)^{-1} x_0$ and $\rho_{in} \triangleq \|s(sI - A_m)^{-1}\|_{\mathcal{L}_1} \rho_0$. Since A_m is Hurwitz and x_0 is bounded, then $\|x_{in}\|_{\mathcal{L}_\infty} \leq \rho_{in}$.

$$L_{i\delta} \triangleq \frac{\bar{\delta}(\delta)}{\delta} d_{f_{xi}}(\bar{\delta}(\delta)), \quad \bar{\delta}(\delta) \triangleq \max\{\delta + \bar{\gamma}, L_z(\delta + \bar{\gamma})B_z\} \quad (3.51)$$

where $\bar{\gamma}$ is a small positive constant assigned arbitrarily. The objective of the adaptive controller aims in achieving DC gain $C(0) \triangleq \mathbb{I}_m$. K is a feedback gain matrix and $D(s)$ is strictly proper transfer matrix and both of them aim to strictly proper transfer function as follows

$$C(s) \triangleq \omega K D(s) (\mathbb{I}_m + \omega K D(s))^{-1} \quad (3.52)$$

The choice of $D(s)$ needs to ensure also that $C(s)H^{-1}(s)$ is a proper stable transfer matrix. For a particular class of systems, a possible choice for $D(s)$ might be $D(s) = 1/s \cdot \mathbb{I}_m$, which yields a strictly proper $C(s)$ of the form

$$C(s) \triangleq \omega K (s\mathbb{I}_m + \omega K)^{-1} \quad (3.53)$$

Now, for a given ρ_0, k and $D(s)$ should be chosen such that there exist $\rho_r > \rho_{in}$ and the following \mathcal{L}_1 norm condition verified

$$\|G_m(s)\|_{\mathcal{L}_1} + \|G_{um}(s)\|_{\mathcal{L}_1} \ell_0 < \frac{\rho_r - \|H_{xm}(s)C(s)K_g\|_{\mathcal{L}_1} \|r\|_{\mathcal{L}_\infty} - \rho_{in}}{L_{1\rho_r} \rho_r + B_0} \quad (3.54)$$

$$G_m(s) = H_{xm}(s)(\mathbb{I}_m - C(s))$$

$$G_{um}(s) = (\mathbb{I}_m - H_{xm}(s)C(s)H_m^{-1}(s))H_{xum}(s)$$

$$\ell_0 = \frac{L_{1\rho_r}}{L_{2\rho_r}}, \quad B_0 = \max\{B_{10}, B_{20}/\ell_0\}$$

let

$$\gamma_1 \triangleq \frac{\|H_{xm}(s)C(s)H_m^{-1}(s)\|_{\mathcal{L}_1}}{1 - \|G_m(s)\|_{\mathcal{L}_1}L_{1\rho_r} - \|G_{um}(s)\|_{\mathcal{L}_1}L_{2\rho_r}}\gamma_0 + \beta \quad (3.55)$$

where γ_0 and β are arbitrarily small positive constants.

let

$$\rho_u \triangleq \rho_{ur} + \gamma_2 \quad (3.56)$$

where ρ_{ur} and γ_2 are defined as following

$$\begin{aligned} \rho_{ur} \triangleq & \|\omega^{-1}C(s)\|_{\mathcal{L}_1}(\|K_g\|_{\mathcal{L}_1}\|r\|_{\mathcal{L}_\infty} + L_{1\rho_r}\rho_r + B_{10} \\ & + \|H_m^{-1}(s)H_{um}(s)\|_{\mathcal{L}_1}(L_{2\rho_r}\rho_r + B_{20})) \end{aligned} \quad (3.57)$$

$$\begin{aligned} \gamma_2 \triangleq & \|\omega^{-1}C(s)\|_{\mathcal{L}_1}L_{1\rho_r}\gamma_1 + \|H_m^{-1}(s)H_{um}(s)\|_{\mathcal{L}_1}L_{2\rho_r}\gamma_1 \\ & + \|H_m^{-1}(s)C(s)\|_{\mathcal{L}_1}\gamma_0 \end{aligned} \quad (3.58)$$

and finally let

$$\theta_{b_i} \triangleq L_{i_p}, \quad \sigma_{b_i} \triangleq L_{i_p}B_z + B_i + \epsilon_i, \quad i = 1, 2 \quad (3.59)$$

where ϵ is an arbitrary positive constant.

3.4.3 \mathcal{L}_1 Adaptive Control Architecture

State Predictor: We consider the following state predictor:

$$\begin{aligned} \dot{\hat{x}}(t) = & A_m\hat{x}(t) + B_m(\hat{\omega}u(t) + \hat{\theta}_1\|x(t)\|_\infty + \hat{\sigma}_1) \\ & + B_{um}(\hat{\theta}_2\|x(t)\|_\infty + \hat{\sigma}_2), \quad \hat{x}(0) = x(0) \\ \hat{y}(t) = & c\hat{x}(t) \end{aligned} \quad (3.60)$$

where $\hat{\omega} \in \mathbb{R}^{m \times m}$, $\hat{\theta}_1(t) \in \mathbb{R}^m$, $\hat{\theta}_2(t) \in \mathbb{R}^{n-m}$, $\hat{\sigma}_1(t) \in \mathbb{R}^m$ and $\hat{\sigma}_2(t) \in \mathbb{R}^{n-m}$ are the adaptive estimates defined by the following adaptive laws.

$$\begin{aligned} \dot{\hat{\omega}} = & \Gamma Proj(\hat{\omega}, -(\tilde{x}^\top PB_m)^\top(u(t)^\top)), \quad \hat{\omega}(0) = \hat{\omega}_0 \\ \dot{\hat{\theta}}_1 = & \Gamma Proj(\hat{\theta}_1, -(\tilde{x}^\top PB_m)^\top\|x(t)\|_\infty), \quad \hat{\theta}_1(0) = \hat{\theta}_{10} \\ \dot{\hat{\theta}}_2 = & \Gamma Proj(\hat{\theta}_2, -(\tilde{x}^\top PB_{um})^\top\|x(t)\|_\infty), \quad \hat{\theta}_2(0) = \hat{\theta}_{20} \\ \dot{\hat{\sigma}}_1 = & \Gamma Proj(\hat{\sigma}_1, -(\tilde{x}^\top PB_m)^\top), \quad \hat{\sigma}_1(0) = \hat{\sigma}_{10} \\ \dot{\hat{\sigma}}_2 = & \Gamma Proj(\hat{\sigma}_2, -(\tilde{x}^\top PB_m)^\top), \quad \hat{\sigma}_2(0) = \hat{\sigma}_{20} \end{aligned} \quad (3.61)$$

where $\tilde{x} \triangleq \hat{x} - x(t)$, $\Gamma \in \mathbb{R}^+$ is the adaptation gain, and $P = P^\top > 0$ is defined by solving the algebraic Lyapunov equation $A_m^\top P + PA_m = -Q$ for arbitrary symmetric $Q = Q^\top > 0$. The

projection operator ensures that $\hat{\omega} \in \Omega$, $\|\hat{\theta}_i\|_\infty \in \Theta_i$, $\|\hat{\sigma}_i\| \leq \Delta_i$, with θ_{bi} and δ_{bi} are being defined by (3.59)

Control Law: Control signal can be calculated as following

$$u(s) = -kD(s)\hat{\eta}(s) \quad (3.62)$$

where $r(s)$ and $\hat{\eta}(s)$ are the Laplace transforms of $r(t)$ and $\hat{\eta}(t) = \hat{\omega}u(t) + \hat{\eta}_1 + \hat{\eta}_2 - K_g r(t)$ respectively; and the necessary feedforward gain in order to get unity steady state is calculated by $K_g \triangleq -(CA_m^{-1}B)^{-1}$; the feedback gain k is positive constant and $D(s)$ is a strictly proper transfer function where both of them lead to a strictly proper stable closed loop system.

$$\hat{\eta}_1 \triangleq \hat{\theta}_1 \|x(t)\|_\infty + \hat{\sigma}_1$$

$$\hat{\eta}_2 \triangleq \hat{\theta}_2 \|x(t)\|_\infty + \hat{\sigma}_2$$

3.4.4 \mathcal{L}_1 Adaptive Control Stability Analysis

Transient and Steady-State Performance: The error between system dynamics in (3.49) and state predictor in (3.60) can be written as

$$\dot{\tilde{x}}(t) = A_m \tilde{x}(t) + B_m(\tilde{\omega}u(t) + \tilde{\eta}_1(t)) + B_{um}\tilde{\eta}_2(t) \quad (3.63)$$

Where $\tilde{x} = \hat{x} - x$, $\tilde{\theta}_i = \hat{\theta}_i - \theta_i$, $\tilde{\omega} = \hat{\omega} - \omega$, $\tilde{\sigma}_i = \hat{\sigma}_i - \sigma_i$ and $\tilde{\eta}_i = \hat{\eta}_i - \eta_i$ where $i = 1, 2$.

Lemma 3 *The prediction error $\tilde{x}(t)$ is uniformly bounded,*

from Lemma 3 and equations (3.33) and (3.34), the derivatives of ω , θ and σ are bounded:

$$\|\theta_i\|_\infty \leq \theta_{bi}(\rho_r) < \infty, \quad \|\dot{\theta}_i\|_\infty \leq d_{\theta_i}(\rho_r) < \infty \quad (3.64)$$

$$\|\sigma_i\|_\infty \leq \sigma_{bi}(\rho_r) < \infty, \quad \|\dot{\sigma}_i\|_\infty \leq d_{\sigma_i}(\rho_r) < \infty \quad (3.65)$$

Then

$$\|\tilde{x}\|_\infty \leq \sqrt{\frac{\theta_m}{\lambda_{\min}(P)\Gamma}} \quad (3.66)$$

where

$$\begin{aligned} \theta_m \triangleq & 4 \left((\theta_{b_1}^2 + \sigma_{b_1}^2)m + (\theta_{b_2}^2 + \sigma_{b_2}^2)(n-m) + \max_{\omega \in \Omega} \text{tr}(\omega^\top \omega) + \right. \\ & \left. 4 \frac{\lambda_{\max}(P)}{\lambda_{\min}(Q)} ((d_{\theta_1}\theta_{b_1} + d_{\sigma_1}\sigma_{b_1})m + (d_{\theta_2}\theta_{b_2} + d_{\sigma_2}\sigma_{b_2})(n-m)) \right) \end{aligned} \quad (3.67)$$

which will be verified as following

Stability proof: Consider the Lyapunov function candidate

$$V(\tilde{x}, \tilde{\omega}, \tilde{\theta}_i, \tilde{\sigma}_i) = \tilde{x}^\top P \tilde{x} + \frac{1}{\Gamma} (tr(\tilde{\omega}^\top \tilde{\omega}) + \tilde{\theta}^\top \tilde{\theta} + \tilde{\sigma}^\top \tilde{\sigma}) \quad (3.68)$$

Since $\hat{x}(0) = x(0)$ then we can verify that

$$\begin{aligned} V(0) &\leq \frac{4}{\Gamma} (\max_{\omega \in \Omega} tr(\omega^\top \omega) + \theta_{b_1}^2 + \sigma_{b_1}^2)m + (\theta_{b_2}^2 + \sigma_{b_2}^2)(n - m)) \leq \frac{\theta_m}{\Gamma} \\ \dot{V} &\leq \tilde{x}^\top Q \tilde{x} + \frac{2}{\Gamma} (\dot{\hat{\theta}} + \tilde{x}^\top P B \|x\|_\infty) + \frac{2}{\Gamma} (\dot{\hat{\sigma}} + \tilde{x}^\top P B) + \frac{2}{\Gamma} (\dot{\hat{\omega}} + \tilde{x}^\top P B u) \\ &\quad - \frac{2}{\Gamma} \sum_{i=1}^2 (\tilde{\theta}_i^\top \dot{\theta}_i + \tilde{\sigma}_i^\top \dot{\sigma}_i) \\ \dot{V} &= -\tilde{x}^\top Q \tilde{x} + \frac{2}{\Gamma} \sum_{i=1}^2 (|\tilde{\theta}_i^\top \dot{\theta}_i| + |\tilde{\sigma}_i^\top \dot{\sigma}_i|) \end{aligned} \quad (3.69)$$

$$\dot{V} \leq -\tilde{x}^\top Q \tilde{x} + \frac{4}{\Gamma} ((d_{\theta_1} \theta_{b_1} + d_{\sigma_1} \sigma_{b_1})m + (d_{\theta_2} \theta_{b_2} + d_{\sigma_2} \sigma_{b_2})(n - m)) \quad (3.70)$$

Now we can say

$$\sum_{i=1}^2 (\tilde{\theta}_i^\top \dot{\theta}_i + \tilde{\sigma}_i^\top \dot{\sigma}_i) \leq \sum_{i=1}^2 (d_{\theta_i} \theta_{b_i} + d_{\sigma_i} \sigma_{b_i}) \quad (3.71)$$

Moreover, the projection operator also ensures that

$$\max_{t \geq 0} \left(\frac{1}{\Gamma} (\tilde{\theta}^\top \tilde{\theta} + tr(\tilde{\omega}^\top \tilde{\omega}) + \tilde{\sigma}^\top \tilde{\sigma}) \right) \leq \frac{1}{\Gamma} (\theta_b^2 m + \Delta^2 m + \max_{\omega \in \Omega} tr(\omega^\top \omega)) \quad (3.72)$$

which holds for all $t \geq 0$. If at any time $t_1 > 0$, one has $V(t_1) \geq \theta_m/\Gamma$, then it follows from (3.67) and (3.68) that

$$\tilde{x}^\top(t_1) P \tilde{x}(t_1) > \frac{4}{\Gamma} \frac{\lambda_{\max}(P)}{\lambda_{\min}(Q)} ((d_{\theta_1} \theta_{b_1} + d_{\sigma_1} \sigma_{b_1})m + (d_{\theta_2} \theta_{b_2} + d_{\sigma_2} \sigma_{b_2})(n - m)) \quad (3.73)$$

thus

$$\begin{aligned} \tilde{x}(t_1)^\top Q \tilde{x}(t_1) &\geq \frac{\lambda_{\min}(Q)}{\lambda_{\max}(P)} \tilde{x}^\top(t_1) P \tilde{x}(t_1) \\ &> \frac{4}{\Gamma} \sum_{i=1}^2 ((d_{\theta_1} \theta_{b_1} + d_{\sigma_1} \sigma_{b_1})m + (d_{\theta_2} \theta_{b_2} + d_{\sigma_2} \sigma_{b_2})(n - m)) \end{aligned} \quad (3.74)$$

Hence, if $V(t_1) \geq \theta_m/\Gamma$, then from (3.70) and (3.74) we have

$$\dot{V} \leq 0 \quad (3.75)$$

3.4.5 Problem Formulation and Simulation

Example 3.4.1 MIMO System with Nonlinear Unmatched Uncertainties.

\mathcal{L}_1 adaptive control will be implemented to high nonlinear system with unmatched uncertainties in order to investigate output performance and control signals. Consider the system in [28].

$$\begin{aligned} \dot{x}(t) &= (A_m + A_\Delta)x(t) + B_m\omega u(t) + f_\Delta(x(t), z(t), t) \\ y(t) &= Cx(t) \end{aligned}$$

where

$$A_m = \begin{bmatrix} -1 & 0 & 0 \\ 0 & 0 & 1 \\ 0 & -1 & -1.8 \end{bmatrix}, \quad B_m = \begin{bmatrix} 1 & 0 \\ 0 & 0 \\ 1 & 1 \end{bmatrix}, \quad C = \begin{bmatrix} 1 & 0 & 0 \\ 0 & 1 & 0 \end{bmatrix}$$

while $A_\Delta \in \mathbb{R}^{3 \times 3}$ and $\omega_\Delta \in \mathbb{R}^{2 \times 2}$ are unknown constant matrices satisfying

$$\omega \in \begin{bmatrix} [0.6, 1.2] & [-0.2, 0.2] \\ [-0.2, 0.2] & [0.6, 1.2] \end{bmatrix} = \Omega$$

and f_Δ is the (unknown) nonlinear function

$$f_\Delta(x(t), z(t), t) = \begin{bmatrix} \frac{k_1}{3}x^\top x + \tanh(\frac{k_2}{2}x_1)x_1 + k_3z \\ \frac{k_4}{2}\sec(x_2)x_2 + \frac{k_5}{5}x_3^2 + k_6(1 - e^{-\lambda t}) + \frac{k_7}{2}z \\ k_8x_3\cos(\omega_u t) + k_9z^2 \end{bmatrix}$$

where $k_1 = -1$, $k_2 = 1$, $k_3 = 0$, $k_4 = 1$, $k_5 = 0$, $k_6 = 0.2$, $k_7 = 1$, $k_8 = 0.6$, $k_9 = -0.7$, $\lambda = 0.3$ and $\omega_u = 5$. The internal unmodeled dynamics are given by

$$\begin{aligned} \dot{x}_{z1} &= x_{z2}(t) \\ \dot{x}_{z2} &= -x_{z1}(t) + 0.8(1 - x_{z1}^2(t))x_{z2}(t) \\ z(t) &= 0.1(x_{z1}(t) - x_{z2}(t)) + z_u(t) \\ z(s) &= \frac{-s + 1}{100s^2 + 8s + 1} \begin{bmatrix} 1 & -2 & 1 \end{bmatrix} x(s) \end{aligned}$$

3.4. \mathcal{L}_1 ADAPTIVE CONTROLLER FOR MIMO SYSTEMS IN THE PRESENCE OF UNMATCHED NONLINEAR UNCERTAINTIES AND

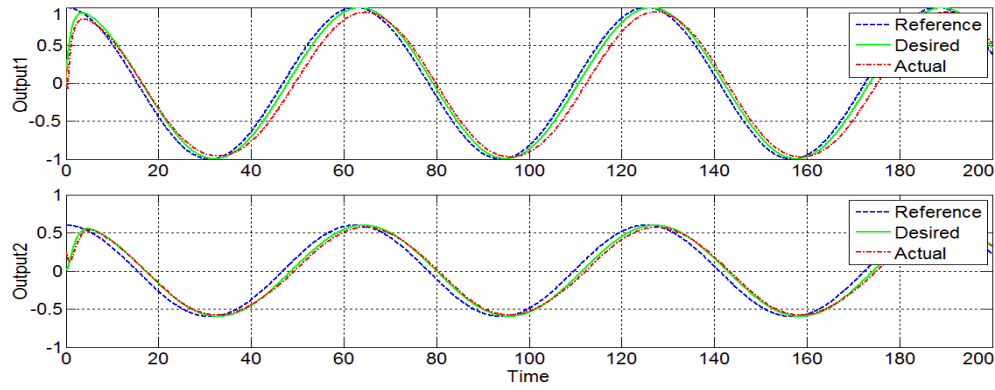


Figure 3.22: Tracking output of \mathcal{L}_1 adaptive control with reference and desired outputs for unmatched MIMO uncertain system.

Desired poles are chosen as $p = -1, -0.9 \pm j0.4359$, $\Gamma = 80000$ and

$$Q = \begin{bmatrix} 1 & 0 & 0 \\ 0 & 1 & 0 \\ 0 & 0 & 1 \end{bmatrix}, \quad K = \begin{bmatrix} 8 & 0 \\ 0 & 8 \end{bmatrix}$$

$$D(s) = \frac{1}{s(s/25 + 1)(s/70 + 1)(s^2/40^2 + 1.8s/40 + 1)} \mathbb{I}_2$$

Adaptive estimates belong to the following bounds $\hat{\theta}_1(t) \in [-40, 40]\mathbb{I}_2$, $\hat{\theta}_2(t) \in [-40, 40]$, $\hat{\sigma}_1(t) \in [-5, 5]\mathbb{I}_2$, $\hat{\sigma}_2(t) \in [-5, 5]$, $\hat{\omega}_{11}(t), \hat{\omega}_{22}(t) \in [0.25, 3]$, and $\hat{\omega}_{12}(t), \hat{\omega}_{21}(t) \in [-0.2, 0.2]$. Also other uncertainties and modeled input parameters will be defined by

$$A_\Delta = \begin{bmatrix} 0.2 & -0.2 & -0.3 \\ -0.2 & -0.2 & 0.6 \\ -0.1 & 0 & -0.9 \end{bmatrix}, \quad \omega = \begin{bmatrix} 0.6 & -0.2 \\ 0.2 & 1.2 \end{bmatrix}$$

Figure 3.22 and 3.23 show output response and control signals of \mathcal{L}_1 adaptive control.

Example 3.4.2 Nonlinear Twin Rotor MIMO System (TRMS) with Strong Coupling.

Twin rotor was designed for training high nonlinear control applications to mimic the behavior of the helicopter dynamics in terms of angle orientation [69]. The model and parameters of the system are defined in [70]. Complexity of the twin rotor comes from high nonlinearities in addition to strong coupling between control signals. Figure 3.24 demonstrates TRMS set up. \mathcal{L}_1 adaptive control will be implemented on high nonlinear TRMS with strong coupling effect in order to evaluate the control performance on output response and control signals. Adaptive estimates were defined as $\hat{\theta}_1(t) \in [-50, 50]\mathbb{I}_2$, $\hat{\theta}_2(t) \in [-50, 50]$, $\hat{\sigma}_1(t) \in [-15, 15]\mathbb{I}_2$, $\hat{\sigma}_2(t) \in [-15, 15]$, $\hat{\omega}_{11}(t), \hat{\omega}_{22}(t) \in [0.25, 5]$, $\Gamma = 100000$ and the desired poles are assigned to

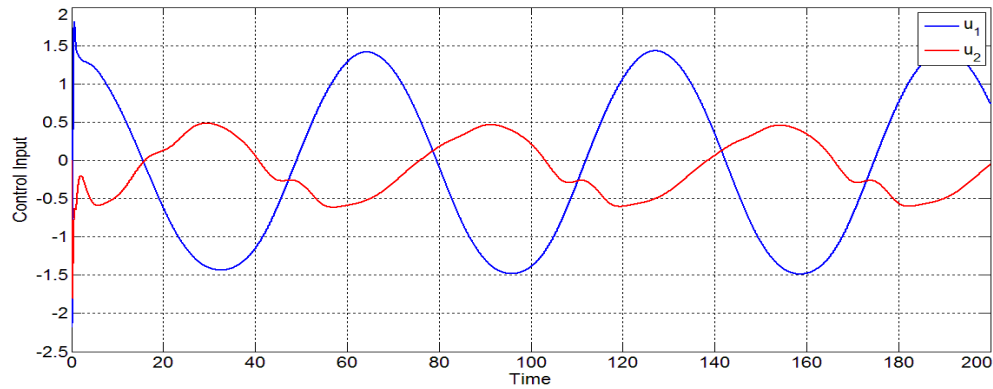


Figure 3.23: Control signal of \mathcal{L}_1 adaptive control for unmatched MIMO uncertain system.

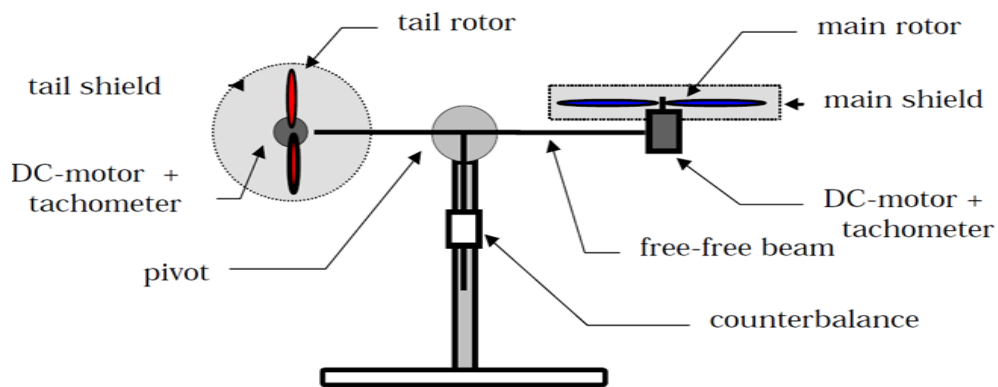


Figure 3.24: Laboratory set-up of TRMS.

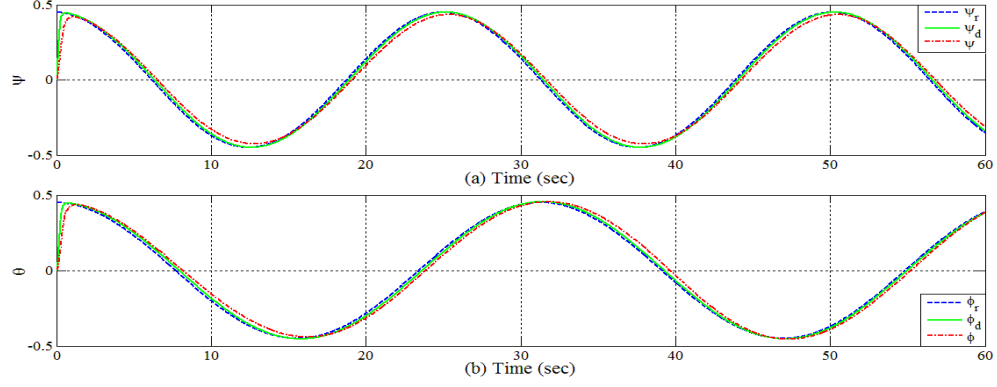


Figure 3.25: Tracking output of \mathcal{L}_1 adaptive control with reference and desired outputs for TRMS.

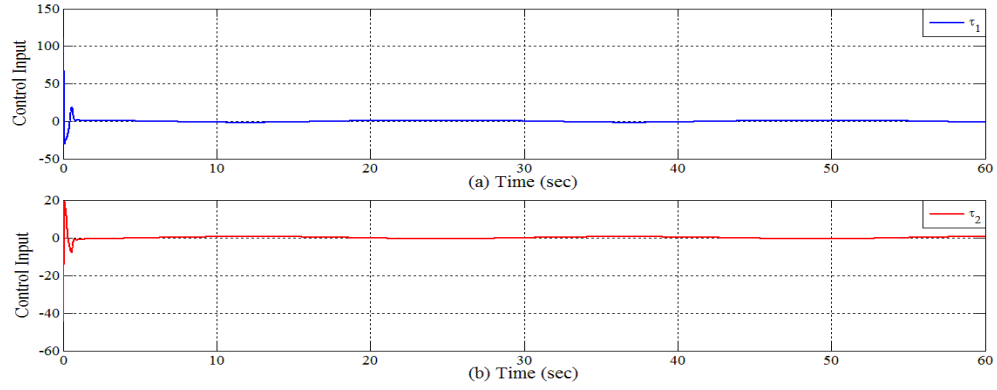


Figure 3.26: Control signal of \mathcal{L}_1 adaptive control for TRMS.

$-15 \pm 0.3i$, $-17 \pm 0.5i$ and $-20 \pm 0.5i$ and finally the feedback gain $= 5 \begin{pmatrix} 1 & 0 \\ 0 & 1 \end{pmatrix}$.

Figure 3.25 and 3.26 show output response and control signals of \mathcal{L}_1 adaptive control for TRMS.

3.5 Conclusion

This chapter mainly handled \mathcal{L}_1 adaptive controller from different perspectives and for different classes of nonlinear systems. The robustness, transient performance and tracking trajectory are prominent features of \mathcal{L}_1 adaptive controller. All previous features have been validated through different cases of studies including reproducing recent results. From the literature, the relation between improving robustness, enhancing transient performance and control signal range have been demonstrated. In conclusion, improving robustness and enhancing the transient performance have a direct effect on the control signal range. We will present a satisfactory solution will be studied in subsequent chapters.

Chapter 4

A Fuzzy Logic Feedback Filter Design Tuned with PSO for \mathcal{L}_1 Adaptive Controller

4.1 Introduction

The structure of \mathcal{L}_1 adaptive controller offers three features including the implementation of a low pass filter in order to limit the frequency range of the control signal and reduce the effect of the uncertainties (see Figure (4.1)). The structure allows decoupling of the adaption and robustness using high-gain for fast adaption. The filter is selected such that the system's

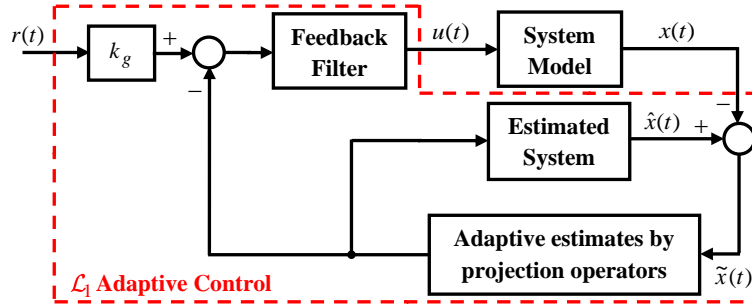


Figure 4.1: The general structure of L1 adaptive controller.

output tracks properly the reference input and the undesirable uncertainties and frequencies are filtered (see [35] or [43]). Using the low pass filter, \mathcal{L}_1 controller reduces the coupling between robustness and fast adaptation and provides infinity norm boundedness of the transient and steady state responses. \mathcal{L}_1 adaptive control was first introduced by [35]. It has been applied successfully to uncertain linear systems [26], uncertain nonlinear single-input-single-

output (SISO) systems [36], [27], and nonlinear system multi-input-multi-output (MIMO) with unmatched uncertainties [71]. And, the control approach showed satisfactory results on experimental flight tests [37], [28]. The optimal structure of \mathcal{L}_1 filter has been studied extensively in [43]. The trade-off between fast desired closed loop dynamics and filter parameters has been debated for long [35, 43–47]. Increasing the bandwidth of the low pass filter will reduce robustness margin, which will require slowing the desired closed loop performance in order to regain the robustness. However, slower selection of desired closed loop performance will deteriorate the output performance especially during the transient period [43]. Limitations of \mathcal{L}_1 adaptive controller and the interconnection between adaptive estimates and the feedback filter were studied in [46], where several filter designs were considered based on the use of disturbance observer. The authors showed that it is crucial to select the appropriate coefficients for a given filter to achieve the desired performance. Several attempts on identifying these optimal coefficients have been made in the literature. This includes convex optimization based on linear matrix inequality (LMI) [43], [44] and multi-objective optimization using MATLAB optimization solver [45]. More recently, a systematic approach was presented in [47] to determine the optimal feedback filter coefficients in order to increase the zone of robustness margin. The authors proposed the use of greedy randomized algorithms.

One can observe that while the previous approaches to determine the optimal coefficients have different degrees of complexity, they agree on the fact that the selection of the appropriate coefficients is performed off-line; and once selected, these coefficients remain unchanged. This study claims that increasing the robustness while guaranteeing fast adaptation requires dynamic and on-line tuning of the feedback filter's coefficients and any proposed method should be relatively simple and easily implementable. To this end, this study proposes fuzzy tuning of the filter's coefficients optimized using PSO taking into account the rate and value of the tracking error between the model reference output and the system's output. The complete structure of fuzzy- \mathcal{L}_1 adaptive controller is presented in Figure 4.2. The FLC-based tuning is performed on-line during operation. On the other hand, PSO identifies the optimal values of output membership functions through off-line tuning.

Fuzzy logic controller (FLC) is classified as an intelligent technique and was first proposed in [72]. FLC showed impressive results in control applications and it has been presented as a robustifying tool with adaptive controllers in [29], [73]. It has been used to compensate unknown nonlinearities of twin rotor MIMO system with adaptive sliding mode control [29]. In [73], the authors suggested an observer-based adaptive backstepping control scheme and used FLC to approximate unknown uncertainties and to handle bounds of dead zone nonlinearity. On the other hand, evolutionary algorithms are introduced as potential optimization techniques in

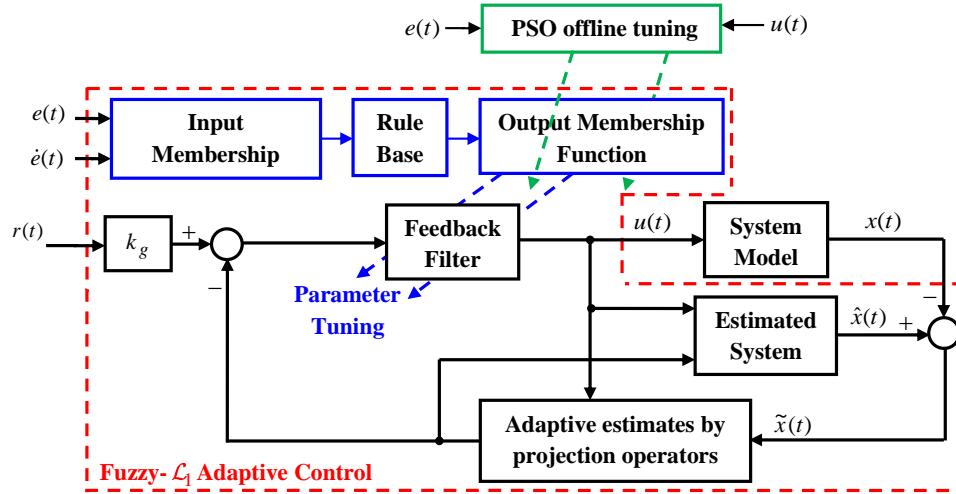


Figure 4.2: Proposed fuzzy- adaptive control structure.

various control applications. They gained the interest of researchers and witnessed rapid developments over the past few decades. In particular, Particle swarm optimization (PSO) was introduced as a global search technique in [74]. PSO has been applied successfully to optimize the structure and parameters of adaptive fuzzy controller in [75] and optimize the variables of FLC membership functions in [76], [77]. The need to tune controller systems with originally fixed coefficients has been widely recognized. In particular, fuzzy tuning has been investigated in several studies (see for instance [78], [79], and [80]) and controllers based on such approach have been implemented in many applications (see for instance [80], [81], [82], [83]). This allows to conclude that the proposed approach is practical and can definitely be implemented with great benefit.

To summarize, in this work, fuzzy- \mathcal{L}_1 adaptive controller is proposed to tune the filter's coefficients in order to improve the trade-off between robustness and fast adaptation. The coefficients are dynamically tuned and not kept fixed as in the literature, thus allowing for better performance. In the proposed approach, FLC is in charge of online tuning of the filter coefficients taking into account the range and rate of the tracking error. The use of FLC to tune the coefficients improves the stability and the robustness of the system and allows faster closed loop dynamics. Input membership functions and other FLC parameters are assigned arbitrarily while PSO optimizes the optimal variables of the fuzzy output membership functions. The approach is validated using different nonlinear systems and the extensive simulation results are benchmarked to the \mathcal{L}_1 adaptive controller with fixed constant gain. The method is simpler than those in the literature and easily implementable.

This chapter is organized as follows: In section two, brief review of \mathcal{L}_1 adaptive control in-

cluding adaptation laws and the general structure is discussed. Section three presents the idea of filter design and the structure of the proposed control. Section four states the optimization problem and presents the particle swarm optimization algorithm. Illustrative examples will be presented in section five in order to clarify and verify the proposed approach. Finally, last section contains the conclusion.

4.2 Review of \mathcal{L}_1 adaptive controller

Consider the following dynamics for nonlinear system

$$\begin{aligned}\dot{x}(t) &= A_m x(t) + b(\omega u(t) + f(x(t), u(t), t)) \\ y(t) &= c x(t)\end{aligned}\tag{4.1}$$

where $x(t) \in \mathbb{R}^n$ is the system state vector (assumed measured); $u(t) \in \mathbb{R}$ is the control input; $y(t) \in \mathbb{R}$ is the system output; $b, c \in \mathbb{R}^n$ are constant vectors (known); A_m is $\mathbb{R}^{n \times n}$ Hurwitz matrix (known) refers to the desired closed-loop dynamics; $\omega(t) \in \mathbb{R}$ is an unknown time variant parameter describes unmodeled input gain with known sign, and $f(x(t), u(t), t) : \mathbb{R}^n \times \mathbb{R} \times \mathbb{R} \rightarrow \mathbb{R}$ is an unknown nonlinear continuous function.

Assumption 1 (Partially known with known sign control input) *Let the upper and the lower input gain bounds be defined by ω_l and ω_u respectively, where*

$$\omega \in \Omega \triangleq [\omega_l, \omega_u], \quad |\dot{\omega}| < \omega$$

Ω is assumed to be known convex compact set and $0 < \omega_l < \omega_u$ are uniformly known conservative bounds.

Assumption 2 (Uniform boundedness of $f(0, u(t), t)$) *Let $B > 0$ such that $f(0, u(t), t) \leq B$ for all $t \geq 0$*

Assumption 3 (Partial derivatives are semiglobal uniform bounded) *For any $\delta > 0$, there exist $d_{f_x}(\delta) > 0$ and $d_{f_t}(\delta) > 0$ such that for arbitrary $\|x\|_\infty \leq \delta$ and any u , the partial derivatives of $f(x(t), u(t), t)$ is piecewise-continuous and bounded,*

$$\left\| \frac{\partial f(x(t), u(t), t)}{\partial x} \right\| \leq d_{f_x}(\delta), \quad \left| \frac{\partial f(x(t), u(t), t)}{\partial t} \right| \leq d_{f_t}(\delta)$$

Assumption 4 (Asymptotically stable of initial conditions) *The system assumed to start initially with x_0 inside an arbitrarily known set ρ_0 i.e., $\|x_0\|_\infty \leq \rho_0 < \infty$.*

$$\theta_b \triangleq d_{f_x}(\delta), \quad \Delta \triangleq B + \epsilon \quad (4.2)$$

Lemma: If $\|x\|_{\mathcal{L}_\infty} \leq \rho$ and there exist $u(\tau)$, $\omega(\tau)$, $\theta(\tau)$ and $\sigma(\tau)$ over $[0, t]$ such that

$$\omega_l < \omega < \omega_u \quad (4.3)$$

$$|\theta(\tau)| < \theta_b \quad (4.4)$$

$$|\sigma(\tau)| < \sigma_b \quad (4.5)$$

$$f(x(\tau), u(\tau), \tau) = \omega u(\tau) + \theta(\tau)\|x(\tau)\|_\infty + \sigma(\tau)$$

If $\dot{x}(\tau)$ and $\dot{u}(\tau)$ are bounded then $\omega(\tau)$, $\theta(\tau)$ and $\sigma(\tau)$ are differentiable with finite derivatives.

The \mathcal{L}_1 adaptive controller is composed of three parts defined as the state predictor, the adaption algorithm based on projection and the feedback filter (see Figure (4.1)). The main function of the state predictor is developed based on the adaptation laws

$$\begin{aligned} \dot{\hat{x}}(t) &= A_m \hat{x}(t) + b(\hat{\omega}u(t) + \hat{\theta}\|x(t)\|_\infty + \hat{\sigma}) \\ \hat{y}(t) &= c\hat{x}(t) \end{aligned} \quad (4.6)$$

The adaptive estimates $\hat{\omega} \in \mathbb{R}$, $\hat{\theta} \in \mathbb{R}$ and $\hat{\sigma} \in \mathbb{R}$ are defined as follows

$$\begin{aligned} \dot{\hat{\omega}} &= \Gamma \text{Proj}(\hat{\omega}, -\tilde{x}^\top P b u(t)), \quad \hat{\omega}(0) = \hat{\omega}_0 \\ \dot{\hat{\theta}} &= \Gamma \text{Proj}(\hat{\theta}, -\tilde{x}^\top P b \|x(t)\|_\infty), \quad \hat{\theta}(0) = \hat{\theta}_0 \\ \dot{\hat{\sigma}} &= \Gamma \text{Proj}(\hat{\sigma}, -\tilde{x}^\top P b), \quad \hat{\sigma}(0) = \hat{\sigma}_0 \end{aligned} \quad (4.7)$$

where $\tilde{x} \triangleq \hat{x} - x(t)$, $\Gamma \in \mathbb{R}^+$ is the adaptation gain, and the solution of Lyapunov equation $A_m^\top P + P A_m = -Q$ with symmetric $P > 0$ and $Q > 0$. The projection operator ensures that $\hat{\omega} \in \Omega \triangleq [\omega_l, \omega_u]$, $\hat{\theta} \in \Theta \triangleq [-\theta_b, \theta_b]$, $|\hat{\sigma}| \leq \Delta$ with θ_b and Δ being defined in (4.2). Projection operators will be evaluated as defined in [84]

With special interest to this paper, the control law is defined as

$$u(s) = -k D(s)(\hat{\eta}(s) - k_g r(s)) \quad (4.8)$$

where $k > 0$ is a feedback gain and $D(s)$ is a strictly proper transfer function leading to a strictly proper and stable transfer function. The Laplace transforms of $r(t)$ and $\hat{\eta}(t) = \hat{\omega}u(t) + \hat{\theta}x(t) + \hat{\sigma}$ are $r(s)$ and $\hat{\eta}(s)$. Finally, k_g is a necessary feedforward gain ensuring a unity steady state gain where $k_g \triangleq -1/(cA_m^{-1}b)$; $k > 0$. Thus, after a certain transient determined by

its bandwidth, the effect of the filter will vanish from the dynamic of the closed loop system. Thus, in this case, the filter

$$C(s) = \frac{\omega k D(s)}{1 + \omega k D(s)} \quad (4.9)$$

With DC gain $C(0) = 1$. The general structure of \mathcal{L}_1 adaptive controller is depicted in Figure 4.1.

Remark 1 *The main objective of this work is to design a FLC in order to tune the feedback gain of \mathcal{L}_1 adaptive controller and ensure that $y(t)$ tracks a continuous reference signal $r(t)$. In addition, it is aimed at improving the robustness and tracking capability and reducing the control signal range when compared to \mathcal{L}_1 adaptive controller with constant parameters.*

4.3 Optimal Fuzzy-tuning of the feedback filter

FLC has been used widely for various control applications. In this work, FLC is developed in order to tune the feedback filter gain of the \mathcal{L}_1 adaptive controller. The importance of tuning this filter is crucial to improve the robustness and to reduce the control signal range.

4.3.1 Structure of Fuzzy Logic Controller

The error $e(t)$ is the difference between reference input $r(t)$ and regulated output $y(t)$. k_p and k_d are proportional and differential weights respectively. These parameters will be assigned before designing the membership functions and their values rely on the expected range of both $e(t)$ and $\dot{e}(t)$ in order to normalize fuzzy input between 1 and 0.

$$k_p \leq \frac{1}{\|e\|_\infty}, \quad k_d \leq \frac{1}{\|\dot{e}\|_\infty} \quad (4.10)$$

The existence of these norms is guaranteed by \mathcal{L}_1 adaptive controller in case of stable dynamics. In addition, they can also be dynamically assigned. The fuzzy filter has a triangular membership functions for both inputs and output. The fuzzy filter has two inputs represented by the error and its rate and one output which is the inverse of the feedback gain k_f . Fuzzy inputs are the absolute values of $e(t)$ and $\dot{e}(t)$ multiplied by weighted gains k_p and k_d . \mathcal{L}_1 adaptive controller will consider the fuzzy output k_f as a feedback gain if the error is greater than k_e . Adversely, the controller will consider a constant feedback gain k if the error is less than or equal k_e as shown in figure 4.4.

4.4 Particle Swarm Optimization

Particle swarm optimization is an intelligent evolutionary computation algorithm. PSO algorithm deploys a set of particles in the space as a population and each particle is a candidate solution. Each particle in the search space moves randomly in swarm of particles to find the optimal solution. Each solution is defined by a particle position in the space and the velocity of swarming is necessary to target the best position. The proper setting of the algorithm variables ensures swarming in the vicinity space of the optimal solution and increases the probability of fast convergence. The velocity and position of the particle are defined according to the following two equations (4.11) and (4.12) respectively

$$v_{i,j}(t) = \alpha(t)v_{i,j}(t-1) + c_1r_1(x_{i,j}^*(t-1) - x_{i,j}(t-1)) + c_2r_2(x_{i,j}^{**}(t-1) - x_{i,j}(t-1)) \quad (4.11)$$

$$x_{i,j}(t) = v_{i,j}(t) + x_{i,j}(t-1) \quad (4.12)$$

where $i = 1, 2, \dots, N_p$ and N_p is the population size, $j = 1, 2, \dots, P_s$ and P_s is the number of parameters. In each particle, $x_{i,j}^*$ and $x_{i,j}^{**}$ represent the local and global solutions respectively, $\alpha(t)$ is an exponential decreasing inertia, c_1 and c_2 represent personal and social influence of parameters and finally r_1 and r_2 are random numbers where $r_1, r_2 \in [0, 1]$. The objective function is defined to enhance the tracking capability and improve the control signal range as follows

$$Obj = \sum_{t=0}^{t_{sim}} (\gamma_1 e^2(t) + \gamma_2 u^2(t)) \quad (4.13)$$

where $e(t) = r(t) - y(t)$, $e(t)$ and $u(t)$ are the system error and control signal respectively. γ_1 and γ_2 are weights that can be selected arbitrarily. Obviously, the output membership functions have 18 parameters and they should be optimized to minimize the objective function. Particle swarm optimization is developed to search for the optimal values of aforementioned parameters. It must be noted that triangular nodes of output membership function represent position $x_{i,j}$, each two triangular intersect on the horizontal axis on one node. The computational flow diagram of PSO algorithm is illustrated in Figure 4.3. The algorithm will be used with \mathcal{L}_1 adaptive controller to define the optimal parameters of output membership functions for a specific number of generations as mentioned in [74], [1].

Remark 2 *In the proposed approach, the properties of the filter, such as strictly proper, low pass with $C(0)=1$, are preserved. Consequently, stability of the Fuzzy-based- \mathcal{L}_1 adaptive controller is guaranteed by the same analysis of stability done in [35].*

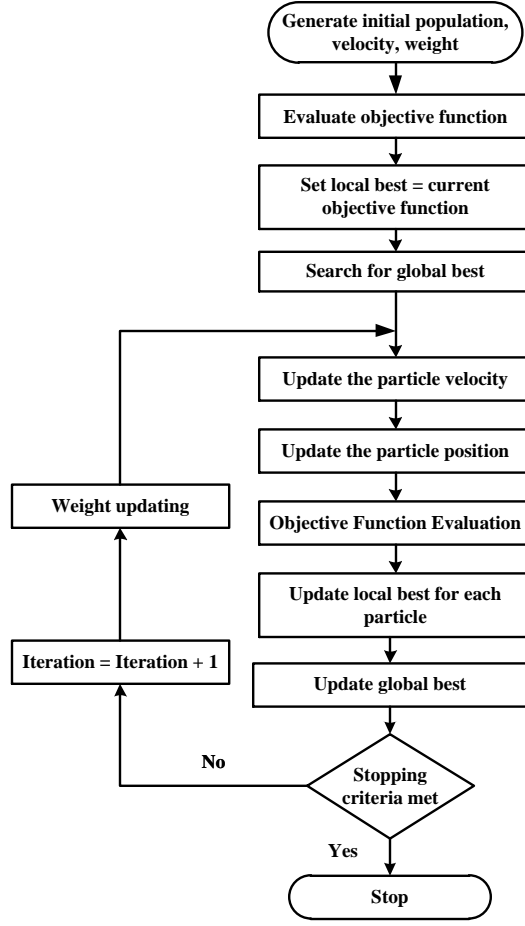


Figure 4.3: Flowchart of particle swarm Optimization [1].

4.5 Results and Discussions

4.5.1 Fuzzy \mathcal{L}_1 adaptive controller implementation:

Problem in [43] has been considered here with additive nonlinearities added to the system as follows

$$\dot{x}(t) = A_m x(t) + B(\omega u(t) + f(x(t), t))$$

$$y(t) = Cx(t)$$

where $x(t) = [x_1(t), x_2(t)]^\top$ are the system states, $u(t)$ is the control input, $y(t)$ is the regulated output and $f(t, x(t))$ includes high nonlinearity assumed to be unknown. In addition,

$$A = \begin{bmatrix} 0 & 1 \\ 0 & 0 \end{bmatrix}, \quad B = \begin{bmatrix} 0 \\ 1 \end{bmatrix}, \quad C = \begin{bmatrix} 0 & 1 \end{bmatrix}$$

and

$$f(x(t), t) = 2x_1^2(t) + 2x_2^2(t) + x_1 \sin(x_1^2) + x_2 \cos(x_2^2)$$

$$\omega = \frac{75}{s + 75}$$

ω is a function with fast dynamic to ensure smoothness of the control signal. The compact sets of the projection operators for unmodeled input parameters, uncertainties and disturbances were assigned to $[\omega_{min}, \omega_{max}] \in [0, 10]$, $\Delta = 100$ and $\theta_b = 10$. The control objective is to design a fuzzy- \mathcal{L}_1 adaptive controller to enhance each of control signal range and tracking capability of a bounded reference input $r(t)$ for the output signal $y(t)$. Desired poles are set to $-21 \pm j0.743$, the constant feedback gain(k) = 20, the adaptation gain(γ) = 1000000 and $Q = \begin{bmatrix} 1 & 0 \\ 0 & 1 \end{bmatrix}$. Fuzzy control parameters are $k_p = 0.1$, $k_d = 0.05$ and $k_e = 0.1$. Figure 4.4 illustrates the FLC with \mathcal{L}_1 adaptive controller.

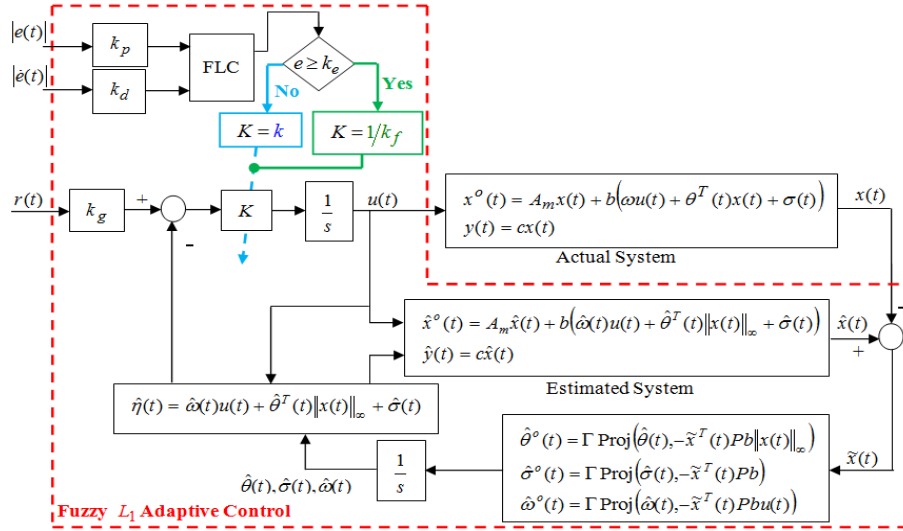


Figure 4.4: Fuzzy- \mathcal{L}_1 adaptive controller for nonlinear SISO system.

4.5.2 Membership Function Optimization

The objective of this work is to construct output membership function for FLC capable of reducing the error and the control signal. Values of input membership functions and constraints of the output membership functions were chosen based on trying different values by running a certain number of experiments. The range of input membership functions was adjusted between 0.08 and 1 and their values were selected as shown in Figure 4.5. The fuzzy inputs and output have triangular membership functions with five linguistic variables. Linguistic variables are assigned as very large (VL), large (L), small (S), very small (VS) and zero (Z) where values of input membership function will be assigned arbitrarily. Values of output membership

Table 4.1: Rule base of FLC.

$\Delta e/e$	VL	L	S	VS	Z
VL	VL	VL	VL	VL	L
L	VL	VL	VL	L	S
S	VL	VL	L	S	VS
VS	VL	L	S	VS	VS
Z	L	S	VS	VS	Z

functions are optimized using PSO. Rule base of the proposed filter is demonstrated in Table 4.1.

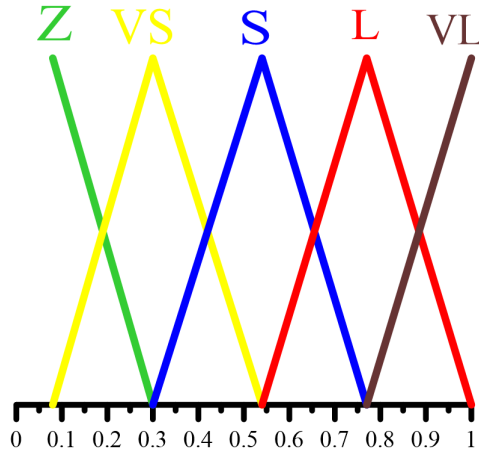


Figure 4.5: Error and rate of error membership functions.

Constraint values of output membership functions are represented by three parameters as lower (l), center (c) and higher (h) values. These three parameters of each triangular membership function will constrain between minimum and maximum bounds. Constraints bounds of the problem can be defined as follows

$$\begin{aligned}
[4, 8, 8] &\leq [VL_l, VL_c, VL_h] \leq [8, 12, 12] \\
[1.5, 3, 6] &\leq [L_l, L_c, L_h] \leq [3, 6, 10] \\
[0.3, 1.5, 4] &\leq [S_l, S_c, S_h] \leq [1.5, 4, 8] \\
[0, 0.5, 1.5] &\leq [VS_l, VS_c, VS_h] \leq [0.5, 1.5, 3] \\
[0.0, 0.0, 0.3] &\leq [Z_l, Z_c, Z_h] \leq [0.0, 0.0, 1.5]
\end{aligned} \tag{4.14}$$

With VL , ML , L , S , MS , VS and Z were mentioned before as a linguistic variables. Also, we assigned $VL_c = VL_h$, $VL_l = S_h$, $L_l = VS_h$, $S_l = Z_h$, $VS_l = z_c$ and $z_c = Z_l$ which means that we have only nine parameters to be optimized.

4.5.3 PSO Simulation results

The population size is set arbitrarily as 150 particles and each particle include 9 parameters will be optimized based on a minimization objective function and these parameter are VL_c , VL_l , L_l , L_c , L_h , S_l , S_c , VS_l and VS_c in (4.13). The initial settings of PSO algorithm are demonstrated in Table 4.2 and the maximum numbers of generations is 100.

Table 4.2: Parameters setting for PSO.

Parameter	λ	α	c_1	c_2
Settings	10	0.99	2	2

4.5.4 PSO Results

The system was simulated for 8 seconds and the data was recorded every 0.01 seconds. The reference input was defined by $\cos(0.5t)$ with zero initial conditions. The optimal variables of output triangular membership functions are illustrated in Figure 4.6. The fitness reduction during the search process is demonstrated in Figure 4.7. However, it is clear that objective function is reduced significantly and enormously to a suitable value which is reflected on the output performance as revealed in Figure 4.8. Figure 4.8.(a) demonstrates the optimal output performance and Figure 4.8.(b) shows the control signal of the considered problem.

In this study, three different scenarios are considered to demonstrate the robustness of fuzzy-

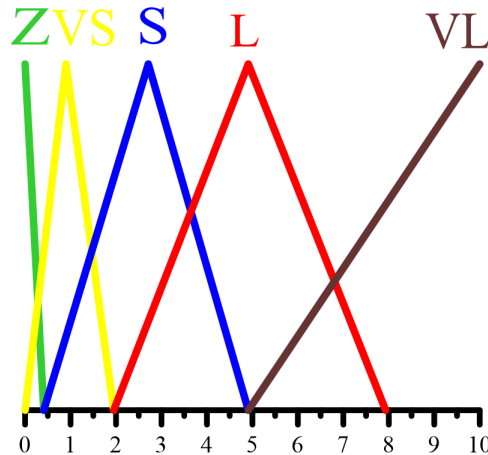


Figure 4.6: Graphical illustration of output membership functions.

\mathcal{L}_1 adaptive controller. All cases will be simulated for 40 seconds. The first case will discuss the nonlinear system included in the search process. Case 2 includes the nonlinear model with

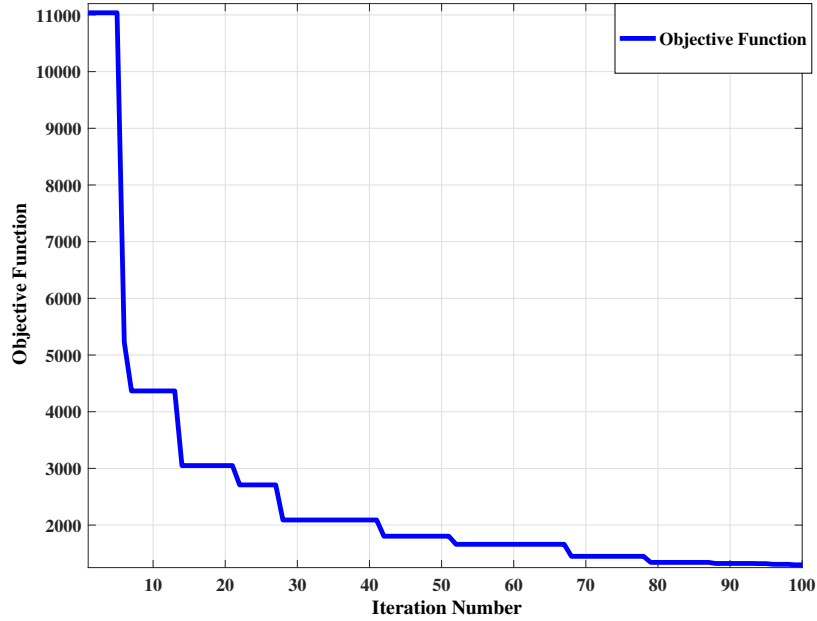


Figure 4.7: Objective function minimization with PSO search process.

high uncertainties, unmodeled input parameters and adding some disturbances in order to validate the robustness of fuzzy filter with \mathcal{L}_1 adaptive controller. Case 3 consider all assumptions in case 2 in addition to investigate the system with faster desired closed loop dynamics.

Case 1: Figure 4.9 presents the output performance of fuzzy- \mathcal{L}_1 adaptive controller versus \mathcal{L}_1 adaptive controller and their control signals. Fuzzy- \mathcal{L}_1 adaptive controller guarantees uniform transient and smooth tracking performance. In addition, its major contribution lies in reducing the control signal range by tuning the feedback gain. Tuning feedback gain enhances the robustness of the system and reduces the control signal range. The correspondence difference of feedback gain between fuzzy- \mathcal{L}_1 adaptive controller and \mathcal{L}_1 adaptive controller is illustrated in Figure 4.10.(a). The errors of both controllers are presented in Figure 4.10.(b).

Case 2: To illustrate the effectiveness of the proposed fuzzy filter with \mathcal{L}_1 adaptive controller, robustness of fuzzy filter is examined against any existing of high uncertainties, unmodeled input parameters and disturbances. Here, the nonlinear model and other assumptions mentioned in case 1 are similar the nonlinear function; however, the nonlinearity includes high time variant uncertainties and disturbances and these changes will except be presented as fol-

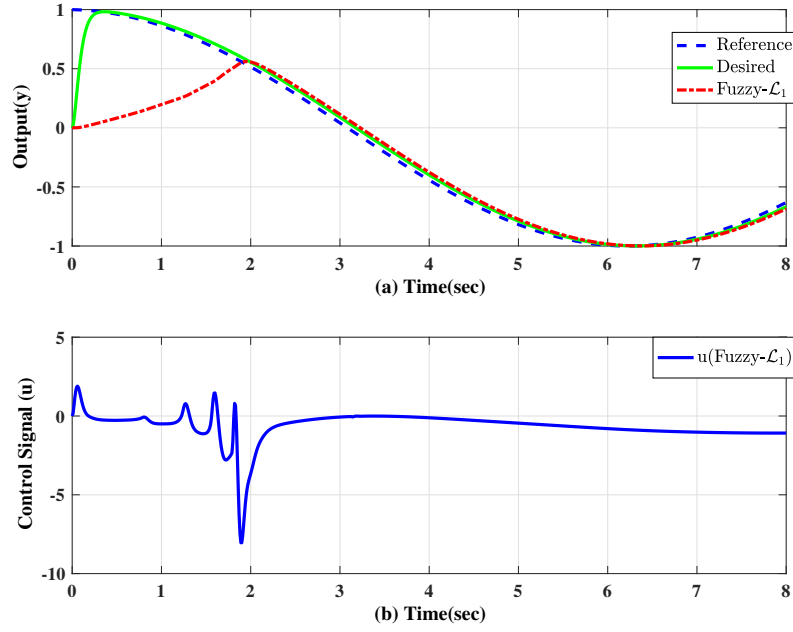


Figure 4.8: Performance of fuzzy- \mathcal{L}_1 adaptive controller after 100 iterations search process.

lows

$$\begin{aligned}
 f(x(t), t) = & (\sin(0.4t) + 1)x_1^2(t) + (2\cos(0.35t) + 0.5)x_2^2(t) \\
 & + (\sin(0.3t) + 0.3)x_1\sin(x_1^2) + \sin(0.35t)\cos(0.4t) \\
 & + 0.5x_2\cos(x_2^2 + 0.5\cos(0.3t)) + \sin(0.3t)\cos(0.4t)z^2
 \end{aligned}$$

where

$$z(s) = \frac{s-1}{s^2+3s+2}v(s), \quad v(t) = x_1\sin(0.2t) + x_2$$

The robustness of fuzzy feedback filter gain with \mathcal{L}_1 adaptive controller has been validated in Figure 4.11 and presented versus \mathcal{L}_1 adaptive controller. The significant impact and the advantage of fuzzy- \mathcal{L}_1 controller is revealed on control signals performance as shown Figure 4.11. Figure 4.12.(a) presents the performance of feedback gain for fuzzy- \mathcal{L}_1 adaptive controller and \mathcal{L}_1 adaptive controller. Finally, Figure 4.12.(b) shows the error of both controllers. Uniform transient and tracking capability are validated as shown in Figure 4.9 and 4.11. The benefits of fuzzy- \mathcal{L}_1 adaptive controller can be summarized in including fast desired dynamics and improving the tracking capability and robustness with less range of control signal.

Case 3: The robustness of fuzzy- \mathcal{L}_1 adaptive controller and \mathcal{L}_1 adaptive controller will reveal more in this case. All aforementioned assumptions in case 2 are similar here except the desired closed loop dynamics assumed to be faster than case 2. Desired poles are set to

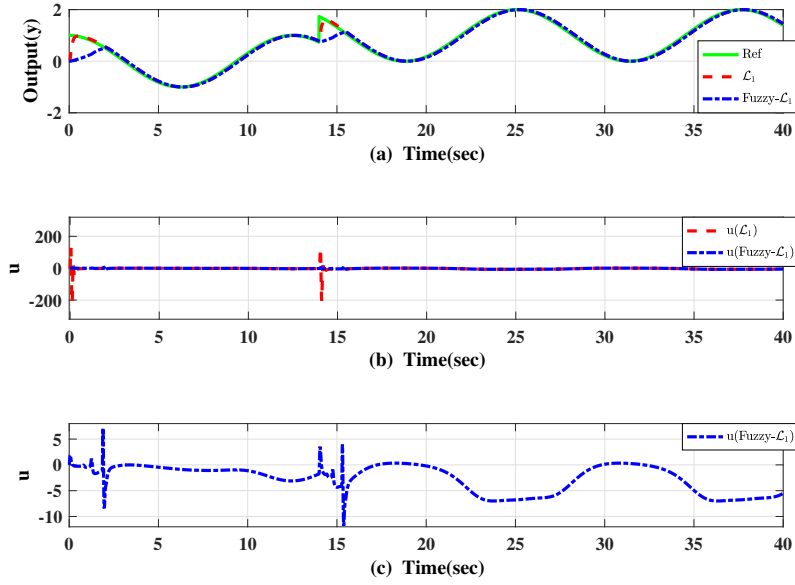


Figure 4.9: Performance of fuzzy- \mathcal{L}_1 adaptive controller and \mathcal{L}_1 adaptive controller for nonlinear system of case 1.

$p = -84 \pm j0.743$. According to this change in closed loop poles, the robustness of \mathcal{L}_1 adaptive controller will be violated and the system will no longer be stable. However, fuzzy- \mathcal{L}_1 adaptive controller will be able to track the output under this new condition with limitation in increasing the control signal range. Figure 4.13 illustrate the output performance of fuzzy- \mathcal{L}_1 adaptive controller for case 3.

The robustness of this criterion has been simulated and validated with \mathcal{L}_1 adaptive controller on high nonlinear system with different forms of nonlinearities and uncertainties in addition to fast closed loop dynamics compared to normal structure of \mathcal{L}_1 adaptive controller. It can be concluded based on the cases considered and results obtained that the proposed fuzzy-based approach to tune the feedback filter improves greatly the performance of \mathcal{L}_1 adaptive controller. The proposed fuzzy- \mathcal{L}_1 adaptive controller guarantee boundedness of the output and control signal and insures fast tracking and low range of control signal.

4.6 Conclusion

This paper presents a new FLC-PSO design of the feedback gain filter part of \mathcal{L}_1 adaptive controller. PSO determines the optimal variables of the output membership functions. The proposed algorithm tunes on-line the filter parameters, which in turn contributed to improving

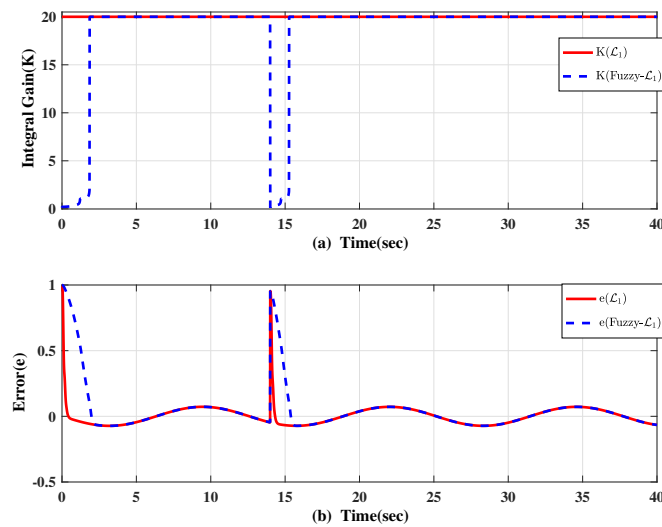


Figure 4.10: Feedback gain and output error of fuzzy- \mathcal{L}_1 adaptive controller and \mathcal{L}_1 adaptive controller of case 1.

robustness and stability of \mathcal{L}_1 adaptive controller. Moreover, owing to a smooth tuning of the filter the control signal range has been greatly reduced. Illustrative examples were developed and simulated to compare fuzzy- \mathcal{L}_1 adaptive controller with \mathcal{L}_1 adaptive controller with constant filter parameters and to validate the advantages of the proposed approach. The results show improved performance and robustness with high levels of time variant uncertainties and disturbances in addition to fast desired closed loop adaptation.

There are several directions for future work. One important area is to implement this approach on a real system and compare the performance with existing techniques. One should note that computation power is relatively cheap and the technology offers several hardware option over which this controller can be implemented. This study aimed at proposing an effective way of tuning the coefficients of the control filter. During this work, the structure of the filter was fixed. Extending this work to determine automatically the appropriate filter's structure has the potential to further improve the robustness and stability. Such an extension will take into account the health of the system and may lead to the design a failure tolerant robust controller. In this study, PSO has been implemented off-line. To our knowledge, recursive PSO for online implementation is not explored. A recursive and online PSO will impose hard constraints on hardware capacity. The implementation of PSO as it is now is not feasible for online control implementation. A comparison between PSO and other evolutionary algorithms can be established to define the most effective solution for the fuzzy- \mathcal{L}_1 adaptive control problem.

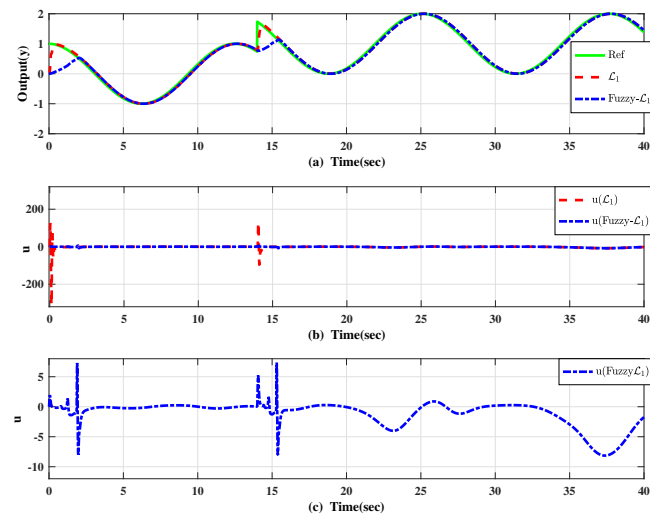


Figure 4.11: Performance of fuzzy- \mathcal{L}_1 adaptive controller and \mathcal{L}_1 adaptive controller for non-linear system of case 2.

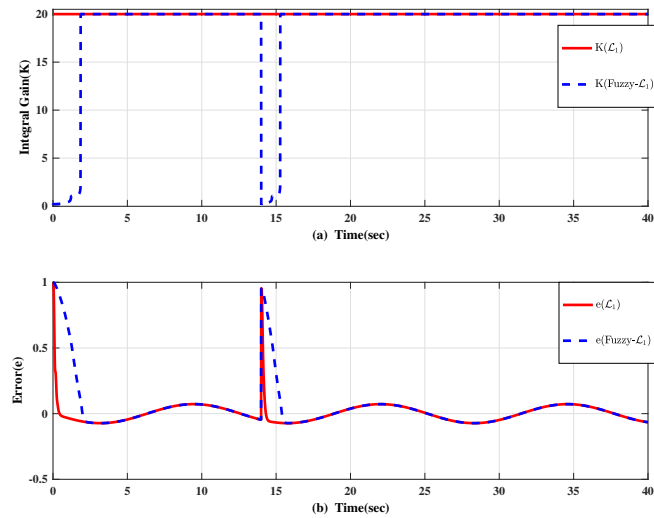


Figure 4.12: Feedback gain and output error of fuzzy- \mathcal{L}_1 adaptive controller and \mathcal{L}_1 adaptive controller of case 2.

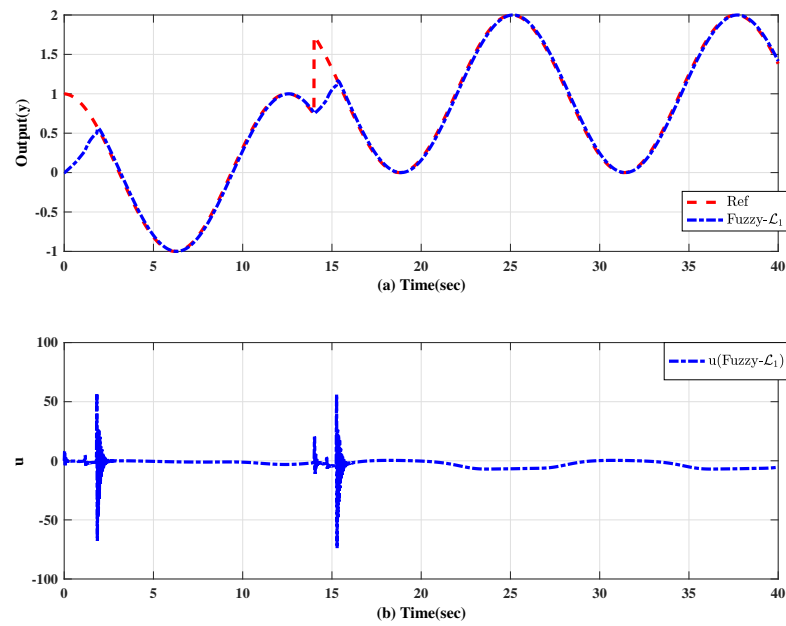


Figure 4.13: Performance of fuzzy- \mathcal{L}_1 adaptive controller for nonlinear system of case 3.

Chapter 5

NEURO-ADAPTIVE FOR STRICT FEEDBACK MIMO SYSTEMS WITH PPF

5.1 Introduction

This chapter is mainly concerned in reproducing recent study of robust neuro adaptive control with prescribed performance function on strict feedback MIMO system. The importance of this chapter relies on capturing prescribed performance idea on transient performance, tracking trajectory and smoothness of the control signal. This chapter consists of six sections with first section is an introduction. The second section presents introduction and necessary conditions of prescribed performance. The third section describes the problem formulation and the main idea of prescribed performance function. The fourth section presents neural network for nonlinearity approximation. Section five includes control law formulation and stability analysis. Section six presents simulation and controller benchmark results. The last section is a conclusion.

5.2 Introduction of Prescribed Performance

Prescribed performance simply means tracking error into an arbitrarily small residual set and the convergence error should be within pre-assigned range. In addition, the convergence rate has to be less than a prescribed value and maximum overshoot should be less than a prescribed constant. Prescribed performance with robust adaptive control was mainly developed to provide a smooth control signal for soft tracking and to solve the problem of accurate com-

putation of the upper bounds for systematic convergence. Due to nonexistence adaptive control for nonlinear systems with error convergence into a predefined small set, the controller with prescribed performance function is demanded. In this chapter, robust adaptive control with prescribed performance should have the ability to approximate the nonlinear model assuming completely unknown dynamics and provide smooth control signal to track the output into the desired trajectory smoothly and accurately.

The main features of the prescribed performance is its ability of tracking the error into a defined small set. Prescribed performance should guarantee many factors

- the convergence of the error within a prescribed bound,
- a maximum overshoot less than a prescribed value,
- a uniform ultimate boundedness property for the transformed output error,
- adaptive and smooth tracking.

Neural network will be used to estimate the nonlinear model as an online estimation tool in the adaptive control problem. Adaptive control will be offered to stabilize the system by canceling undesired dynamics using neural network. Also, it will be used to provide robust tracking and forcing the error to be bounded in predefined set. The prescribed set will be reduced into a very small set according to a pre-assigned prescribed performance function. Number of neurons of the neural network and their types are defined based on try and error which can be considered as a main drawback of this method.

The work in this section is mainly based on reproducing [23] to catch the idea of prescribed performance function and to evaluate the function with adaptive control.

5.3 Problem Formulation and Preliminaries

For compactness and easy reading of the chapter, this section presents the concept of prescribed performance (for more details the reader is invited to consult [23]).

Consider the general case of nonlinear affine system as follows

$$\begin{aligned}
 x_1^{(n_1)} &= f_1(x) + g_{11}(x)u_1 + \cdots + g_{1m}(x)u_m \\
 &\vdots \\
 x_m^{(n_m)} &= f_m(x) + g_{m1}(x)u_1 + \cdots + g_{mm}(x)u_m
 \end{aligned} \tag{5.1}$$

which can be adequately written in the form:

$$x^{(n)} = f(x) + G(x)u$$

where

$$\begin{aligned} x^{(n)} &= \begin{bmatrix} x_1^{(n_1)} & \cdots & x_m^{(n_m)} \end{bmatrix}^\top \\ f(x) &= \begin{bmatrix} f_1(x) & \cdots & f_m(x) \end{bmatrix}^\top \\ G(x) &= \begin{bmatrix} g_{11}(x) & \cdots & g_{1m}(x) \\ \vdots & \ddots & \vdots \\ g_{m1}(x) & \cdots & g_{mm}(x) \end{bmatrix} \end{aligned}$$

The use of Prescribed performance with robust adaptive control demand considering four basic assumptions.

Assumption 14 *The matrix $\frac{G(x)G^\top(x)}{2}$ has to be known with either uniformly positive definite or uniformly negative definite for all $x \in \Omega_x$ where $\Omega_x \subseteq \mathbb{R}^n$ is a compact set to guarantee system controllability.*

$$\underline{\sigma}\left(\frac{G(x)G^\top(x)}{2}\right) \geq g^* > 0 \quad \forall x \in \Omega_x \quad (5.2)$$

where $\underline{\sigma}(W)$ is the smallest singular value of the matrix W and g^* represents its lower bound. In addition, if $G(x)$ satisfies Assumption 14 then system is uniformly strongly controllable [23].

Assumption 15 *The desired trajectories are known bounded functions of time with bounded known derivatives.*

Assumption 16 *The system states are available for measurement.*

Assumption 17 *The functions $f_i(x)$ and $g_{ij}(x)$, $i, j = 1, \dots, m$ are continuous but otherwise completely unknown.*

Prescribed performance can be defined as the effort of tracking a generic error

$e(t) = [e_1(t), e_2(t), \dots, e_m(t)] \in \mathbb{R}^n$ such that each element of $e(t)$ evolves within PPB in a form of decaying functions of time that define the range of the residual error, the speed of convergence to the residual set, and the allowable overshoot or undershoot. In addition, prescribed performance with robust adaptive control was mainly developed to provide an adequate command signal for smooth tracking and solve the problem of accurate computation of the transient

and steady state error bounds by guarantying uniform ultimate boundedness property of the error.

A smooth function $\rho_i(t) : \mathbb{R}_+ \rightarrow \mathbb{R}_+$ is defined as a performance function associated with error component $e_i(t)$, $i = 1, \dots, m$, if $\rho_i(t)$ is positive, decreasing and $\lim_{t \rightarrow \infty} \rho_i(t) = \rho_{i\infty} > 0$.

5.3.1 Performance Functions

A smooth function $\rho_i(t) : \mathbb{R}_+ \rightarrow \mathbb{R}_+$ is defined as a performance function associated with error component $e_i(t)$, $i = 1, \dots, m$, if $\rho_i(t)$ is positive, decreasing and $\lim_{t \rightarrow \infty} \rho_i(t) = \rho_{i\infty} > 0$. A possible choice of such function can be

$$\rho_i(t) = (\rho_{i0} - \rho_{i\infty}) \exp^{-\ell_i t} + \rho_{i\infty} \quad (5.3)$$

where $\rho_{i0}, \rho_{i\infty}$ and ℓ_i are appropriately defined positive constants. The control objective is to guarantee that

$$-\delta_i \rho_i(t) < e_i(t) < \rho_i(t), \quad \text{if } e_i(0) > 0 \quad (5.4)$$

$$-\rho_i(t) < e_i(t) < \delta_i \rho_i(t), \quad \text{if } e_i(0) < 0 \quad (5.5)$$

for all $t \geq 0$ and $0 \leq \delta_i \leq 1$, and $i = 1, \dots, m$. Figure 5.1 illustrates the prescribed performance function and tracking error evolving from a large to a small set as per equations (5.4) and (5.5).

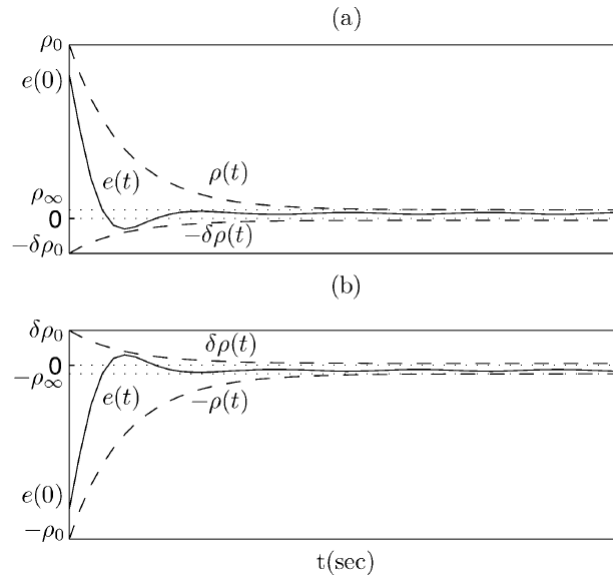


Figure 5.1: Graphical illustration of PPF for the tracking error behavior (a) graphical illustration of (5.4); (b) graphical illustration of (5.5).

Error Transformation

To implement the prescribing performance, one needs to solve a constrained control problem. To avoid such difficulty, the following error transformation is used

$$\epsilon_i = T_i\left(\frac{e_i(t)}{\rho_i(t)}\right) \quad (5.6)$$

or equivalently,

$$e_i(t) = \rho_i(t) S(\epsilon_i) \quad (5.7)$$

where ϵ_i , $i = 1, 2, \dots, m$ is the transformed error and $S_i(\cdot)$ and $T_i^{-1}(\cdot)$ are two smooth functions such that $S_i(\cdot) = T_i^{-1}(\cdot)$ and $S_i(\cdot)$ satisfy the following properties:

1. $S_i(\epsilon_i)$ is smooth and strictly increasing.
2. $-\delta_i < S_i(\epsilon_i) < 1$, if $e_i(0) > 0$
 $-1 < S_i(\epsilon_i) < \delta_i$, if $e_i(0) < 0$
3. $\left. \begin{aligned} \lim_{\epsilon_i \rightarrow -\infty} S_i(\epsilon_i) &= -\delta_i \\ \lim_{\epsilon_i \rightarrow +\infty} S_i(\epsilon_i) &= 1, \end{aligned} \right\} \quad \text{if } e_i(0) \geq 0$
 $\left. \begin{aligned} \lim_{\epsilon_i \rightarrow -\infty} S_i(\epsilon_i) &= -1 \\ \lim_{\epsilon_i \rightarrow +\infty} S_i(\epsilon_i) &= \delta_i, \end{aligned} \right\} \quad \text{if } e_i(0) < 0$

where

$$S(\epsilon) = \begin{cases} \frac{\bar{\delta}e^\epsilon - \underline{\delta}e^{-\epsilon}}{e^\epsilon + e^{-\epsilon}}, & \bar{\delta} = 1 \text{ and } \underline{\delta} = 0 \text{ if } e(0) \geq 0 \\ \frac{\bar{\delta}e^\epsilon - \underline{\delta}e^{-\epsilon}}{e^\epsilon + e^{-\epsilon}}, & \underline{\delta} = 1 \text{ and } \bar{\delta} = 0 \text{ if } e(0) < 0 \end{cases} \quad (5.8)$$

One should note that the overshoot/undershoot in equation (5.8) is assumed to be zero.

where the overshoot in equation (5.8) assumed to be zero. To continue, an error transformation that modulates $e_i(t)$ with respect to the corresponding performance bounds has to be defined. More specifically, we define the following transformed errors:

$$\epsilon = S^{-1}\left(\frac{\rho(t)}{e(t)}\right) \quad (5.9)$$

Next a metric error $E(t)$ will be defined to describe the system dynamics in a new form of system error.

$$E_i(t) = \left(\frac{d}{dt} + \lambda_i\right)^{n-1} \epsilon_i \quad (5.10)$$

$$\dot{E}(t) = V + R\dot{x} \quad (5.11)$$

where $\dot{E}(t) = [E_1 \ \cdots \ E_n]^\top$ and $V = [v_1 \ \cdots \ v_n]^\top$.

$$R = \begin{bmatrix} \frac{1}{2\rho_1(t)}(\partial S_1^{-1}/\partial(\frac{\rho_1(t)}{e_1(t)})) & \cdots & 0 \\ \vdots & \ddots & \vdots \\ 0 & \cdots & \frac{1}{2\rho_n(t)}(\partial S_n^{-1}/\partial(\frac{\rho_n(t)}{e_n(t)})) \end{bmatrix} \quad (5.12)$$

Equations (5.11) and (5.12) can be driven easily. All foregoing equations in addition to approximated nonlinear model will be implemented in order to define the required control signal. Online training of linearly parameterized neural network is mainly implemented to estimate the nonlinear model as presented in the following subsection.

5.4 Neural Approximations

Neural network with linear parameterization can be expressed by the following relation

$$y = Z^\top(x)\theta \quad (5.13)$$

where $y \in \mathbb{R}^m$ is the neural net output, $x \in \mathbb{R}^n$ is the neural input, $\theta \in \mathbb{R}^p$ is a p-dimensional vector of synaptic weights and $Z(x)$ is a p-dimensional vector of regressor terms. Regressor terms may include high order functions of radial basis function [85], sigmoid functions [86] and shifted sigmoids [87] are defined as high order neural network.

The nonlinear system is considered to be unknown functions and may be represented by one layer neural network structure with linear in weights plus modeling error term $\forall x \in \Omega_x$ obtaining:

$$f(x) = Z_f^\top(x)\theta^* + \omega_f(x) \quad (5.14)$$

$$G(x) = \begin{bmatrix} Z_{G_{11}}^\top(x)\theta^* & \cdots & Z_{G_{1m}}^\top(x)\theta^* \\ \vdots & \ddots & \vdots \\ Z_{G_{m1}}^\top(x)\theta^* & \cdots & Z_{G_{mm}}^\top(x)\theta^* \end{bmatrix} + \omega_G(x) \quad (5.15)$$

where $Z_f(x) = [Z_{f_1}(x) \ \cdots \ Z_{f_m}(x)]$, $Z_{f_i}(x)$ and $Z_{G_{ij}}(x) \in \mathbb{R}^p, i, j = 1, \dots, m$ are selected basis functions and $\theta^* \in \mathbb{R}^p$ are constants but unknown parameters which are used to minimize the approximation errors $\omega_f(x), \omega_G(x) \forall x \in \Omega_x$. Number of regressor p should be chosen appropriately and sufficiently large in order to have a suitable representation of the nonlinear system. The approximated errors $\omega_f(x), \omega_G(x)$ should satisfy the following conditions

$$\|\omega_f(x)\| \leq W_f, \forall x \in \Omega_x \quad (5.16)$$

$$\|\omega_G(x)\| \leq W_G, \forall x \in \Omega_x \quad (5.17)$$

where $W_f > 0$ and $W_G > 0$ and they are constants.

Furthermore, if we define:

$$f(x, \theta) = Z_f^\top(x)\theta \quad (5.18)$$

$$G(x, \theta) = \begin{bmatrix} Z_{G_{11}}^\top(x)\theta & \cdots & Z_{G_{1m}}^\top(x)\theta \\ \vdots & \ddots & \vdots \\ Z_{G_{m1}}^\top(x)\theta & \cdots & Z_{G_{mm}}^\top(x)\theta \end{bmatrix} \quad (5.19)$$

Then, defining the control law require the following variables

$$F_G(x, \theta)v = A_F(x, \theta)\theta \quad (5.20)$$

where

$$A_F(x, \theta) = \begin{bmatrix} Z_{G_{11}}^\top(x)v_1 + \cdots + Z_{G_{1m}}^\top(x)v_m \\ \vdots \\ Z_{G_{m1}}^\top(x)v_1 + \cdots + Z_{G_{mm}}^\top(x)v_m \end{bmatrix} \quad (5.21)$$

5.5 Robust Adaptive Control Design

The control law may be formulated as following

$$u = v_a - (\eta_{G_a}|v_a|^2 + \eta_{G_b}|v_b|^2) \frac{R^\top E}{\text{sign}(G(x))} \quad (5.22)$$

$$v_a(x, \hat{\theta}) = -\frac{\text{Adj}(F_G(x, \hat{\theta}))\text{Det}(F_G(x, \hat{\theta}))}{\text{Det}^2(F_G(x, \hat{\theta})) + \delta_d} v_b(x, \hat{\theta}) \quad (5.23)$$

$$v_b(x, \hat{\theta}) = F_f(x, \hat{\theta}) + R^{-1}V + kR^{-1}E + n_f R^\top + E \quad (5.24)$$

For $\eta_{G_a}, \eta_{G_b}, n_f, k$ and δ_d are positive constants and $F_f(x, \hat{\theta})$ and $F_G(x, \hat{\theta})$ are the approximations of $f(x)$ and $G(x)$. δ_d is necessary to make equation (5.23) free of singularities. In order to validate equations (5.22), (5.23) and (5.24), let's formulate Lyapunov candidate function as

$$L = \frac{1}{2}E^\top E + \frac{1}{2}\tilde{\theta}^\top \Gamma^{-1} \tilde{\theta} \quad (5.25)$$

$$\dot{L} = \frac{1}{2}\dot{E}^\top E + \frac{1}{2}E^\top \dot{E} + \frac{1}{2}\dot{\tilde{\theta}}^\top \Gamma^{-1} \tilde{\theta} + \frac{1}{2}\tilde{\theta}^\top \Gamma^{-1} \dot{\tilde{\theta}}$$

$$\dot{L} = \frac{1}{2}(V + R(f(x) + G(x)u))^\top E + \frac{1}{2}E^\top (V + R(f(x) + G(x)u)) + \frac{1}{2}\dot{\tilde{\theta}}^\top \Gamma^{-1} \tilde{\theta} + \frac{1}{2}\tilde{\theta}^\top \Gamma^{-1} \dot{\tilde{\theta}}$$

And after some manipulations, next equation will be chosen to validate global stability of the control law

$$\dot{\hat{\theta}} = \Gamma((Z_f^\top(x) + A_F(x, v_a))^\top R^\top E - \sigma(\theta - \theta_0)) \quad (5.26)$$

Where $\sigma > 0$ and θ_0 a parameter vector used to incorporate a good guess of θ . Finally, \dot{L} will be equivalent to

$$\begin{aligned} \dot{L} \leq & -k|E|^2 - \frac{\sigma}{2}|\tilde{\theta}|^2 - \eta_f|R^\top E|^2 + |R^\top E|W_f + |R^\top E|^2|v_a|W_G \\ & - \eta_{G_a}g^*|v_a|^2|R^\top E|^2 + |R^\top E||v_b| - \eta_{G_b}g^*|v_b|^2|R^\top E|^2 + \frac{\sigma}{2}|\theta^* - \theta|^2 \end{aligned}$$

Finally we will have

$$\dot{L} \leq -k|E|^2 - \frac{\sigma}{2}|\tilde{\theta}|^2 + \frac{W_f^2}{4\eta_f} + \frac{W_G^2}{4\eta_{G_a}g^*} + \frac{1}{4\eta_{G_b}g^*} + \frac{\sigma}{2}|\theta^* - \theta|^2$$

and if we choose $d = \frac{W_f^2}{4\eta_f} + \frac{W_G^2}{4\eta_{G_a}g^*} + \frac{1}{4\eta_{G_b}g^*} + \frac{\sigma}{2}|\theta^* - \theta|^2$, then the value of d will be reflected on the value of E or/and $\tilde{\theta}$. For more details look [23].

5.6 Problem Simulation and Results

Consider equations of motion of 2 DOF planner robot in example 3.3.1, the nonlinear plant assumed to be completely unknown. Single layer neural network with 30 neurons sigmoid basis function were used to estimate the system nonlinearities $-M^{-1}(q)(C(\dot{q}, q)\dot{q} + G_0(q))$ and $M^{-1}(q)$. The parameters of the sigmoid basis function $\zeta_j(x) = 1/(1 + e^{-\omega_j^\top - b_j})$ with $\omega_j \in \mathbb{R}^4$, $b_j \in \mathbb{R}^4$, $j = 1, 2, \dots, 30$ were chosen by off-line training try and error on the simulation then kept constant throughout the simulation. θ_0 is a vector represents the good guess of the initial conditions of the parameter estimates and was taken to be a zero vector referring to completely unknown nonlinear dynamics.

The robot assumed to start initially from the origin while the desired trajectory for both angles were chosen to be

$$q_d = \begin{bmatrix} 0.5\cos(0.7t) & -0.6\cos(0.65t) \end{bmatrix}^\top$$

Prescribed performance function was chosen as

$$\rho_i(t) = (\rho_{i0} - \rho_{i\infty})e^{-l_i t} + \rho_{i\infty}, \quad i = 1, 2$$

Prescribed performance parameters are demonstrated in table 5.1 and parameters of controller are defined table 6.1

Table 5.1: Prescribed performance function parameters

ρ_{10}	$\rho_{1\infty}$	l_1	ρ_{20}	$\rho_{2\infty}$	l_2
1.1	0.005	2.0	1.1	0.005	2.0

Table 5.2: Adaptive PPF Controller parameters

k	n_f	η_{G_a}	η_{G_b}	δ_d	σ	Γ	λ_1	λ_2
0.5	0.2	0.2	0.2	0.1	7.5	0.11	0.75	0.75

In figure 5.2, angular positions of both actual and desired trajectory had verified the control efficacy. Figure 5.3 demonstrates the smoothness of the control signal along the trajectory. Figure 5.4 presents bounds of the prescribed performance function and verify that the error of each joint is bounded within a large set and ended within a small preassigned set. Finally, transformed errors both joints are demonstrated in figure 5.4.

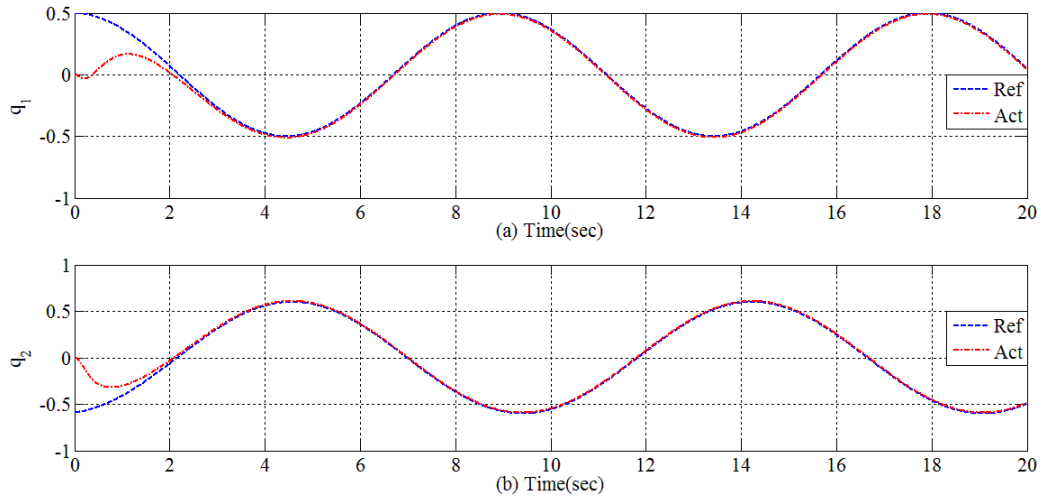


Figure 5.2: Output response of the robust adaptive control with PPF for q_1 and q_2 versus desired trajectory q_{d1} and q_{d2}

5.7 Conclusion

This chapter illustrated the significant role of prescribed performance function with robust adaptive control. The main idea of Prescribed performance has been gained and the controller showed smoothness in the control signal and impressive tracking performance. In a subsequent

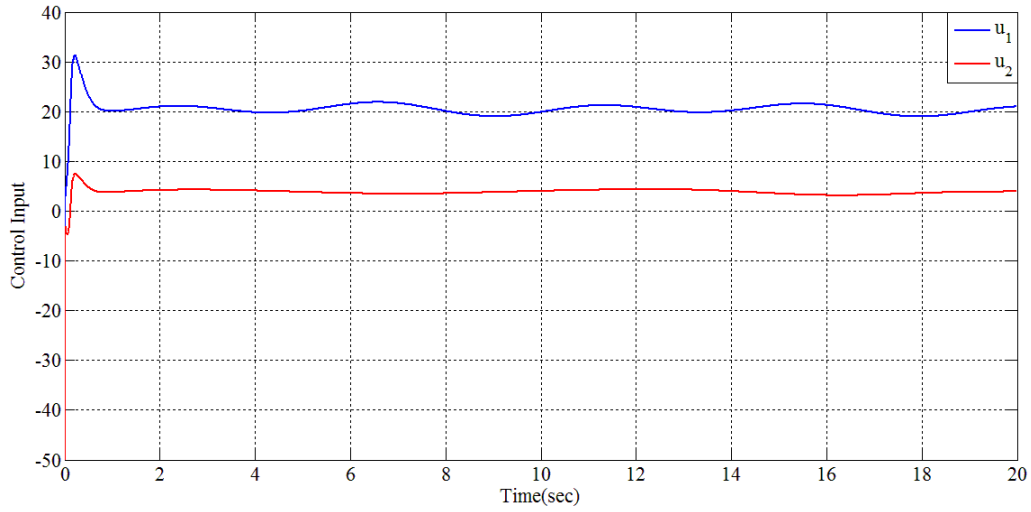


Figure 5.3: Control input provided by robust adaptive control with PPF where u_1 is τ_1 and u_2 is τ_2 .

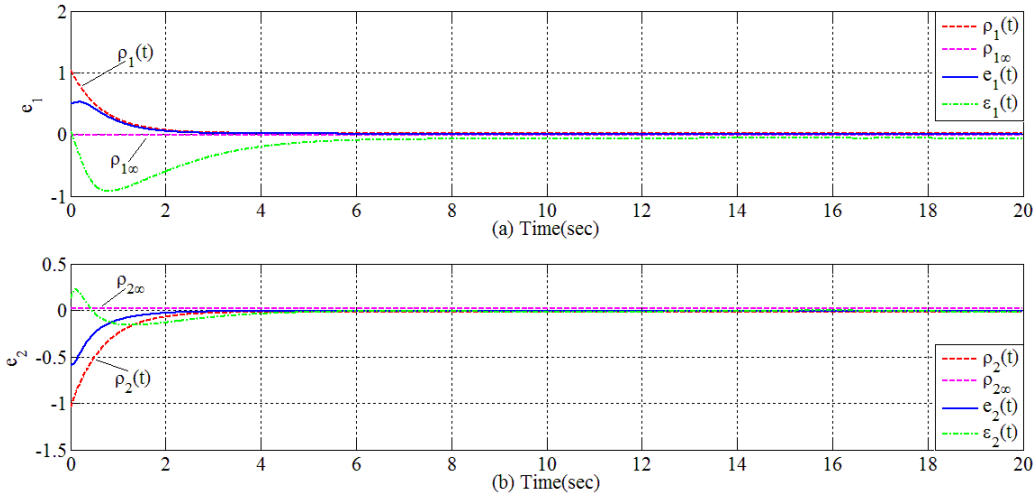


Figure 5.4: Prescribed error bounds between ρ_0 and ρ_∞ and ϵ for both joints (a) q_1 and (b) q_2 .

chapter, new controller stands on PPF will be developed relies on the result of this chapter.

Chapter 6

ROBUST MRAC WITH PPF FOR NONLINEAR MIMO SYSTEMS

6.1 Introduction

In this work, we are motivated by the limitations of the studies presented in the literature and mentioned in chapter 3 and 5 to propose a robust MRAC with PPF. We show that the robust stabilization of the transformed error guaranties the stability and convergence of the constrained tracking error within the set of time varying constraints representing the performance limits. Simulation results benchmark the performance of the proposed approach with \mathcal{L}_1 adaptive control and neuro-adaptive control with prescribed performance. The rest of the chapter is organized as follows. In section two, the problem formulation with important remark are presented. The design and analysis of the proposed robust MRAC-PPF, which represents the main contribution, is presented in section three. In section four, simulation results verify the effectiveness of the proposed control and show that the MRAC-PPF considerably improves the transient performance when compared to \mathcal{L}_1 adaptive control and Neuro-Adaptive controller with PPF. We conclude the chapter in section five.

6.2 Problem Formulation

We consider the following uncertain system defined by

$$\begin{aligned}\dot{x} &= Ax(t) + Bu(t) + \theta^\top x(t) + \Delta f(x, u, t) + d(t), \quad x(0) = x_0. \\ y(t) &= Cx(t).\end{aligned}\tag{6.1}$$

where Δf is an unknown uncertainty and $d(t)$ is the system unknown but bounded disturbance. And Let the desired dynamics be defined as following

$$\dot{x}_m(t) = A_m x(t) + B_m r(t), \quad B_m = B k_g. \quad (6.2)$$

where A_m is a Hurwitz matrix, and both pairs (A, B) and (A_m, B) are controllable. Consider $u(t) = u_m(t) + u_{ad}(t)$ where $u_m(t) = -k_m x(t)$ and k_m is a state feedback gain such that $A_m = A - k_m x(t)$.

$$\dot{x}(t) = A_m x(t) + B u_{ad}(t) + \theta^\top x(t) + \Delta f(x, u, t) + d(t) \quad (6.3)$$

Remark B is not necessary a square matrix but satisfies

$$\underline{\sigma}\left(\frac{B B^\top}{2}\right) \geq g^* > 0 \quad (6.4)$$

$A \in \mathbb{R}^{n \times n}$, $B \in \mathbb{R}^{n \times m}$, $x(t) \in \mathbb{R}^n$, $u(t)$ and $r(t)$ are $\in \mathbb{R}^m$, $\Delta f(x, u, t) \in \mathbb{R}^n$ and $d(t) \in \mathbb{R}^n$.

Let the error be $e = x - x_m$, then

$$\dot{e} = \dot{x} - \dot{x}_m = A_m e + B(u_{ad} - k_g r) + \theta^\top x(t) + \Delta f(x, u, t) + d(t) \quad (6.5)$$

6.3 Controller Structure

Let

$$e(t) = \rho(t) S(\epsilon) \quad (6.6)$$

$$\rho(t) = (\rho_0 - \rho_\infty) e^{-lt} + \rho_\infty \quad (6.7)$$

the transformed error is then

$$\epsilon = S^{-1}\left(\frac{\rho(t)}{e(t)}\right) \quad (6.8)$$

where

$$S(\epsilon) = \begin{cases} \frac{\bar{\delta} e^\epsilon - \underline{\delta} e^{-\epsilon}}{e^\epsilon + e^{-\epsilon}}, & \bar{\delta} = 1 \text{ and } \underline{\delta} = 0 \text{ if } e(0) \geq 0 \\ \frac{\bar{\delta} e^\epsilon - \underline{\delta} e^{-\epsilon}}{e^\epsilon + e^{-\epsilon}}, & \bar{\delta} = 1 \text{ and } \underline{\delta} = 0 \text{ if } e(0) \geq 0 \end{cases} \quad (6.9)$$

and

$$\epsilon = S^{-1}\left(\frac{\rho(t)}{e(t)}\right) = \frac{1}{2} \ln(\underline{\delta} + e(t)/\rho(t)) - \frac{1}{2} \ln(\bar{\delta} - e(t)/\rho(t)) \quad (6.10)$$

Let

$$\frac{1}{2\rho(t)} (\partial S^{-1}(\epsilon)/\epsilon) = \frac{1}{2\rho(t)} \left(\frac{1}{\underline{\delta} + e(t)/\rho(t)} - \frac{1}{e(t)/\rho(t) - \bar{\delta}} \right) \quad (6.11)$$

which can be written in matrix form as

$$\Gamma = \begin{pmatrix} \frac{1}{2\rho_1(t)}(\partial S^{-1}(\epsilon_1)/\epsilon_1) & \cdots & 0 \\ \vdots & \ddots & \vdots \\ 0 & \cdots & \frac{1}{2\rho_n(t)}(\partial S^{-1}(\epsilon_n)/\epsilon_n) \end{pmatrix}$$

Let

$$\Phi = -\Gamma \begin{pmatrix} e_1(t)/\rho_1(t) & \cdots & 0 \\ \vdots & \ddots & \vdots \\ 0 & \cdots & e_n(t)/\rho_n(t) \end{pmatrix}$$

$$\epsilon = \begin{pmatrix} \epsilon_1 \\ \vdots \\ \epsilon_n \end{pmatrix}$$

and

$$\rho = \begin{pmatrix} \rho_1 \\ \vdots \\ \rho_n \end{pmatrix}$$

then

$$\dot{\epsilon} = \Gamma \dot{\epsilon} + \Phi \dot{\rho} = \Gamma(A_m e + B(u_a d - k_g r) + \theta^\top x(t) + \Delta f(x, u, t) + d(t)) + \Phi \dot{\rho} \quad (6.12)$$

Let

$$\gamma(x) = \theta^\top x(t) + \Delta f(x, u, t) + d(t) \quad (6.13)$$

Assume

$$\gamma(x) = \theta^\top x(t) + \sigma^\top \psi(x, u) + \alpha(x, u) \quad (6.14)$$

where $\alpha(x, u)$ represents all the unknown nonlinear in parameters terms such that $\alpha(x) \leq \bar{\alpha}_i$.

Let

$$V = \Gamma(A_m e - Bk_g r) + \Phi \dot{\rho} \quad (6.15)$$

and define

$$V_n = \Gamma^{-1} V \quad (6.16)$$

Consider

$$\hat{\gamma}(x) = \hat{\theta}^\top x(t) + \hat{\sigma}^\top \psi(x, u) \quad (6.17)$$

where $(\hat{\cdot})$ stands for the estimate. Then

$$\begin{aligned}
 \gamma(x) - \hat{\gamma}(x, \hat{\theta}, \hat{\sigma}) &= \tilde{\theta}^\top x(t) + \tilde{\sigma}^\top \psi(x) + \alpha(x). \\
 \tilde{\theta} &= \hat{\theta} - \theta, \tilde{\sigma} = \hat{\sigma} - \sigma \\
 \epsilon^\top \dot{\epsilon} &= \epsilon^\top (\Gamma(-\hat{\gamma}(x, \hat{\theta}, \hat{\sigma}) - V_n) + V) \\
 \epsilon^\top \dot{\epsilon} &= - \sum_{i=1}^n \epsilon_i \Gamma_{i,i} \tilde{\theta}_{:,i}^\top x(t) - \sum_{i=1}^n \epsilon_i \Gamma_{i,i} \tilde{\sigma}_{:,i}^\top \psi(x) + \sum_{i=1}^n \epsilon_i \Gamma_{i,i} \bar{\alpha}_i
 \end{aligned} \tag{6.18}$$

It is important to notice that

$$\begin{aligned}
 \tilde{\theta}_{:,i}^\top \hat{\theta}_{:,i} &= \frac{1}{2} \tilde{\theta}_{:,i}^\top \tilde{\theta}_{:,i} + \frac{1}{2} (\hat{\theta}_{:,i} - \theta_{:,i})^\top (\hat{\theta}_{:,i} + \theta_{:,i}) \geq \frac{1}{2} \tilde{\theta}_{:,i}^\top \tilde{\theta}_{:,i} - \frac{1}{2} \theta_{:,i}^\top \theta_{:,i} \\
 -\tilde{\theta}_{:,i}^\top \hat{\theta}_{:,i} &\leq -\frac{1}{2} \tilde{\theta}_{:,i}^\top \tilde{\theta}_{:,i} + \frac{1}{2} \theta_{:,i}^\top \theta_{:,i}
 \end{aligned}$$

The control signal can be selected as

$$u_{ad}(t) = B^{-1}(-\hat{\theta}^\top x(t) - \hat{\sigma}^\top \psi(x) - V_n) + u_r(t) \tag{6.19}$$

where B^{-1} can be replaced by its Moore–Penrose inverse when it is not square owing to Assumption. Let the adaption rules for $\hat{\theta}$ and $\hat{\sigma}$ be defined as follows respectively

$$\dot{\hat{\theta}}_{:,i} = -\gamma_{1i} \epsilon_i \Gamma_{i,i} x(t) \tag{6.20}$$

$$\dot{\hat{\sigma}}_{:,i} = \int_0^\infty \Gamma_{i,i} (-\gamma_{2i} |\epsilon_i| v_i \hat{\sigma}_{:,i} + \gamma_{2i} \epsilon_i \psi(x)) d\tau - \beta_i \delta_i \tag{6.21}$$

$$\delta_i = \gamma_{2i} |\epsilon_i| v_i \hat{\sigma}_{:,i} + \gamma_{2i} \epsilon_i \psi(x) \tag{6.22}$$

$$\hat{\alpha} \geq \bar{\alpha}_i + \frac{1}{2} \|\sigma_{:,i}\|^2 \Gamma_{i,i} v_i \tag{6.23}$$

and the robustifying term

$$u_r = [u_{ri}] = [-\text{sign}(\epsilon)_i \cdot \hat{\alpha}] \tag{6.24}$$

We are now ready to announce the following theorem.

Theorem 1 *Under Assumption 1 with the prescribed performance defined by (5.3), the MRAC of System (6.1) with reference model (6.2) having the error dynamic (6.5) and the transformed error dynamic (6.12), the control input defined by (6.19), equations (6.17)-(6.16), and the adaption rule (6.20)-(6.22) and the robustifying term (6.23)-(6.24), forces the transformed error to asymptotically reach zero and therefore the tracking error to satisfy the prescribed*

performance.

6.4 Stability Analysis

The proof is similar to the one in [53]. We adapted it to our case. Let us consider the Lyapunov candidate The Lyapunov candidate may be chosen as

$$W = W_1 + W_2 \quad (6.25)$$

$$W_1 = \epsilon^\top \epsilon$$

$$W_2 = \sum_{i=1}^n \frac{1}{2\gamma_{1i}} \tilde{\theta}_{:,i}^\top \tilde{\theta}_{:,i} + \sum_{i=1}^n \frac{1}{2\gamma_{2i}} (\tilde{\sigma}_{:,i} + \beta_i \delta_i)^\top (\tilde{\sigma}_{:,i} + \beta_i \delta_i)$$

$$\dot{W} = \dot{W}_1 + \dot{W}_2$$

$$\dot{W}_1 = \dot{\epsilon}^\top \epsilon + \epsilon^\top \dot{\epsilon}$$

$$\dot{W}_2 = \sum_{i=1}^n \frac{1}{2\gamma_{1i}} \tilde{\theta}_{:,i}^\top \dot{\tilde{\theta}}_{:,i} + \sum_{i=1}^n \frac{1}{\gamma_{2i}} (\tilde{\sigma}_{:,i} + \beta_i \delta_i)^\top (\dot{\tilde{\sigma}}_{:,i} + \beta_i \dot{\delta}_i) \quad (6.26)$$

$$\begin{aligned} \dot{W}_1 \leq & - \sum_{i=1}^n \epsilon_i \Gamma_{i,i} \tilde{\theta}_{:,i}^\top x(t) - \sum_{i=1}^n \epsilon_i \Gamma_{i,i} \tilde{\sigma}_{:,i}^\top \psi(x) + \sum_{i=1}^n |\epsilon_i| \Gamma_{i,i} \bar{\alpha}_i \\ & - \sum_{i=1}^n \epsilon_i \Gamma_{i,i} K_{i,i} \epsilon_i + \sum_{i=1}^n \epsilon_i \Gamma_{i,i} u_{ri} \end{aligned} \quad (6.27)$$

$$\begin{aligned} \sum_{i=1}^n \frac{1}{\gamma_{2i}} (\tilde{\sigma}_{:,i} + \beta_i \delta_i)^\top (\dot{\tilde{\sigma}}_{:,i} + \beta_i \dot{\delta}_i) \leq & - \sum_{i=1}^n \frac{1}{2} \|\tilde{\sigma}_{:,i}\|^2 |\epsilon_i| \Gamma_{i,i} v_i + \sum_{i=1}^n \frac{1}{2} \|\sigma_{:,i}\|^2 |\epsilon_i| \Gamma_{i,i} v_i + \\ & \sum_{i=1}^n \frac{1}{2} \tilde{\sigma}_{:,i} \epsilon_i \Gamma_{i,i} \psi(x) - \sum_{i=1}^n \beta_i \|\delta_i\| \end{aligned}$$

$$\begin{aligned} \dot{W} = \dot{W}_1 + \dot{W}_2 \leq & - \sum_{i=1}^n \epsilon_i \Gamma_{i,i} \tilde{\theta}_{:,i}^\top x(t) - \sum_{i=1}^n \epsilon_i \Gamma_{i,i} \tilde{\sigma}_{:,i}^\top \psi(x) + \sum_{i=1}^n |\epsilon_i| \Gamma_{i,i} \bar{\alpha}_i - \sum_{i=1}^n \epsilon_i \Gamma_{i,i} K_{i,i} \epsilon_i \\ & + \sum_{i=1}^n \epsilon_i \Gamma_{i,i} u_{ri} + \sum_{i=1}^n \frac{1}{2\gamma_{1i}} \tilde{\theta}_{:,i}^\top \dot{\tilde{\theta}}_{:,i} + \sum_{i=1}^n \frac{1}{\gamma_{2i}} (\tilde{\sigma}_{:,i} + \beta_i \delta_i)^\top (\dot{\tilde{\sigma}}_{:,i} + \beta_i \dot{\delta}_i) \leq 0 \end{aligned}$$

Then by choosing

$$\dot{\tilde{\sigma}}_{:,i} = \int_0^\infty \Gamma_{i,i} (-\gamma_{2i} |\epsilon_i| v_i \hat{\sigma}_{:,i} + \gamma_{2i} \epsilon_i \psi(x)) d\tau - \beta_i \delta_i$$

$$\delta_i = \gamma_{2i} |\epsilon_i| v_i \hat{\sigma}_{:,i} + \gamma_{2i} \epsilon_i \psi(x)$$

and

$$u_{ri} = -\text{sign}(\epsilon)_i \cdot \hat{\alpha}$$

one gets

$$\begin{aligned} \dot{W} \leq & - \sum_{i=1}^n \epsilon_i \Gamma_{i,i} \tilde{\theta}_{:,i}^\top x(t) - \sum_{i=1}^n \epsilon_i \Gamma_{i,i} \tilde{\sigma}_{:,i}^\top \psi(x) + \sum_{i=1}^n |\epsilon_i| \Gamma_{i,i} \bar{\alpha}_i - \sum_{i=1}^n \epsilon_i \Gamma_{i,i} K_{i,i} \epsilon_i \\ & - \sum_{i=1}^n |\epsilon_i| \Gamma_{i,i} \hat{\alpha} + \sum_{i=1}^n \frac{1}{2\gamma_{1i}} \tilde{\theta}_{:,i}^\top \dot{\hat{\theta}}_{:,i} - \sum_{i=1}^n \frac{1}{2} \|\tilde{\sigma}_{:,i}\|^2 |\epsilon_i| \Gamma_{i,i} v_i \\ & + \sum_{i=1}^n \frac{1}{2} \tilde{\sigma}_{:,i} \epsilon_i \Gamma_{i,i} \psi(x) - \sum_{i=1}^n \beta_i \|\delta_i\| + \sum_{i=1}^n \frac{1}{2} \|\sigma_{:,i}\|^2 |\epsilon_i| \Gamma_{i,i} v_i \leq 0 \end{aligned} \quad (6.28)$$

Using the adaption rule

$$\dot{\hat{\theta}}_{:,i} = -\gamma_{1i} \epsilon_i \Gamma_{i,i} x(t)$$

and leads to

$$\begin{aligned} & + \sum_{i=1}^n |\epsilon_i| \Gamma_{i,i} \bar{\alpha}_i - \sum_{i=1}^n \epsilon_i \Gamma_{i,i} K_{i,i} \epsilon_i - \sum_{i=1}^n |\epsilon_i| \Gamma_{i,i} \hat{\alpha} \\ & - \sum_{i=1}^n \frac{1}{2} \|\tilde{\sigma}_{:,i}\|^2 |\epsilon_i| \Gamma_{i,i} v_i + \sum_{i=1}^n \frac{1}{2} \|\sigma_{:,i}\|^2 |\epsilon_i| \Gamma_{i,i} v_i - \sum_{i=1}^n \beta_i \|\delta_i\| \leq 0 \end{aligned} \quad (6.29)$$

The following terms are negative $-\sum_{i=1}^n \epsilon_i \Gamma_{i,i} K_{i,i} \epsilon_i$, $-\sum_{i=1}^n \frac{1}{2} \|\tilde{\sigma}_{:,i}\|^2 |\epsilon_i| \Gamma_{i,i} v_i$ and $-\sum_{i=1}^n \beta_i \|\delta_i\|$,
Therefore one can select

$$\sum_{i=1}^n |\epsilon_i| \Gamma_{i,i} \bar{\alpha}_i - \sum_{i=1}^n |\epsilon_i| \Gamma_{i,i} \hat{\alpha} + \sum_{i=1}^n \frac{1}{2} \|\sigma_{:,i}\|^2 |\epsilon_i| \Gamma_{i,i} v_i \leq 0 \quad (6.30)$$

Which leads to

$$\sum_{i=1}^n |\epsilon_i| \Gamma_{i,i} \hat{\alpha} \geq \sum_{i=1}^n |\epsilon_i| \Gamma_{i,i} \bar{\alpha}_i + \sum_{i=1}^n \frac{1}{2} \|\sigma_{:,i}\|^2 |\epsilon_i| \Gamma_{i,i} v_i \quad (6.31)$$

which is satisfied if $\hat{\alpha}$ is selected as

$$\hat{\alpha} \geq (\bar{\alpha}_i + \frac{1}{2} \|\sigma_{:,i}\|^2 v_i)$$

In the next section, several simulation results to validate the approach and assess its stability will be presented.

6.5 Simulation Examples

the performance of the proposed robust MRAC control design is demonstrated using two different cases. In each case, the control performance and its ability to guarantee the desired performance are benchmarked to first \mathcal{L}_1 adaptive controller and Neuro-adaptive controller.

Example 6.5.1

$$\dot{x} = Ax(t) + Bu(t) + \theta^\top x(t) + \Delta f + d(t), \quad x(0) = x_0.$$

$$y(t) = Cx(t).$$

$$A = \begin{bmatrix} -36 & 36 & 0 \\ 0 & 20 & 0 \\ 0 & 0 & -3 \end{bmatrix}, B = \begin{bmatrix} 1 & 0 & 0 \\ 0 & 1 & 0 \\ 0 & 0 & 1 \end{bmatrix}, C = \begin{bmatrix} 1 & 0 & 0 \\ 0 & 1 & 0 \\ 0 & 0 & 1 \end{bmatrix}$$

$$\Delta f = \begin{bmatrix} x_3^2 + 0.2\sin(x_1) \\ -x_1x_3 - 0.2\cos(x_3)x_1 \\ x_1x_2 \end{bmatrix}, d(t) = \begin{bmatrix} 1 + \sin(t) \\ 1.2 + \cos(t) \\ \sin(t) + \cos(t) - 1 \end{bmatrix}$$

$$, \theta(t) = \begin{bmatrix} 3\sin(0.5t) & 2\sin(0.4t)\cos(0.3t) & 0.7\sin(0.2t) \\ 0.9\sin(0.2t) & 2.5\sin(0.3t) + 0.3\cos(t) & \sin(0.1t) \\ 0.5\sin(0.13t) & 0.6\cos(0.15t) & 1.5\cos(0.7t) + 1.6\sin(0.3t) \end{bmatrix}$$

Example 6.5.2

$$\dot{x} = Ax(t) + Bu(t) + \theta^\top x(t) + \Delta f + d(t), \quad x(0) = x_0.$$

$$y(t) = Cx(t).$$

$$A = \begin{bmatrix} -36 & 36 & 0 \\ 0 & 20 & 0 \\ 0 & 0 & -3 \end{bmatrix}, B = \begin{bmatrix} 1 & 0 & 0 \\ 0 & 1 & 0 \\ 0 & 0 & 1 \end{bmatrix}, C = \begin{bmatrix} 1 & 0 & 0 \\ 0 & 1 & 0 \\ 0 & 0 & 1 \end{bmatrix}$$

$$\Delta f = \begin{bmatrix} x_3^2 + 0.2\sin(x_1) - 2.5u_3\cos(u_1) \\ -x_1x_3 - 0.2\cos(x_3)x_1 + 0.7u_3^2 \\ x_1x_2 \end{bmatrix}, d(t) = \begin{bmatrix} 1 + \sin(t) \\ 1.2 + \cos(t) \\ \sin(t) + \cos(t) - 1 \end{bmatrix}$$

$$, \theta(t) = \begin{bmatrix} 3\sin(0.5t) & 2\sin(0.4t)\cos(0.3t) & 0.7\sin(0.2t) \\ 0.9\sin(0.2t) & 2.5\sin(0.3t) + 0.3\cos(t) & \sin(0.1t) \\ 0.5\sin(0.13t) & 0.6\cos(0.15t) & 1.5\cos(0.7t) + 1.6\sin(0.3t) \end{bmatrix}$$

Desired poles are selected as $p = -70, -60 \pm i$.

Robust Adaptive Prescribed Performance Parameters $\rho_{i0} = 2, \rho_{i\infty} = 0.05, l_i = 1.5$, and estimator parameters $\beta_i = 2, \gamma_{1i} = 50000, \gamma_{2i} = 50000, v_i = 0.05$ where $i = 1, 2, 3$ and finally $\psi(x) = [2 \ 2 \ 2]^\top, \hat{\epsilon} = [10 \ 10 \ 10]^\top, K = 0.1\text{diag}(3)$

Reference input assigned to be $r(t) = [\cos(0.75t) \ \cos(0.8t) \ \cos(0.7t)]^\top$,

\mathcal{L}_1 **Adaptive Controller Parameters** $\theta_b \in [-5, 5]$, $\Delta \in 20$, $\hat{\omega} \in [0.3, 10]$,

The parameters of the sigmoid basis function $\zeta_j(x) = 1/(1 + e^{-\omega_j^\top - b_j})$ with $\omega_j \in \mathbb{R}^3$, $b_j \in \mathbb{R}^3$, $j = 1, 2, \dots, 80$ were chosen by off-line training try and error on the simulation then kept constant throughout the simulation. θ_0 is a vector represents the good guess of the initial conditions of the parameter estimates and was taken to be a zero vector referring to completely unknown nonlinear dynamics. Prescribed performance parameters are $\rho_{i0} = 2$, $\rho_{i\infty} = 0.05$, $l_i = 1.5$. Figure 6.1 shows the output performance of the proposed approach versus \mathcal{L}_1 adaptive

Table 6.1: Robust Neuro Adaptive Control with PPF parameters

k	n_f	η_{G_a}	η_{G_b}	δ_d	σ	Γ
0.5	0.2	0.2	0.2	0.1	7.5	0.1I

controller, the control signal of these two controllers are presented in figure 6.2. Figure 6.3 and 6.4 reveal the idea of prescribed performance and demonstrates the error of these three controllers with respect to pre-assigned prescribed values with high nonlinear uncertainties and nonlinearities as mentioned in case 1.

The following figures of case 2 overlay the simulation results of the proposed approach as well as two controllers from the literature. we can see in figure 6.5 the output performance of three controllers, their control signal is presented in 6.6, error and transformed error are presented in figure 6.7, and finally figure 6.8 highlights the advantage of the proposed controller. In all, the performance of the proposed approach, its efficiency, and robustness compete with \mathcal{L}_1 and *Neuro – Adaptive*.

6.6 Conclusion

In this chapter, we proposed an adaptive control of multi-input multi-output uncertain high-order nonlinear system capable of guaranteeing a predetermined prescribed performance. The robust stabilization of the transformed error, guaranties the stability and convergence of the constrained tracking error within the set of time varying constraints representing the performance limits. Simulation results demonstrated the efficiency of the proposed approach when compared to \mathcal{L}_1 adaptive control and to the neuro-adaptive approach with similar requirement.

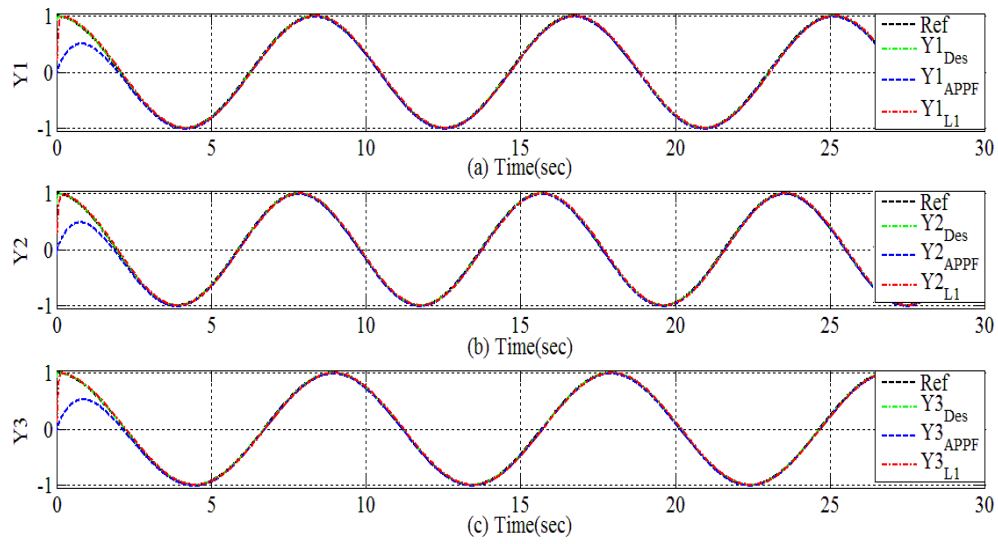


Figure 6.1: Output Performance of robust MRAC-PPF and \mathcal{L}_1 adaptive controller for case 1.

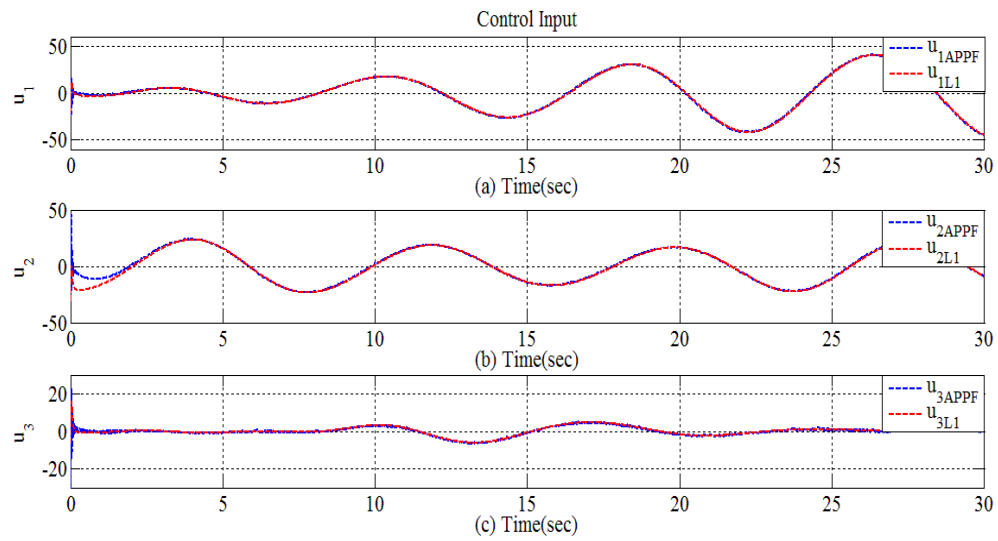


Figure 6.2: Control Signal of robust MRAC-PPF and \mathcal{L}_1 adaptive controller for case 1.

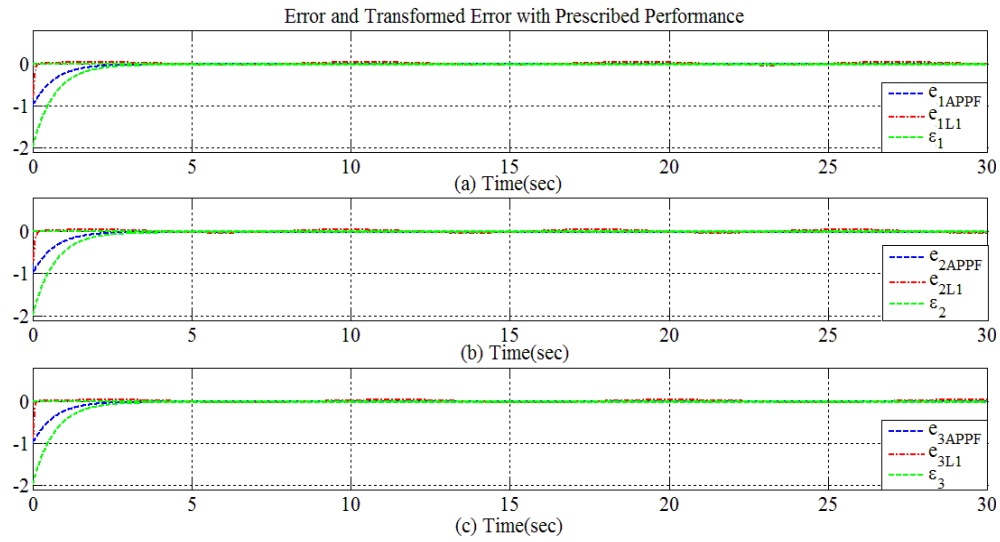


Figure 6.3: e_2 and ϵ_2 of robust MRAC-PPF and \mathcal{L}_1 adaptive controller for case 1.

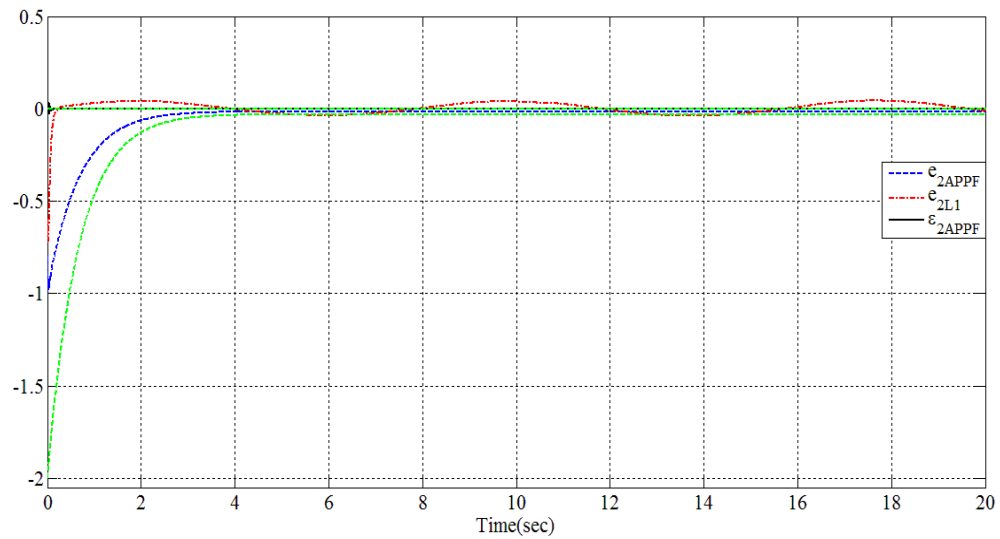


Figure 6.4: e_2 and ϵ_2 of robust MRAC-PPF and \mathcal{L}_1 adaptive controller for case 1.

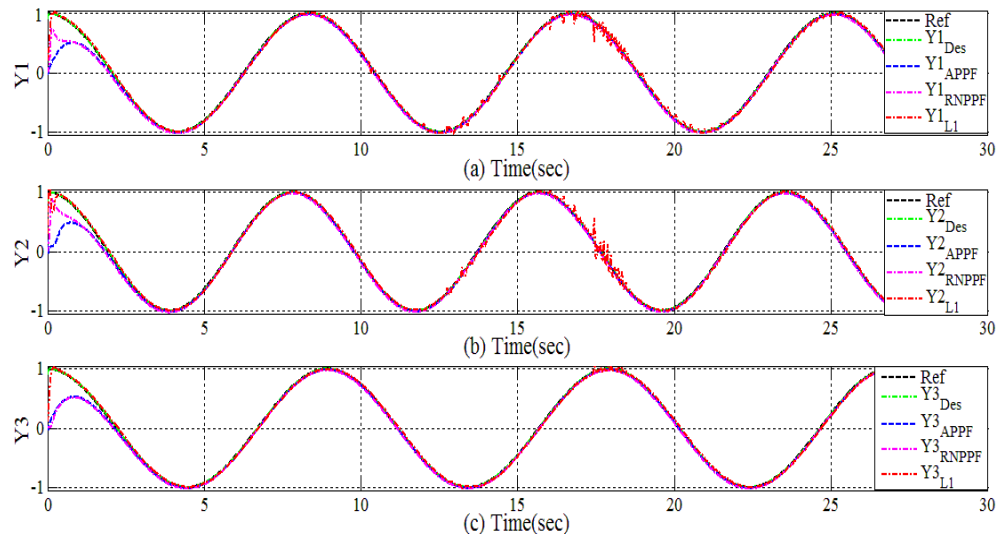


Figure 6.5: Output Performance of robust MRAC-PPF, \mathcal{L}_1 adaptive controller and *Neuro – Adaptive* with PPF for case 2.

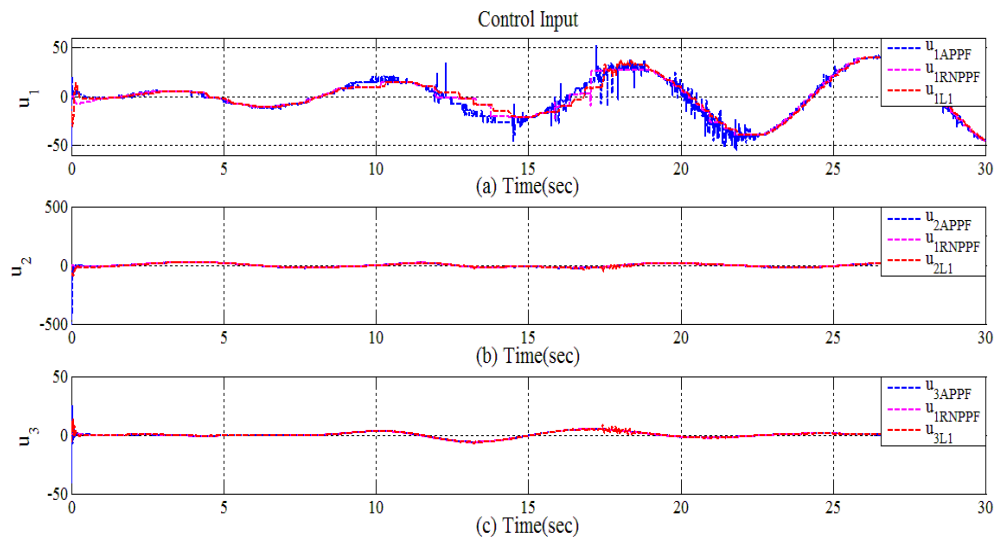


Figure 6.6: Control Signal of robust MRAC-PPF, \mathcal{L}_1 adaptive controller and *Neuro – Adaptive* controller with PPF for case 2.

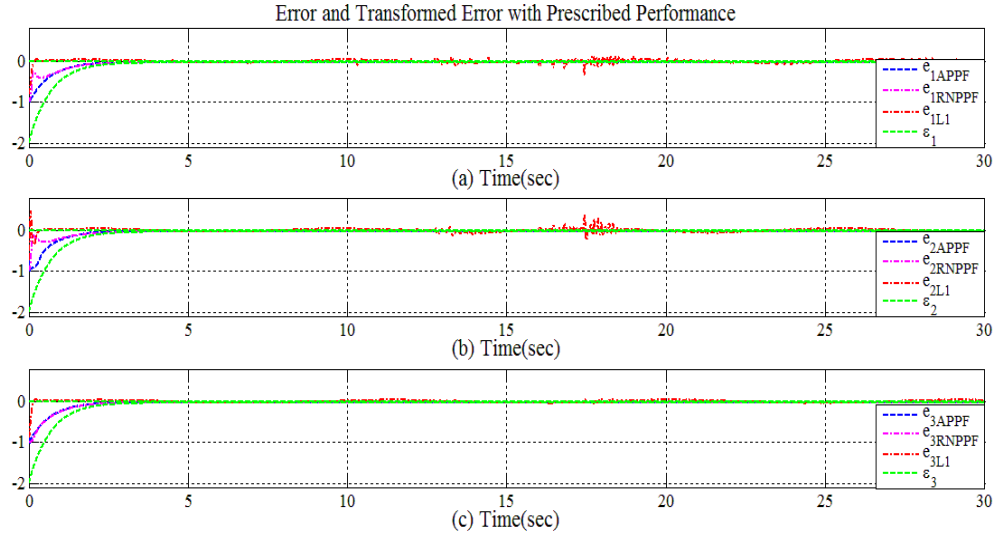


Figure 6.7: e_2 and ϵ_2 of robust MRAC-PPF, \mathcal{L}_1 adaptive controller and *Neuro – Adaptive* controller with PPF for case 2.

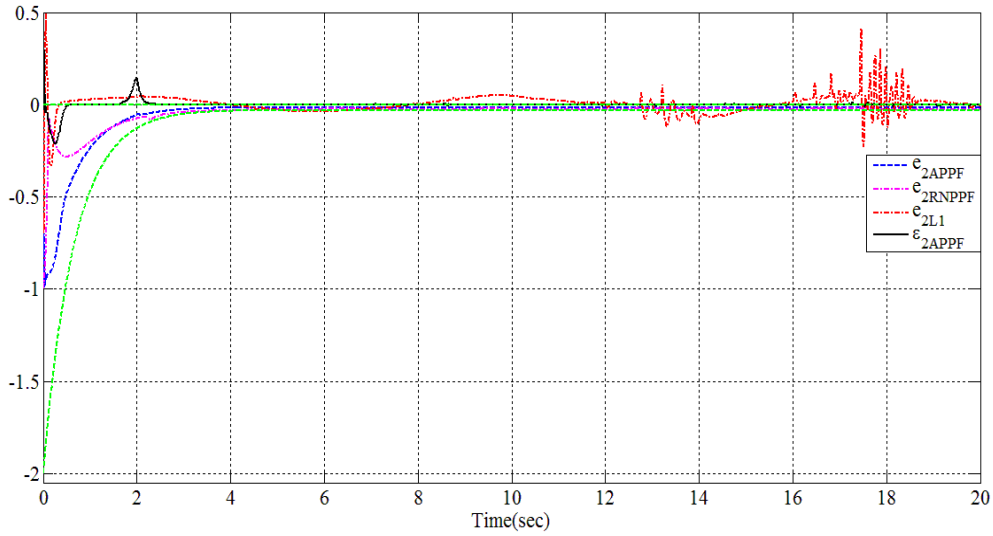


Figure 6.8: e_2 and ϵ_2 of robust MRAC-PPF, \mathcal{L}_1 adaptive controller and *Neuro – Adaptive* controller with PPF for case 2.

Chapter 7

ROBUST ADAPTIVE OBSERVER FOR \mathcal{L}_1 ADAPTIVE CONTROLLER

7.1 Introduction

Designing a robust adaptive observer for nonlinear systems could be headed in order to estimate inaccessible states from the measured output but can be challenging due to unmodeled dynamics, presence high nonlinearities and time varying uncertainties. In this chapter, robust adaptive observer design for \mathcal{L}_1 adaptive controller is mainly adopted from [63]. The work in [63] was designed to deal with SISO and MIMO systems with high level of nonlinearities that are assumed to be completely unknown in addition to the presence of structured uncertainties. The chapter is organized as following: section one is an introduction. Problem formulation is presented in section two. The observer design and stability analysis are presented in section three. In section four, discussion of illustrative examples validate the effectiveness of the observer design with \mathcal{L}_1 adaptive controller. Finally, the chapter is concluded.

7.2 Problem formulationn

Consider the following problem:

$$\begin{aligned}\dot{x}(t) &= Ax(t) + Bf(x, u, t) + g(y, u) \\ y &= Cx(t)\end{aligned}\tag{7.1}$$

where $x \in \mathbb{R}^n$, $u \in \mathbb{R}^m$ and $y \in \mathbb{R}^p$ are the system stats (unmeasured), the control input (unmeasured) and the system output (measured) respectively. $g(y, u)$ is nonlinear function with known parameters and $f(x, u, t)$ is an unknown nonlinear function. Finally, A , B and C are constant

matrices (known) with appropriate sizes.

The objective of this chapter is to design an adaptive observer for uncertain nonlinear system with unknown dynamics in order to estimate states values for \mathcal{L}_1 adaptive controller from the regulated output value. Four basic assumptions will be considered

Assumption 18 *The pair (A, B) is controllable and the pair (A, C) is detectable.*

Assumption 19 *Lyapunov function of the system $V(v)$ is uniformly bounded and satisfies*

$$\alpha_1(\|v\|) \leq V_v(v) \leq \alpha_2(\|v\|) \quad (7.2)$$

$$\frac{\partial \leq V_v(v)}{\partial v} S(y, v) \leq -\alpha_3(\|v\|) \quad (7.3)$$

$$\alpha_3(\|v\|) = \tau_0 V_v(v) - \gamma(\|y\|) - d_0 \quad (7.4)$$

where α_1 , α_2 and α_3 are positive definite class K_∞ functions [88], and $\tau_0 > 0$; $d_0 > 0$ are positive constants. γ_0 is a smooth nonnegative function and has the form of $\gamma(s) = s^2 \gamma_0(s^2)$ which will be equivalent to $y^2 \gamma_0(y^2)$ as mentioned in [89] and $\bar{\epsilon}_0$ is a small positive number.

Assumption 20 *The nonlinear function can be written in the form of*

$$\|f(x, u, t)\| \leq \lambda_1 + \lambda_2 \|x\| \xi(y, u) + \lambda_3 \zeta(y, u) + \lambda_4 \alpha(\|v\|) \quad (7.5)$$

with $\lambda_i \geq 0$, $i = 1, 2, 3, 4$ are unknown nonnegative constants, $\alpha(\|\cdot\|)$ is a class K_∞ function and both of $\xi(y, u)$ and $\zeta(y, u)$ are functions assigned arbitrarily nonnegative.

Assumption 21 *Q, P are positive definite matrices satisfying*

$$\begin{aligned} (A - k_l C)^T P + P(A - k_l C) + Q &\leq 0 \\ PB &= C^T \end{aligned} \quad (7.6)$$

7.3 Robust adaptive observer

The observer design is given by

$$\dot{\check{x}} = A\check{x} - k_l(\check{y} - y) - \check{\beta}B(\check{y} - y)\beta_l + g(y, u) \quad (7.7)$$

where $\check{y} = C\check{x}$.

Let $e = \check{x} - x$, $A_l = A - k_l C$ and $\bar{e}_l = \check{y} - y$

$$\dot{e}_l = A_l e_l - \check{\beta}B\bar{e}_l\beta_l - Bf(x, u, t) \quad (7.8)$$

The adaptation law of parameter $\check{\beta}$ given by

$$\dot{\check{\beta}} = \Gamma_l \|\bar{e}_l\| \beta_l - \Gamma_l \sigma_l \check{\beta} \quad (7.9)$$

Where Γ_l and σ_l are positive constants and β_l can be defined by

$$\beta_l = 1 + \xi^2(y, u) + \|\check{x}\| \xi^2(y, u) + \eta^2(y, u) + [\alpha(\alpha_1^{-1}(2\delta))]^2 \quad (7.10)$$

δ is a dynamic signal include unmodeled dynamics and it has the following form

$$\dot{\delta} = -\lambda_0 \delta + \delta_l, \delta(0) > 0 \quad (7.11)$$

where $\tau_0 \in [0, \tau_0]$ and $\delta_l(y)$ is a smooth nonnegative function $\delta_l(y) = \|y\|^2 \gamma_0(\|y\|^2) + d_0$. As mentioned in [63, 89] that the relation between dynamic signal and Lyapunov function is

$$\begin{aligned} V_v(v) &\leq \delta + D \\ D &= \max 0, e^{-\tau_0 t} V_v(v) - e^{-\lambda_0 \delta_0 t} \end{aligned} \quad (7.12)$$

where $\tau_0 > \lambda_0 > 0$.

The full illustration of L1 adaptive controller with robust adaptive observer is depicted in figure 7.1.

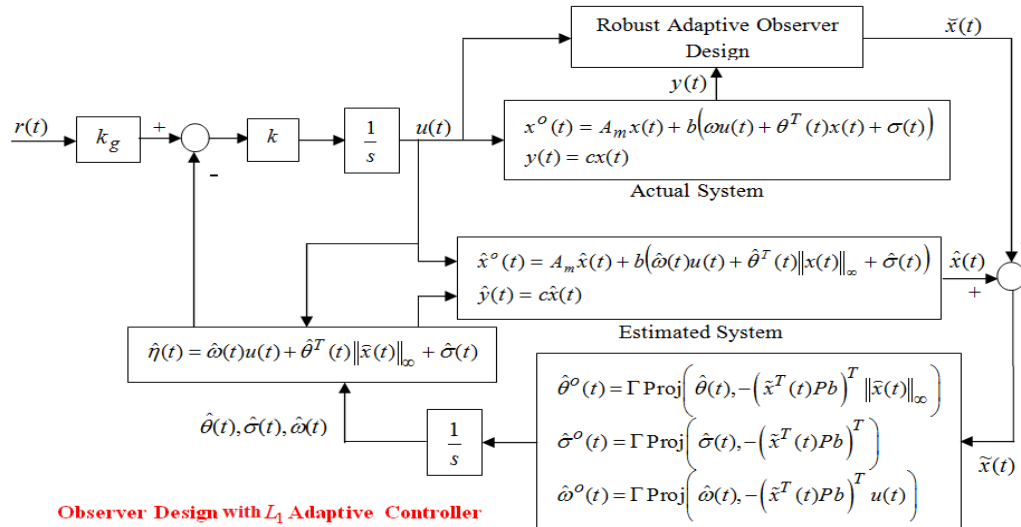


Figure 7.1: Robust adaptive observer design with \mathcal{L}_1 adaptive controller.

7.3.1 Lyapunov function

consider the following Lyapunov candidate

$$V_v = \frac{1}{2}[e_l^T P e_l + \Gamma_l \tilde{\beta}^2] \quad (7.13)$$

where $\tilde{\beta} = \beta - \beta^*$ and $\beta^* > 0$ is a constant representing the desired value of β . The derivative of (7.13) in addition to the use of (7.9), (7.10) and assumption 7.3.

$$\begin{aligned} \dot{V}_v &= \frac{1}{2}e_l(A_l^T P + P A_l)e_l - e_l^T P \hat{\beta} B \bar{e}_l \beta_l - e_l^T P B f(x, t) + \Gamma_l^{-1} \tilde{\beta} \dot{\tilde{\beta}} \\ \dot{V}_v &= \frac{1}{2}e_l Q e_l - e_l^T P \hat{\beta} B \bar{e}_l \beta_l - e_l^T P B f(x, t) + \Gamma_l^{-1} \tilde{\beta} \dot{\tilde{\beta}} \\ \dot{V}_v &= \frac{1}{2}e_l Q e_l - \hat{\beta} \|\bar{e}_l\|^2 [1 + \xi^2(y, u) + \|\tilde{x}\| \xi^2(y, u) + \eta^2(y, u) + [\alpha(\alpha_1^{-1}(2\delta))]^2] \\ &\quad - \|\bar{e}_l\| [\lambda_1 + \lambda_2 \|x\| \xi(y, u) + \lambda_3 \zeta(y, u) + \lambda_4 \alpha(\|v\|)] + \Gamma_l^{-1} \tilde{\beta} \dot{\tilde{\beta}} \end{aligned} \quad (7.14)$$

$$\begin{aligned} \dot{V}_v &= \frac{1}{2}e_l Q e_l - \|\bar{e}_l\| [\lambda_1 + \lambda_2 \|x\| \xi(y, u) + \lambda_3 \zeta(y, u) + \lambda_4 \alpha(\|v\|)] + \sigma_l \tilde{\beta} \beta \\ &\quad - \beta^* \|\bar{e}_l\|^2 [1 + \xi^2(y, u) + \|\tilde{x}\| \xi^2(y, u) + \eta^2(y, u) + [\alpha(\alpha_1^{-1}(2\delta))]^2] \end{aligned} \quad (7.15)$$

From (7.12)

$$\alpha(\|v\|) \leq \alpha(\alpha_1^{-1}(2\delta)) + \alpha(\alpha_1^{-1}(2D)) \quad (7.16)$$

$$\begin{aligned} \dot{V}_v &= \frac{1}{2}e_l Q e_l - \|\bar{e}_l\| \lambda_1 + \|\bar{e}_l\| \lambda_2 \|x\| \xi(y, u) + \|\bar{e}_l\| \lambda_3 \zeta(y, u) \\ &\quad + \|\bar{e}_l\| \lambda_4 \alpha(\alpha_1^{-1}(2\delta)) + \|\bar{e}_l\| \lambda_4 \alpha(\alpha_1^{-1}(2D)) - \sigma_l \tilde{\beta} \beta \\ &\quad - \beta^* \|\bar{e}_l\|^2 [1 + \xi^2(y, u) + \|\tilde{x}\| \xi^2(y, u) + \eta^2(y, u) + [\alpha(\alpha_1^{-1}(2\delta))]^2] \end{aligned} \quad (7.17)$$

Choosing $\bar{\lambda}_1 = \lambda_1 + \lambda_4 \alpha(\alpha_1^{-1}(2D))$ and $\|x\| \leq \|e_l\| + \|\tilde{x}\|$

$$\begin{aligned} \dot{V}_v &= \frac{1}{2}e_l Q e_l - \|\bar{e}_l\| \bar{\lambda}_1 + \|\bar{e}_l\| \lambda_2 \|e_l\| \xi(y, u) + \|\bar{e}_l\| \lambda_2 \|\tilde{x}\| \xi(y, u) \\ &\quad + \|\bar{e}_l\| \lambda_3 \zeta(y, u) + \|\bar{e}_l\| \lambda_4 \alpha(\alpha_1^{-1}(2\delta)) - \sigma_l^{-1} \tilde{\beta} \beta \\ &\quad - \beta^* \|\bar{e}_l\|^2 [1 + \xi^2(y, u) + \|\tilde{x}\| \xi^2(y, u) + \eta^2(y, u) + [\alpha(\alpha_1^{-1}(2\delta))]^2] \end{aligned} \quad (7.18)$$

$$\dot{V}_v = \frac{1}{2}e_l Q e_l - \sigma_l^{-1} \tilde{\beta} \beta - \beta^* \|\bar{e}_l\|^2 \beta_l + M \quad (7.19)$$

Where M includes the rest terms which is equivalent to equation (7.3).

7.4 Results and Discussions

Two cases will validate the robustness of robust adaptive observer design with \mathcal{L}_1 adaptive controller. The first case represent the observer with high nonlinear SISO system and in the second case and the observer is designed for high nonlinear MIMO system. The nonlinearity, states and control input are assumed to be completely unknown for previous two cases.

Example 7.5.1 Consider the following nonlinear SISO system

$$\begin{aligned}\dot{x} &= Ax + B(\omega u + f(x, t)) \\ y &= Cx\end{aligned}$$

where $x = [x_1, x_2]^T$ are system states (unmeasured), u is the control input (unmeasured), y is the output (measured). A , B and C are known matrices and they indicate that the system is controllable and detectable. The unknown nonlinearity is $f(x, t)$.

$$A = \begin{bmatrix} 0 & 1 \\ 0 & 0 \end{bmatrix}, B = \begin{bmatrix} 0 \\ 1 \end{bmatrix}, C = \begin{bmatrix} 1 & 1 \end{bmatrix}$$

and

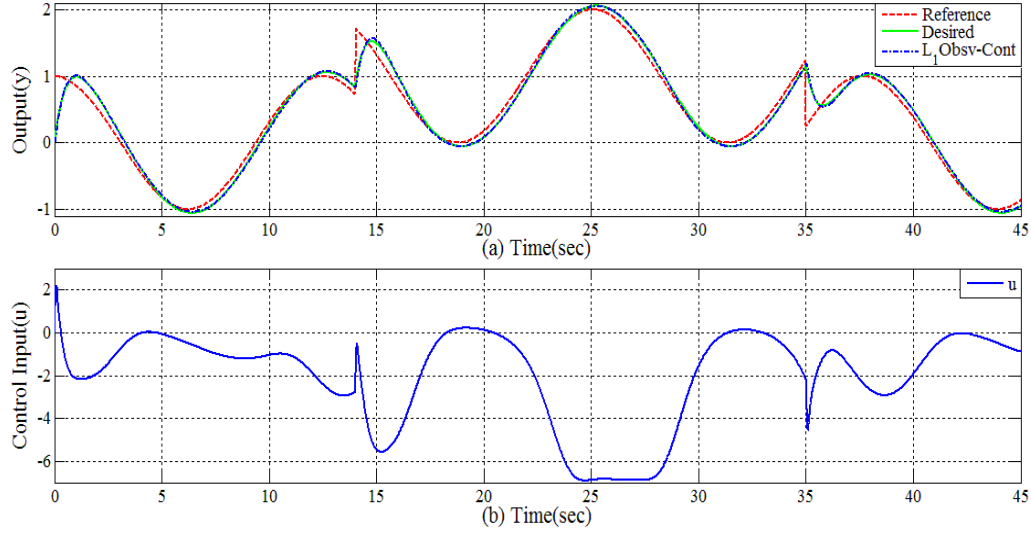
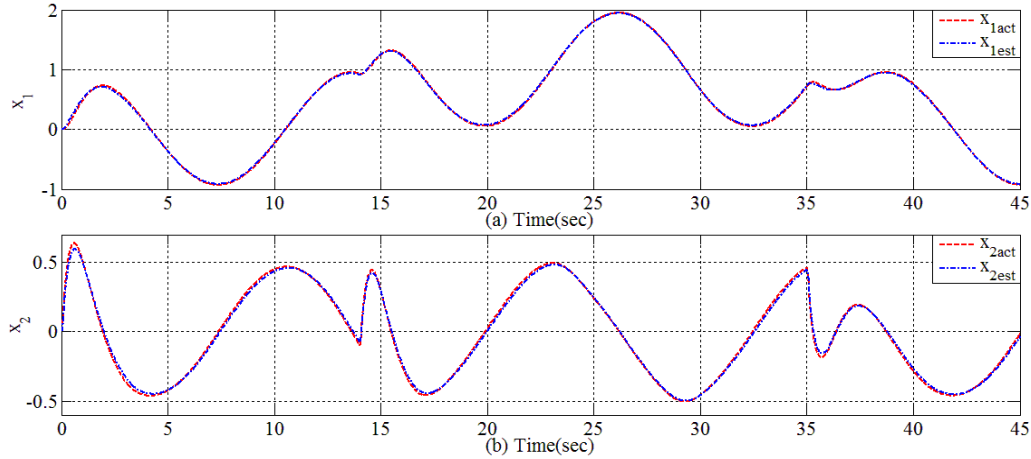
$$\omega = \frac{75}{s + 75}, z(s) = \frac{s - 1}{s^2 + 3s + 2} v(s), v(t) = x_1 \sin(0.2t) + x_2$$

$$f(x, t) = 2x_1^2 + 2x_2^2 + x_1 \sin(x_1^2) + x_2 \cos(x_2^2) + z^2$$

Each of the unmodeled input parameters, uncertainties in the states and disturbances were assigned in compact sets $[\omega_{min}, \omega_{max}] \in [0, 10]$, $\Delta = 100$ and $\theta_b = 10$. The desired closed loop poles are chosen to be $-1.4 \pm j0.743$, the feedback gain = 20, the adaptation gain(Γ) = 1000000 and $Q = \begin{bmatrix} 1 & 0 \\ 0 & 1 \end{bmatrix}$. The observer design parameters were selected as $\Gamma_l = 10$, $\sigma_l = 0.0001$, $\lambda_0 = 2.5$, $d_0 = 0.625$ and finally $k_l = [8, 64]^T$. The parameter of the adaptive law β_l is defined by $\beta_l = 1 + \|y\|^4 + \|\ddot{x}\|^2 \|y\|^4 + 2\delta$ with $\delta(0) = 1$ and $\check{\beta}(0) = 1$. The reference input was chosen to $r = \cos(0.5t)$ with step change by +1 and -1 at 14 and 35 second respectively in order to validate the robustness of the observer with \mathcal{L}_1 adaptive controller.

Figure (7.2) illustrates the output performance and the control signal of \mathcal{L}_1 adaptive controller with the observer design. The actual and estimated states are demonstrated in figure (7.3). The change in the adaptive estimate during the control process is revealed in figure (7.4).

Example 7.5.2 Consider the following 2-DOF planner robot example 3.3.1 which is similar

Figure 7.2: Output performance of \mathcal{L}_1 adaptive controller with robust adaptive observer.Figure 7.3: x and \tilde{x} of robust observer with \mathcal{L}_1 adaptive controller.

to our case with some time variant uncertainties in the inertia matrix to be

$$M(q) = \begin{bmatrix} M_{11} + d_1(t) & M_{12} + d_2(t) \\ M_{21} + d_2(t) & M_{22} + d_3(t) \end{bmatrix}$$

where $d_1(t) = 0.6\sin(0.3t)$, $d_2(t) = 0.7\sin(0.25t)$ and $d_3(t) = |0.5\sin(0.35t)|$ are time varying uncertain parameters included in the model. Projection operator bounds are $\hat{\omega} \in \begin{bmatrix} [0.3, 9.0] & [0.0, 0.3] \\ [0.0, 0.3] & [0.3, 4] \end{bmatrix}$, $\Delta = 100$ and $\theta_b = 10$. The desired closed loop poles were chosen to $-10 \pm j0.5$, $-15 \pm j0.5$, the feedback gain $= K = \begin{bmatrix} 20 & 0 \\ 0 & 20 \end{bmatrix}$, the adaptation gain $(\Gamma) = 100000$ and $Q = eye(4, 4)$. The observer design parameters were selected as $\Gamma_l = 100$, $\sigma_l = 0.0001$, $\lambda_0 = 2.5$, $d_0 = 0.625$. The parameter of adaptive law β_l is defined by $\beta_l = 1 + \|y\|^4 + \|\tilde{x}\|^2\|y\|^4 + 2\delta$ with $\delta(0) = 1$ and $\check{\beta}(0) = 1$ and

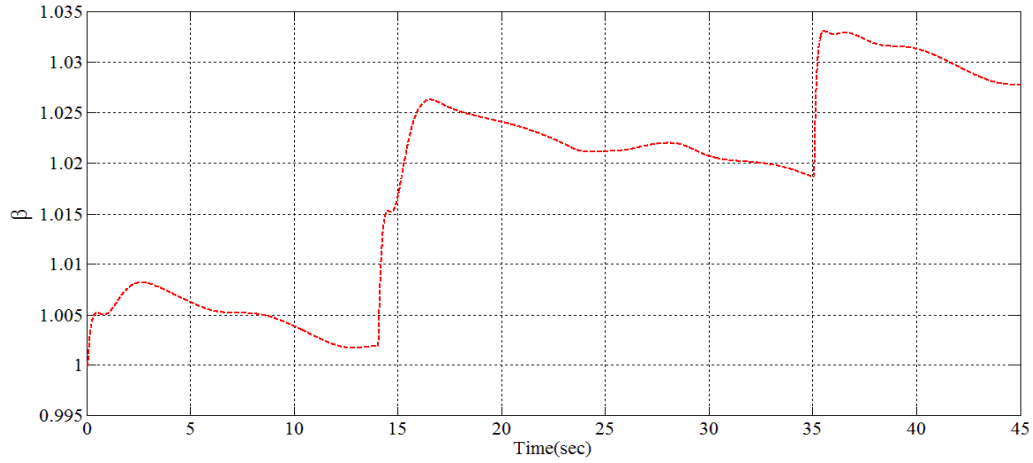


Figure 7.4: $\check{\beta}$ of robust observer with \mathcal{L}_1 adaptive controller.

the desired closed loop poles of observers are $-60 \pm j0.5$, $-50 \pm j0.5$.

Figure 7.5 shows the output performance and the control signal of \mathcal{L}_1 adaptive controller with the observer design for joints q_1 and q_2 . In figure (7.6), actual and observed states are plotted. Finally, figure (7.7) illustrates the change in adaptive estimate $\check{\beta}$ during the control process.

Example 7.5.3 Consider simulation problem of quadrotor in example (3.3.2), The observer

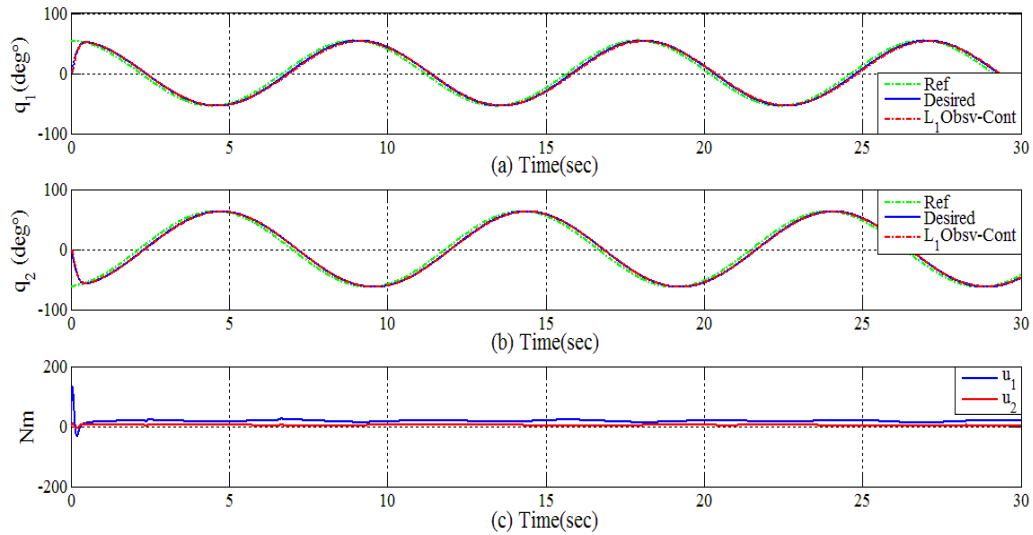


Figure 7.5: Output performance of \mathcal{L}_1 adaptive controller with robust observer for 2 DOF planner robot.

design parameters were selected as $\Gamma_l = 100$, $\sigma_l = 0.0001$, $\lambda_0 = 2.5$, $d_0 = 0.625$. The parameter of adaptive law β_l is defined by $\beta_l = 1 + \|y\|^4 + \|\check{x}\|^2\|y\|^4 + 2\delta$ with $\delta(0) = 1$ and $\check{\beta}(0) = 1$ and the desired closed loop poles of observers are $-70 \pm j0.5$, $75 \pm j0.5$ and $-85 \pm j0.5$.

Figure (7.8) shows the output performance for positions of x , y and z of quadrotor. The angles

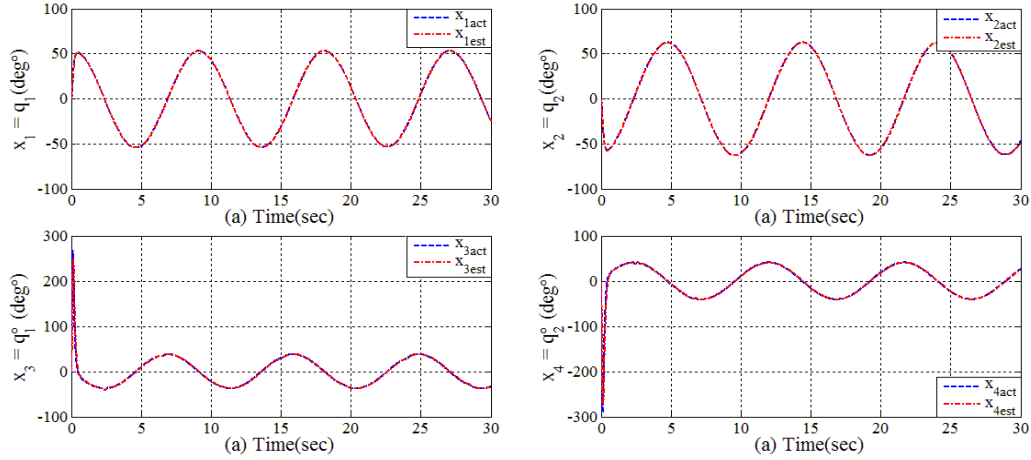


Figure 7.6: x and \hat{x} of robust observer with \mathcal{L}_1 adaptive controller for 2-DOF planer robot.

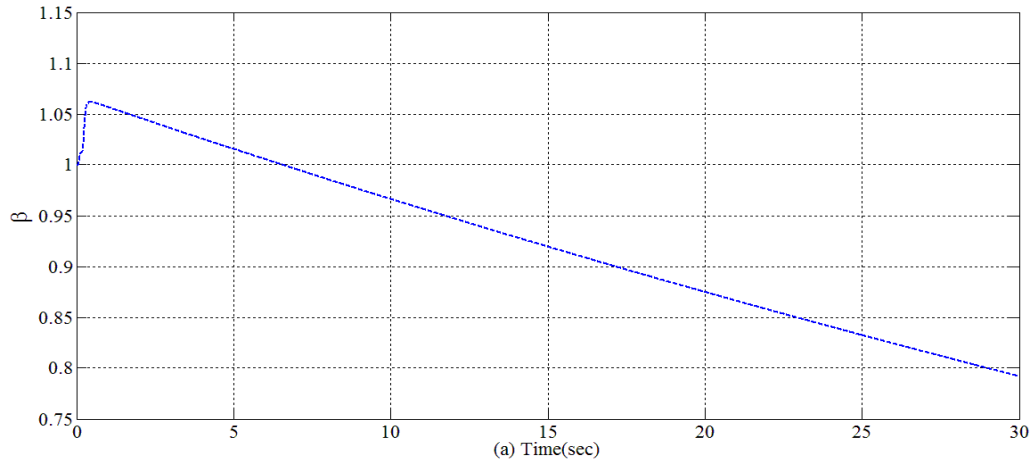


Figure 7.7: $\hat{\beta}$ in the estimate robust observer with \mathcal{L}_1 adaptive controller.

performance and control signal are illustrated in figure (7.9) and (7.10) respectively. Figure (7.11) shows the output position in 3D-frame. Finally, figure (7.12) benchmark the estimated states and actual states. The figure illustrate the robustness of the observer design.

7.5 Conclusion

In this work, robust adaptive observer has been examined with \mathcal{L}_1 adaptive controller for non-linear systems. Nonlinearities are assumed to be completely unknown in addition to unmodeled input parameters and uncertainties. System outputs were available for measurements while states were unmeasurable and control inputs were not used in the observer design. Two illustrative simulations were developed including SISO and MIMO systems to prove the robustness of the observer design with \mathcal{L}_1 adaptive controller and to validate the tracking performance.

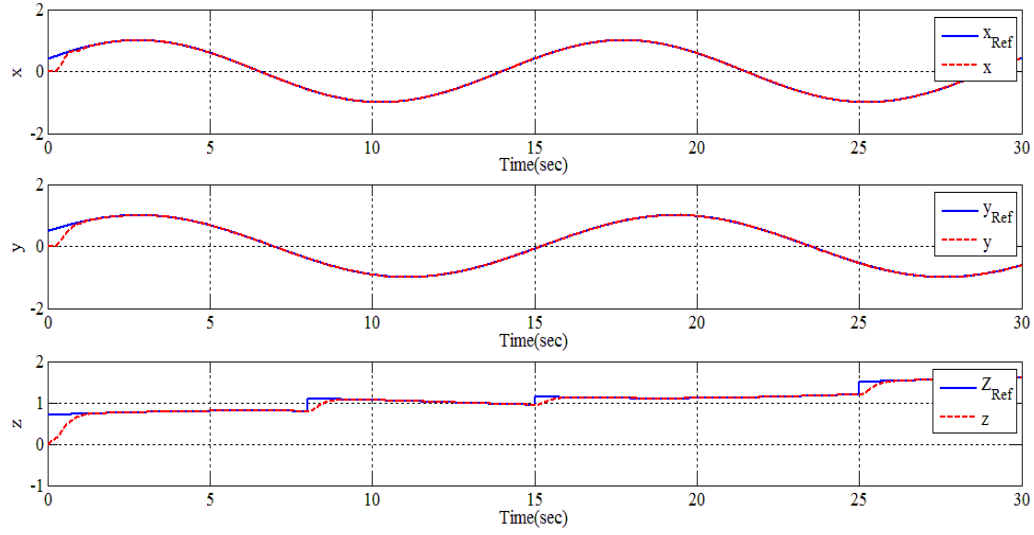


Figure 7.8: Position performance of \mathcal{L}_1 adaptive controller with robust observer for quadrotor.

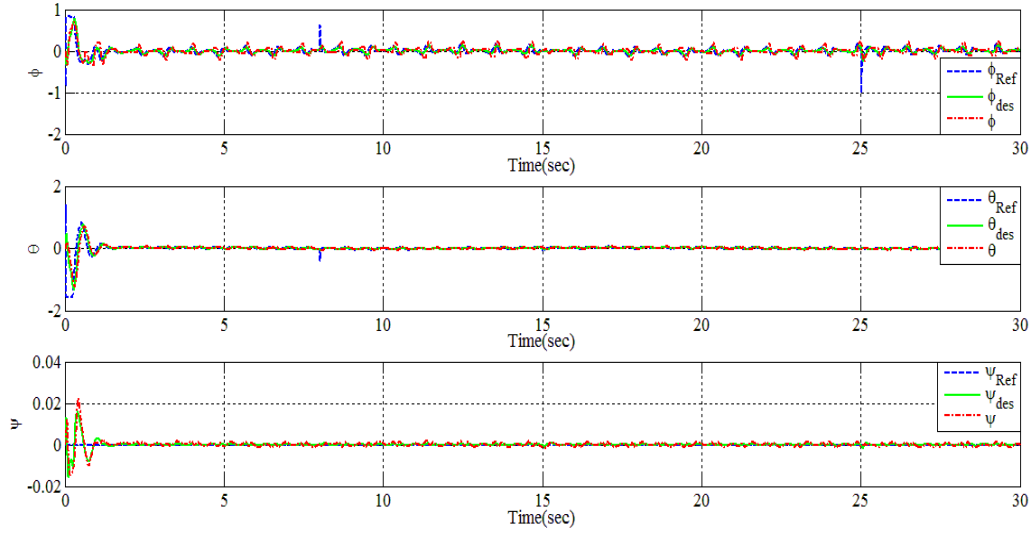


Figure 7.9: Angles performance of \mathcal{L}_1 adaptive controller with robust observer for quadrotor.

The output performance was impressive and both observed and actual states were very close in their values which validate the efficacy of the observer design with \mathcal{L}_1 adaptive controller.

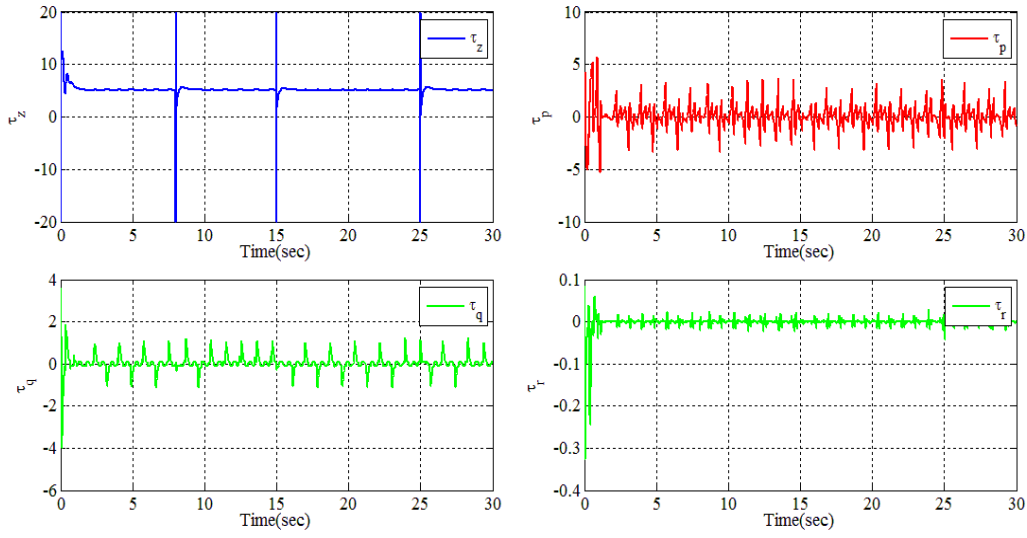


Figure 7.10: Control signal of \mathcal{L}_1 adaptive controller with robust observer for quadrotor.

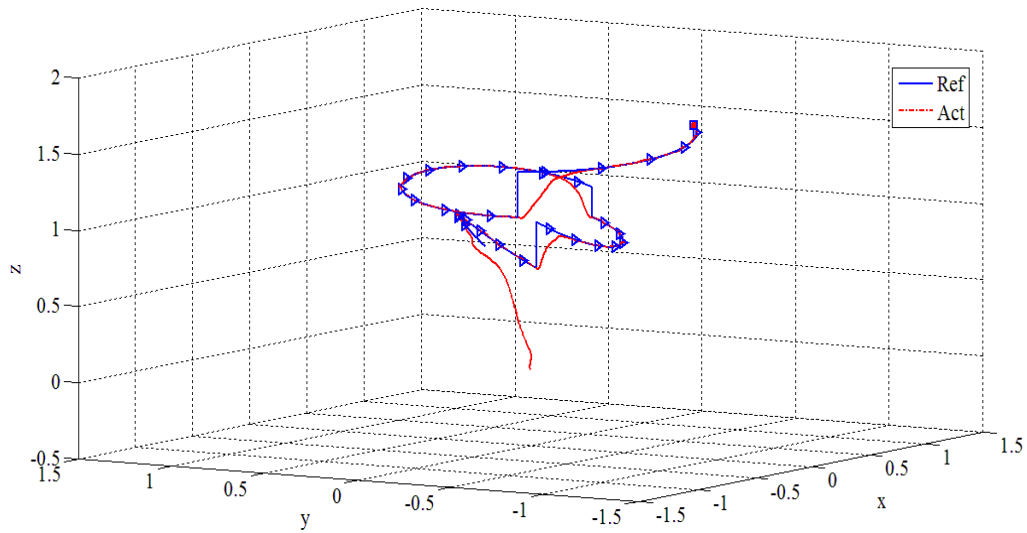


Figure 7.11: Angles performance of \mathcal{L}_1 adaptive controller with robust observer for quadrotor.

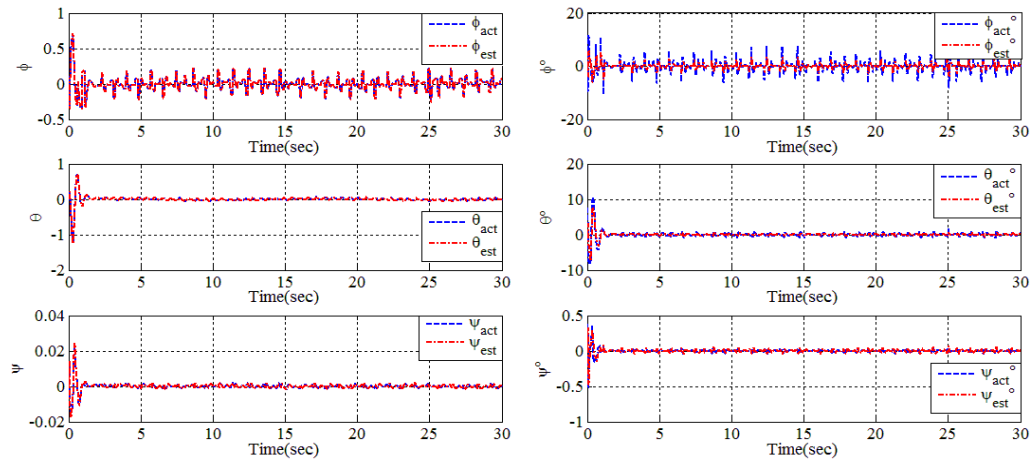


Figure 7.12: Actual and estimated angles of robust observer with \mathcal{L}_1 adaptive controller for quadrotor.

Chapter 8

CONCLUSIONS AND FUTURE WORK

8.1 Summary of Conclusions and Contributions

\mathcal{L}_1 adaptive controller was applied on different structures of nonlinear systems. In addition, the proposed controllers fuzzy- \mathcal{L}_1 adaptive controller and robust MRAC with PPF have been implemented on different nonlinear systems. In this thesis, the following problems and results have been presented

Chapter 3

1. \mathcal{L}_1 adaptive controller has been presented for high nonlinear SISO and MIMO systems with matched and unmatched uncertainties.
2. High nonlinear systems include UVS such as twin rotor, quadrotor and UAV. Also, two degree of freedom planar robot and other nonlinear systems from recent papers have been simulated.

Chapter 4

1. Fuzzy filter for \mathcal{L}_1 adaptive controller has been proposed for high nonlinear uncertain systems.
2. Stability analysis and robustness of the controller has been validated.
3. The proposed controller showed better results in terms of control signal, robustness margin and tracking capability compared to \mathcal{L}_1 adaptive controller.

Chapter 5

1. The work of neuro adaptive control with PPF has been developed successfully.

Chapter 6

1. Robust MRAC with PPF for high nonlinear uncertain systems has been proposed.
2. Stability analysis and robustness of the controller has been validated.
3. The proposed controller showed better results from \mathcal{L}_1 adaptive controller in case of not-affine systems and it solved the limitations of neuro adaptive control with PPF.

Chapter 7

1. Developed and implemented a robust adaptive observer with \mathcal{L}_1 adaptive controller.
2. The observer showed impressive results with the controller applied to different systems.

8.2 Future Work

1. Optimizing fuzzy membership functions on scale of MIMO systems for fuzzy \mathcal{L}_1 -adaptive controller.
2. Propose MRAC with PPF for high nonlinear systems with unmatched uncertainties.
3. Propose \mathcal{L}_1 adaptive controller with PPF for nonlinear systems.

Bibliography

- [1] M. A. Abido, "Optimal power flow using particle swarm optimization," *International Journal of Electrical Power & Energy Systems*, vol. 24, no. 7, pp. 563–571, 2002. (document), 4.4, 4.3
- [2] H. A. Hashim, S. El-Ferik, and M. A. Abido, "A fuzzy logic feedback filter design tuned with pso for 11 adaptive controller," *Expert Systems with Applications*, vol. 42, no. 23, pp. 9077–9085, 2015. 1.4
- [3] H. A. Hashim and M. A. Abido, "Fuzzy controller design using evolutionary techniques for twin rotor mimo system: a comparative study," *Computational intelligence and neuroscience*, vol. 2015, p. 49, 2015. 1.4
- [4] H. A. Hashim, B. O. Ayinde, and M. A. Abido, "Optimal placement of relay nodes in wireless sensor network using artificial bee colony algorithm," *Journal of Network and Computer Applications*, vol. 64, pp. 239–248, 2016. 1.4
- [5] K. J. \AAstrom and B. Wittenmark, "On self tuning regulators," *Automatica*, vol. 9, no. 2, pp. 185–199, 1973. 2.2
- [6] T. R. Fortescue, L. S. Kershenbaum, and B. E. Ydstie, "Implementation of self-tuning regulators with variable forgetting factors," *Automatica*, vol. 17, no. 6, pp. 831–835, 1981. 2.2
- [7] K. J. \AAstrom and T. Hagglund, "Automatic tuning of simple regulators with specifications on phase and amplitude margins," *Automatica*, vol. 20, no. 5, pp. 645–651, 1984. 2.2
- [8] E. Yesil, M. Guzelkaya, and I. Eksin, "Self tuning fuzzy PID type load and frequency controller," *Energy Conversion and Management*, vol. 45, no. 3, pp. 377–390, 2004. 2.2
- [9] W. J. Rugh, "Analytical framework for gain scheduling," *Control Systems, IEEE*, vol. 11, no. 1, pp. 79–84, 1991. 2.2

- [10] P. Apkarian and R. J. Adams, “Advanced gain-scheduling techniques for uncertain systems,” *Control Systems Technology, IEEE Transactions on*, vol. 6, no. 1, pp. 21–32, 1998. 2.2
- [11] W. J. Rugh and J. S. Shamma, “Research on gain scheduling,” *Automatica*, vol. 36, no. 10, pp. 1401–1425, 2000. 2.2
- [12] P. C. Parks, “Liapunov redesign of model reference adaptive control systems,” *Automatic Control, IEEE Transactions on*, vol. 11, no. 3, pp. 362–367, 1966. 2.2, 2.3
- [13] Y.-C. Chen and C.-C. Teng, “A model reference control structure using a fuzzy neural network,” *Fuzzy Sets and Systems*, vol. 73, no. 3, pp. 291–312, 1995. 2.2
- [14] X. Yu and Z. Man, “Model reference adaptive control systems with terminal sliding modes,” *International Journal of Control*, vol. 64, no. 6, pp. 1165–1176, 1996. 2.2
- [15] H. D. Patino and D. Liu, “Neural network-based model reference adaptive control system,” *Systems, Man, and Cybernetics, Part B: Cybernetics, IEEE Transactions on*, vol. 30, no. 1, pp. 198–204, 2000. 2.2
- [16] J. Kim and N. Kasabov, “HyFIS: adaptive neuro-fuzzy inference systems and their application to nonlinear dynamical systems,” *Neural Networks*, vol. 12, no. 9, pp. 1301–1319, 1999. 2.2
- [17] T. Orłowska-Kowalska, M. Dybkowski, and K. Szabat, “Adaptive sliding-mode neuro-fuzzy control of the two-mass induction motor drive without mechanical sensors,” *Industrial Electronics, IEEE Transactions on*, vol. 57, no. 2, pp. 553–564, 2010. 2.2
- [18] E. Kayacan, H. Ramon, and W. Saeys, “Adaptive neuro-fuzzy control of a spherical rolling robot using sliding-mode-control-theory-based online learning algorithm,” *Cybernetics, IEEE Transactions on*, vol. 43, no. 1, pp. 170–179, 2013. 2.2
- [19] A. Astolfi and R. Ortega, “Immersion and invariance: a new tool for stabilization and adaptive control of nonlinear systems,” *Automatic Control, IEEE Transactions on*, vol. 48, no. 4, pp. 590–606, 2003. 2.2
- [20] X. Liu, R. Ortega, H. Su, and J. Chu, “Immersion and invariance adaptive control of nonlinearly parameterized nonlinear systems,” *Automatic Control, IEEE Transactions on*, vol. 55, no. 9, pp. 2209–2214, 2010. 2.2

- [21] J. Hu and H. Zhang, "Immersion and invariance based command-filtered adaptive backstepping control of VTOL vehicles," *Automatica*, vol. 49, no. 7, pp. 2160–2167, 2013. 2.2
- [22] D. Bustan, S. K. H. Sani, and N. Pariz, "Immersion and invariance based fault tolerant adaptive spacecraft attitude control," *International Journal of Control, Automation and Systems*, vol. 12, no. 2, pp. 333–339, 2014. 2.2
- [23] C. P. Bechlioulis and G. A. Rovithakis, "Robust adaptive control of feedback linearizable MIMO nonlinear systems with prescribed performance," *Automatic Control, IEEE Transactions on*, vol. 53, no. 9, pp. 2090–2099, 2008. 2.2, 2.4, 3.3.4, 5.2, 5.3, 5.3, 5.5
- [24] ———, "Adaptive control with guaranteed transient and steady state tracking error bounds for strict feedback systems," *Automatica*, vol. 45, no. 2, pp. 532–538, 2009. 2.2, 2.4
- [25] J. Na, "Adaptive prescribed performance control of nonlinear systems with unknown dead zone," *International Journal of Adaptive Control and Signal Processing*, vol. 27, no. 5, pp. 426–446, 2013. 2.2, 2.4
- [26] C. Cao and N. Hovakimyan, "Design and analysis of a novel adaptive control architecture with guaranteed transient performance," *Automatic Control, IEEE Transactions on*, vol. 53, no. 2, pp. 586–591, 2008. 2.2, 2.3, 4.1
- [27] J. Luo, C. Cao, and N. Hovakimyan, "L 1 adaptive controller for a class of systems with unknown nonlinearities," in *American Control Conference (ACC), 2010*. IEEE, 2010, pp. 1659–1664. 2.2, 2.3, 3.2.4, 4.1
- [28] E. Xargay, N. Hovakimyan, V. Dobrokhodov, I. Kaminer, I. M. Gregory, and C. Cao, "L1 adaptive flight control system: Flight evaluation and technology transition," in *AIAA Infotech@ Aerospace 2010*, 2010. 2.2, 2.3, 3.4.5, 4.1
- [29] C.-W. Tao, J.-S. Taur, Y.-H. Chang, and C.-W. Chang, "A novel fuzzy-sliding and fuzzy-integral-sliding controller for the twin-rotor multi-input-multi-output system," *Fuzzy Systems, IEEE Transactions on*, vol. 18, no. 5, pp. 893–905, 2010. 2.2, 4.1
- [30] S. Mondal and C. Mahanta, "Adaptive second-order sliding mode controller for a twin rotor multi-input-multi-output system," *IET Control Theory & Applications*, vol. 6, no. 14, pp. 2157–2167, 2012. 2.2
- [31] D. Lee, H. J. Kim, and S. Sastry, "Feedback linearization vs. adaptive sliding mode control for a quadrotor helicopter," *International Journal of Control, Automation and Systems*, vol. 7, no. 3, pp. 419–428, 2009. 2.2

- [32] H. Voos, “Nonlinear control of a quadrotor micro-UAV using feedback-linearization,” in *Mechatronics, 2009. ICM 2009. IEEE International Conference on*. IEEE, 2009, pp. 1–6. 2.2
- [33] A. Das, F. Lewis, and K. Subbarao, “Backstepping approach for controlling a quadrotor using lagrange form dynamics,” *Journal of Intelligent and Robotic Systems*, vol. 56, no. 1-2, pp. 127–151, 2009. 2.2, 3.3.4
- [34] S. Barreto, A. G. S. Conceicao, C. E. Dorea, L. Martinez, E. R. de Pieri, and others, “Design and implementation of model-predictive control with friction compensation on an omnidirectional mobile robot,” *Mechatronics, IEEE/ASME Transactions on*, vol. 19, no. 2, pp. 467–476, 2014. 2.2
- [35] C. Cao and N. Hovakimyan, “Design and analysis of a novel l1 adaptive controller, part i: Control signal and asymptotic stability,” in *American Control Conference, 2006*. IEEE, 2006, pp. 3397–3402. 2.3, 4.1, 2
- [36] —, “Guaranteed transient performance with l1 adaptive controller for systems with unknown time-varying parameters and bounded disturbances: Part i,” in *American Control Conference, 2007. ACC’07*. IEEE, 2007, pp. 3925–3930. 2.3, 4.1
- [37] I. M. Gregory, C. Cao, E. Xargay, N. Hovakimyan, and X. Zou, “L1 adaptive control design for NASA AirSTAR flight test vehicle,” in *AIAA Guidance, Navigation, and Control Conference*, vol. 5738, 2009. 2.3, 4.1
- [38] T. J. Leman, E. Xargay, G. Dullerud, N. Hovakimyan, and T. Wendel, “L1 adaptive control augmentation system for the x-48b aircraft,” Ph.D. dissertation, University of Illinois, 2010. 2.3
- [39] I. Kaminer, O. Yakimenko, V. Dobrokhodov, A. Pascoal, N. Hovakimyan, C. Cao, A. Young, and V. Patel, “Coordinated path following for time-critical missions of multiple UAVs via l1 adaptive output feedback controllers,” in *AIAA Guidance, Navigation and Control Conference and Exhibit*, 2007. 2.3
- [40] B. Michini and J. How, “L1 adaptive control for indoor autonomous vehicles: design process and flight testing,” in *Proceeding of AIAA Guidance, Navigation, and Control Conference*, 2009, pp. 5754–5768. 2.3
- [41] J. Wang, V. V. Patel, C. Cao, N. Hovakimyan, and E. Lavretsky, “Novel l1 adaptive control methodology for aerial refueling with guaranteed transient performance,” *Journal of guidance, control, and dynamics*, vol. 31, no. 1, pp. 182–193, 2008. 2.3

- [42] E. Kharisov, I. M. Gregory, C. Cao, and N. Hovakimyan, “L1 adaptive control law for flexible space launch vehicle and proposed plan for flight test validation,” in *AIAA Guidance, Navigation and Control Conference*, 2008. 2.3
- [43] N. Hovakimyan and C. Cao, *L1 adaptive control theory: Guaranteed robustness with fast adaptation*. Siam, 2010, vol. 21. 2.3, 4.1, 4.5.1
- [44] D. Li, N. Hovakimyan, C. Cao, and K. Wise, “Filter design for feedback-loop trade-off of l1 adaptive controller: A linear matrix inequality approach,” in *Proc. AIAA Guidance, Navigation and Control*, 2008. 2.3, 4.1
- [45] D. Li, V. V. Patel, C. Cao, N. Hovakimyan, and K. A. Wise, “Optimization of the time-delay margin of l1 adaptive controller via the design of the underlying filter,” in *Proc. AIAA Guidance, Navigation and Control*, 2007. 2.3, 4.1
- [46] E. Kharisov, K. K. K. Kim, X. Wang, and N. Hovakimyan, “Limiting behavior of l1 adaptive controllers,” in *Proc. AIAA Guidance, Navigation and Control Conference, Portland, OR*, 2011, pp. 451–456. 2.3, 4.1
- [47] K.-K. K. Kim and N. Hovakimyan, “Multi-criteria optimization for filter design of l1 adaptive control,” *Journal of Optimization Theory and Applications*, vol. 161, no. 2, pp. 557–581, 2014. 2.3, 4.1
- [48] J. Wang, N. Hovakimyan, and C. Cao, “Verifiable adaptive flight control: unmanned combat aerial vehicle and aerial refueling,” *Journal of guidance, control, and dynamics*, vol. 33, no. 1, pp. 75–87, 2010. 2.4
- [49] A. K. Kostarigka and G. A. Rovithakis, “Adaptive dynamic output feedback neural network control of uncertain MIMO nonlinear systems with prescribed performance,” *Neural Networks and Learning Systems, IEEE Transactions on*, vol. 23, no. 1, pp. 138–149, 2012. 2.4
- [50] J. Na, Q. Chen, X. Ren, and Y. Guo, “Adaptive prescribed performance motion control of servo mechanisms with friction compensation,” *IEEE Transactions on Industrial Electronics*, vol. 61, no. 1, pp. 486–494, 2014. 2.4
- [51] C. P. Bechlioulis and G. A. Rovithakis, “Prescribed performance adaptive control for multi-input multi-output affine in the control nonlinear systems,” *Automatic Control, IEEE Transactions on*, vol. 55, no. 5, pp. 1220–1226, 2010. 2.4

- [52] M. Chen, S. S. Ge, and B. Ren, “Adaptive tracking control of uncertain MIMO nonlinear systems with input constraints,” *Automatica*, vol. 47, no. 3, pp. 452–465, 2011. 2.4
- [53] Y. Sun and H. Liu, “Fuzzy adaptive prescribed performance control for MIMO uncertain chaotic systems in nonstrict feedback form,” *Discrete Dynamics in Nature and Society*, vol. 2014, 2014. 2.4, 6.4
- [54] K. S. Narendra and A. M. Annaswamy, *Stable adaptive systems*. Courier Dover Publications, 2012. 2.5
- [55] P. A. Ioannou and J. Sun, “Stable and robust adaptive control,” *Englewood Cliffs, NJ: Printice Hall*, vol. 2, 1995. 2.5
- [56] D.-W. Gu and F. W. Poon, “A robust state observer scheme,” *Automatic Control, IEEE Transactions on*, vol. 46, no. 12, pp. 1958–1963, 2001. 2.5
- [57] J. Davila, L. Fridman, and A. Levant, “Second-order sliding-mode observer for mechanical systems,” *IEEE transactions on automatic control*, vol. 50, no. 11, pp. 1785–1789, 2005. 2.5
- [58] Z. Qiao, T. Shi, Y. Wang, Y. Yan, C. Xia, and X. He, “New sliding-mode observer for position sensorless control of permanent-magnet synchronous motor,” *Industrial Electronics, IEEE Transactions on*, vol. 60, no. 2, pp. 710–719, 2013. 2.5
- [59] K.-B. Lee and F. Blaabjerg, “An improved DTC-SVM method for sensorless matrix converter drives using an overmodulation strategy and a simple nonlinearity compensation,” *Industrial Electronics, IEEE Transactions on*, vol. 54, no. 6, pp. 3155–3166, 2007. 2.5
- [60] V. Stepanyan and N. Hovakimyan, “Adaptive disturbance rejection controller for visual tracking of a maneuvering target,” *Journal of guidance, control, and dynamics*, vol. 30, no. 4, pp. 1090–1106, 2007. 2.5
- [61] F. A. Shaik, S. Purwar, and B. Pratap, “Real-time implementation of chebyshev neural network observer for twin rotor control system,” *Expert Systems with Applications*, vol. 38, no. 10, pp. 13 043–13 049, 2011. 2.5
- [62] R. Marine, G. L. Santosuoso, and P. Tomei, “Robust adaptive observers for nonlinear systems with bounded disturbances,” *Automatic Control, IEEE Transactions on*, vol. 46, no. 6, pp. 967–972, 2001. 2.5
- [63] Y. Liu, “Robust adaptive observer for nonlinear systems with unmodeled dynamics,” *Automatica*, vol. 45, no. 8, pp. 1891–1895, 2009. 2.5, 7.1, 7.3

- [64] A. Freddi, A. Lanzon, and S. Longhi, “A feedback linearization approach to fault tolerance in quadrotor vehicles,” in *Proceedings of The 2011 IFAC World Congress, Milan, Italy*, 2011. 3.3.4
- [65] T. I. Fossen, *Guidance and control of ocean vehicles*. Wiley New York, 1994, vol. 199, no. 4. 3.3.4
- [66] B. Ferreira, M. Pinto, A. Matos, and N. Cruz, “Control of the MARES autonomous underwater vehicle,” in *OCEANS 2009, MTS/IEEE Biloxi-Marine Technology for Our Future: Global and Local Challenges*. IEEE, 2009, pp. 1–10. 3.3.4
- [67] —, “Hydrodynamic modeling and motion limits of AUV MARES,” in *Industrial Electronics, 2009. IECON’09. 35th Annual Conference of IEEE*. IEEE, 2009, pp. 2241–2246. 3.3.4
- [68] B. Ferreira, A. Matos, N. Cruz, and M. Pinto, “Modeling and control of the MARES autonomous underwater vehicle,” *Marine Technology Society Journal*, vol. 44, no. 2, pp. 19–36, 2010. 3.3.4
- [69] F. C. , *Twin Rotor MIMO System user manual*. Feedback Co, 1998. 3.4.5
- [70] B. Pratap and S. Purwar, “Sliding mode state observer for 2-DOF twin rotor MIMO system,” in *Power, Control and Embedded Systems (ICPCES), 2010 International Conference on*. IEEE, 2010, pp. 1–6. 3.4.5
- [71] E. Xargay, N. Hovakimyan, and C. Cao, “L1 adaptive controller for multi-input-multi-output systems in the presence of nonlinear unmatched uncertainties,” in *American Control Conference*, 2010, pp. 874–879. 4.1
- [72] L. A. Zadeh, “Fuzzy sets,” *Information and control*, vol. 8, no. 3, pp. 338–353, 1965. 4.1
- [73] Y. Li, S. Tong, Y. Liu, and T. Li, “Adaptive fuzzy robust output feedback control of nonlinear systems with unknown dead zones based on a small-gain approach,” *Fuzzy Systems, IEEE Transactions on*, vol. 22, no. 1, pp. 164–176, 2014. 4.1
- [74] R. C. Eberhart and J. Kennedy, “A new optimizer using particle swarm theory,” in *Proceedings of the sixth international symposium on micro machine and human science*, vol. 1. New York, NY, 1995, pp. 39–43. 4.1, 4.4
- [75] K. Das Sharma, A. Chatterjee, and A. Rakshit, “A hybrid approach for design of stable adaptive fuzzy controllers employing lyapunov theory and particle swarm optimization,” *Fuzzy Systems, IEEE Transactions on*, vol. 17, no. 2, pp. 329–342, 2009. 4.1

- [76] Z. Bingul and O. Karahan, "A fuzzy logic controller tuned with PSO for 2 DOF robot trajectory control," *Expert Systems with Applications*, vol. 38, no. 1, pp. 1017–1031, 2011. 4.1
- [77] C. Wong, H. Wang, and S. Li, "PSO-based motion fuzzy controller design for mobile robots," *International Journal of fuzzy systems*, vol. 10, no. 1, p. 24, 2008. 4.1
- [78] R.-E. Precup, R.-C. David, E. M. Petriu, S. Preitl, and M.-B. Rădac, "Novel adaptive charged system search algorithm for optimal tuning of fuzzy controllers," *Expert Systems with Applications*, vol. 41, no. 4, pp. 1168–1175, 2014. 4.1
- [79] F. Valdez, P. Melin, and O. Castillo, "A survey on nature-inspired optimization algorithms with fuzzy logic for dynamic parameter adaptation," *Expert Systems with Applications*, vol. 41, no. 14, pp. 6459–6466, 2014. 4.1
- [80] V. Kumar, P. Gaur, and A. Mittal, "Ann based self tuned pid like adaptive controller design for high performance pmsm position control," *Expert Systems with Applications*, vol. 41, no. 17, pp. 7995–8002, 2014. 4.1
- [81] N. Mendes and P. Neto, "Indirect adaptive fuzzy control for industrial robots: a solution for contact applications," *Expert Systems with Applications*, 2015. 4.1
- [82] S. Masumpoor, M. A. Khanesar *et al.*, "Adaptive sliding-mode type-2 neuro-fuzzy control of an induction motor," *Expert Systems with Applications*, 2015. 4.1
- [83] W. Zhang, H. Ma, and S. X. Yang, "A neuro-fuzzy decoupling approach for real-time drying room control in meat manufacturing," *Expert Systems with Applications*, vol. 42, no. 3, pp. 1039–1049, 2015. 4.1
- [84] J.-B. Pomet and L. Praly, "Adaptive nonlinear regulation: estimation from the lyapunov equation," *Automatic Control, IEEE Transactions on*, vol. 37, no. 6, pp. 729–740, 1992. 4.2
- [85] M. D. Buhmann, "Radial basis functions," *Acta Numerica 2000*, vol. 9, pp. 1–38, 2000. 5.4
- [86] Y. Ito, "Approximation of continuous functions on \mathbb{R}^d by linear combinations of shifted rotations of a sigmoid function with and without scaling," *Neural Networks*, vol. 5, no. 1, pp. 105–115, 1992. 5.4
- [87] G. Cybenko, "Approximation by superpositions of a sigmoidal function," *Mathematics of control, signals and systems*, vol. 2, no. 4, pp. 303–314, 1989. 5.4

- [88] H. K. Khalil and J. W. Grizzle, *Nonlinear systems*. Prentice hall Upper Saddle River, 2002, vol. 3. 19
- [89] Z.-P. Jiang and L. Praly, “Design of robust adaptive controllers for nonlinear systems with dynamic uncertainties,” *Automatica*, vol. 34, no. 7, pp. 825–840, 1998. 19, 7.3